



TECHNISCHE UNIVERSITÄT  
CHEMNITZ

Emergency Braking in Compact Vehicle Platoons:  
A Cyber-Physical Design

Dissertation  
zur Erlangung des akademischen Grades

Dr.-Ing.

Herr Dharshan Krishna Murthy  
geboren am 19. April 1988 in Mysore, Indien

Fakultät für Informatik  
an der Technischen Universität Chemnitz



# Acknowledgments

First and foremost, this work would not have been completed without my supervisor Prof. Alejandro Masrur. His round the clock availability and the flexibility to barge into his office anytime to discuss anything related to research has helped me immensely whenever I was stuck. His consistent guidance throughout my doctoral thesis along with his motivational words, especially when I was doubting myself resulted in this work. Thank you for the opportunity and your valuable time.

I am sincerely thankful to Prof. Hardt who deepened my interests in the automotive domain. His continuous support during my studies and PhD providing numerous platforms to showcase parts of this work has helped me immensely in shaping this work into its final form. Thank you very much once again.

I am what I am today because of my parents. Their sacrifices and hard work always made me push through difficult times. Just thanking them would be an understatement for all their emotional support and unconditional love.

Lastly, I must confess that there was a time when I considered quitting. I continued not only because of the support from the above mentioned people, but also because of Bhagavadh Geetha's teachings and sages that are definitely worth acknowledging. I will surely devote to them.



To my parents.



# Abstract

With the advent of autonomous driving, concepts like road trains or platoons are becoming more popular. In these arrangements, vehicles travel at separations of only 5 to 10m between them. These short inter-vehicle distances allow compacting vehicle flows resulting in increased throughput on highways. In addition, there are also fuel/energy savings as the magnitude of aerodynamic resistance acting on vehicles is reduced.

These benefits increase when reducing inter-vehicle separations to below 5m. However, it becomes extremely difficult to guarantee safety, especially, when braking in an emergency. The longitudinal and lateral control systems developed so far aim to achieve *string stability* in the cruise scenario, i.e., to prevent that small variations at the lead magnify towards the trail. Unfortunately, this has no relevance during emergency braking, since control systems incur saturation, i.e., the condition where computed output brake forces exceed those that can be applied by actuators. This is because all vehicles have to apply their maximum brake forces in order to minimize the stopping distance of the platoon and reach a complete standstill. As a result, emergency braking requires special attention and needs to be designed and verified independent of the cruise scenario.

Braking in an emergency is mainly characterized by the problem of heterogeneous deceleration capabilities of vehicles, e.g., due to their type and/or loading conditions. As a result, a deceleration rate possible by one vehicle may not be achievable by its immediately leading or following vehicles. Not addressing this heterogeneity leads to inter-vehicle collisions.

Moreover, transitions in the road profile increase the complexity of such brake maneuvers. Particularly, when there is a transition from a flat road to a steep downhill, an already saturated brake controller cannot counteract the effect of the downhill slope. Hence, its deceleration magnitude will be reduced, potentially leading to intra-platoon crashes that would otherwise not occur on a flat road.

In this work, we first analyze the problem of emergency braking in platoons operating at inter-vehicle separations below 5m and under idealized conditions (i.e., flat road, instantaneous deceleration, etc.). For this case, we propose a cyber-physical approach based on exploiting space buffers that are present in the separations between vehicles, and compare it with straightforward schemes (such as Least Platoon Length and Least Stopping Distance) in terms of achieved aerodynamic benefits, overall platoon length, and stopping distance. We then consider realistic conditions (in particular, changing road profiles as mentioned before) and investigate how to design a brake-by-wire controller present at each vehicle that accounts for this. We further extend our proposed cyber-physical approach by adding cooperative behavior. In particular, if an individual vehicle is unable to track its assigned deceleration, it coordinates with all others to avoid inter-vehicle collisions, for which we propose a vehicle-to-vehicle (V2V) communication strategy.

Finally, we present a detailed evaluation of the proposed cyber-physical approach based on high-fidelity vehicle models in Matlab/Simulink. Even though more work is needed towards a real-life implementation, our simulation results demonstrate benefits by the proposed approach and, especially, its feasibility.





# List of Acronyms

<b>V2V</b>	Vehicle-to-Vehicle
<b>V2I</b>	Vehicle-to-Infrastructure
<b>ETSI</b>	European Telecommunications Standards Institute
<b>RSU</b>	Road Side Unit
<b>ADAS</b>	Advanced Driver Assistance Systems
<b>ACC</b>	Adaptive Cruise Control
<b>ABS</b>	Antilock Brake System
<b>LTI</b>	Linear Time Invariant
<b>ITS</b>	Intelligent Transport Systems
<b>ISO</b>	International Organization for Standardization
<b>OSI</b>	Open System Interconnection
<b>DCC</b>	Decentralized Congestion Control
<b>IVS</b>	ITS Vehicle Station
<b>ICS</b>	ITS Central Station
<b>V2X</b>	Vehicle-to-X
<b>CAM</b>	Cooperative Awareness Message
<b>DENM</b>	Decentralized Environmental Notification Message
<b>SPAT</b>	Signal Phase and Timing Message
<b>SAM</b>	Service Announcement Message
<b>CCH</b>	Control Channel
<b>SCH</b>	Service Channel
<b>MAC</b>	Medium Access Control
<b>EDCA</b>	Enhanced Distributed Coordination Access
<b>AIFS</b>	Arbitration Inter Frame Space
<b>CW</b>	Contention Window
<b>AC</b>	Access Category
<b>GCDC</b>	Grand Cooperative Driving Challenge

## *LIST OF ACRONYMS*

<b>CALM</b>	Communication Access of Land Mobiles
<b>LDW</b>	Lane Departure Warning
<b>MPC</b>	Model Predictive Control
<b>CACC</b>	Cooperative Adaptive Cruise Control
<b>CCA</b>	Cooperative/Chain Collision Avoidance
<b>CAC</b>	Cooperative Autonomous Control
<b>GPS</b>	Global Positioning System
<b>IMU</b>	Inertial Measurement Unit
<b>SG</b>	Safeguard
<b>B</b>	Space Buffer
<b>LQR</b>	Linear Quadratic Regulator
<b>PID</b>	Proportional-Integral-Derivative

# Contents

<b>1. Introduction</b>	<b>1</b>
1.1. Scope and Motivation . . . . .	2
1.2. Contributions . . . . .	3
1.3. Models and Assumptions . . . . .	4
1.4. Structure of the work . . . . .	5
<b>2. Principles and fundamentals</b>	<b>7</b>
2.1. Platoon spacing policies . . . . .	7
2.1.1. Constant spacing policy . . . . .	7
2.1.2. Constant time headway policy . . . . .	8
2.1.3. Nonlinear spacing policies . . . . .	8
2.2. Aerodynamic effects . . . . .	9
2.2.1. Factors affecting aerodynamic force . . . . .	9
2.2.2. Aerodynamic effects during platoon operation . . . . .	10
2.3. Braking dynamics . . . . .	12
2.3.1. Forces during braking . . . . .	12
2.3.2. The impact of vehicle loading conditions . . . . .	13
2.3.3. Stopping distance . . . . .	16
2.3.4. Brake-by-wire systems . . . . .	17
2.3.5. A vehicle model in state-space representation . . . . .	18
2.4. Vehicle-to-vehicle communication (V2V) . . . . .	20
2.5. Summary . . . . .	23
<b>3. Related work</b>	<b>25</b>
3.1. Overview of platooning systems . . . . .	25
3.2. Vehicle coordination for platoon formation . . . . .	27
3.3. The platoon cruise scenario . . . . .	28
3.4. The platoon brake scenario . . . . .	30
<b>4. Braking under idealized conditions</b>	<b>33</b>
4.1. Intra-platoon communication . . . . .	33
4.2. Intuitive approaches . . . . .	35
4.2.1. Least Platoon Length . . . . .	35
4.2.2. Least Stopping Distance . . . . .	36
4.3. Subplatoon approach . . . . .	37
4.4. Space-Buffer approach . . . . .	39
4.4.1. Space buffer computations . . . . .	39
4.4.2. Proving collision-free brake maneuvers . . . . .	40
4.5. Parameters for comparison of the approaches . . . . .	42
4.6. Key findings . . . . .	42
<b>5. Considering realistic brake conditions</b>	<b>45</b>
5.1. Controller-based stopping distance . . . . .	45
5.2. Brake-by-wire performance specifications . . . . .	46
5.3. Deriving the controller-based stopping distance . . . . .	47

5.4.	The controller-based Space-Buffer approach . . . . .	50
5.4.1.	The ordering of vehicles . . . . .	51
5.4.2.	Considering uphill road profiles . . . . .	52
5.4.3.	Considering downhill road profiles . . . . .	52
5.5.	Key findings . . . . .	53
<b>6.</b>	<b>Engineering a cooperative behavior</b>	<b>55</b>
6.1.	Actions by distressed vehicles . . . . .	55
6.2.	Actions by less or non-distressed vehicles . . . . .	56
6.3.	Key findings . . . . .	59
<b>7.</b>	<b>Evaluation and simulation</b>	<b>61</b>
7.1.	The impact of platoon braking on stopping distance . . . . .	61
7.2.	Braking under idealized conditions . . . . .	62
7.2.1.	Test data . . . . .	62
7.2.2.	Method of performing the simulations . . . . .	62
7.2.3.	Aerodynamic savings, platoon length, and stopping distance . . . . .	64
7.2.4.	The impact of braking capacities . . . . .	66
7.3.	Braking under realistic conditions . . . . .	69
7.3.1.	The impact of ignoring controller-related effects . . . . .	70
7.3.2.	Braking on a flat road . . . . .	71
7.3.3.	Braking in a downhill . . . . .	73
7.3.4.	Avoiding collisions by distress messages . . . . .	75
7.3.5.	Braking in a steep downhill . . . . .	76
7.4.	Packet losses during platoon operation . . . . .	78
7.5.	Summary . . . . .	80
<b>8.</b>	<b>Concluding remarks</b>	<b>81</b>
8.1.	Outlook . . . . .	82
	<b>Bibliography</b>	<b>83</b>
<b>A.</b>	<b>Principles and Fundamentals</b>	<b>89</b>
A.1.	Platoon joining and operation . . . . .	89
<b>B.</b>	<b>Braking under realistic conditions</b>	<b>91</b>
B.1.	Control design, vehicle and platoon model . . . . .	91
<b>C.</b>	<b>List of Symbols</b>	<b>95</b>

# Chapter 1.

## Introduction

A quarter of Europe’s greenhouse gas emissions are caused by the transportation sector. Specifically in 2014, road transport alone has contributed to more than 70% of these emissions. Therefore, for transitioning to a low-carbon economy, and simultaneously meeting people’s increased mobility demands, areas for action have been identified, e.g., using renewable energy, electrifying vehicles, and making use of digital technologies to increase the efficiency of road transport [5].

The necessity to increase the road transport’s efficiency arises because the existing infrastructure falls short in meeting the requirements of the ever increasing number of vehicles. Even though new roads are being added, they cannot be improved/extended at the same pace with which vehicles are sold. This results in a vehicle throughput of highways of only around 2000 vehicles per hour at an average inter-vehicle spacing of  $35m$  [56], leading to traffic jams, more pollution, and simply a waste of time.<sup>1</sup>

In order to better utilize the existing infrastructure and, thereby, improve vehicle throughput, concepts like cooperative driving or platoons as illustrated in Fig. 1.1 are gaining in importance [43] [20] [17] [82] [72] [56]. In these vehicle arrangements, group of vehicles travel together at very short separations of 5 to  $10m$  between them [24]. The lead vehicle is usually a manually driven truck, whereas the following vehicles (trucks or cars) are automated and experience reduced aerodynamic force, thereby, resulting in fuel/energy savings. The lead vehicle’s actions — braking or accelerating — are communicated to all following vehicles through wireless messages typically based on IEEE 802.11p [36] [37] [13] [29] [45]. Control systems present at each following vehicle perform the necessary longitudinal and lateral maneuvers [24] [43] [42].

The concept of platooning has attracted lot of attention both from academia and industry around the globe, especially, from the goods transportation sector. As a result, with the support from ongoing standardization of vehicle-to-vehicle (V2V) and vehicle-to-infrastructure (V2I) communication, the following topics need to be addressed for platoons:

<sup>1</sup>Although flying cars such as AeroMobil [6] promise to ease this situation, these will presumably make up a small percentage of the total number of vehicles in the future. In addition, they will certainly bring about problems like coordinating take-off and landing that are even more difficult to solve.

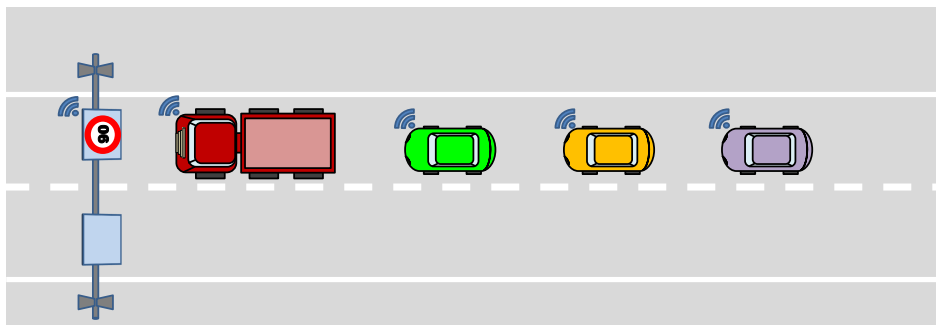


Figure 1.1.: An example of a platoon

- **Coordination and formation:** Platoons can be formed between vehicles with the same destination or using a common road stretch to reach different destinations. Hence, there is a need of a system that coordinates vehicle movements and allows them to join, operate, and leave a platoon [46] [52] [72] [78] [79].
- **Longitudinal and lateral control (i.e., cruise control):** Once a vehicle joins and operates in a platoon, longitudinal and lateral control systems perform vehicle maneuvers by controlling clutch, brakes, acceleration, and steering wheel. These systems maintain a preset cruise speed, and an appropriate distance and alignment to the immediate vehicle ahead [9] [39] [41] [47] [51] [77] [84] [86].
- **Wireless communication:** Critical information needs to be exchanged in a wireless manner. This constitutes the backbone of platoon operation, both in cruise and brake scenarios. Therefore, standards have to be established with respect to messages, technologies, and protocols used [35] [33] [34] [38] [36] [37].
- **Cybersecurity:** It is very important to ensure that malicious attackers do not inject false messages into the platoon network, thereby, affecting vehicle control [27] [28]. The effects of such events are catastrophic as vehicles generally travel at highway speeds of around  $100\text{km/h}$ . On the other hand, the implemented cybersecurity measures should impart a minimum overhead to inter-vehicle communication such that real-time requirements can still be met [31].

In this work, the focus is basically on longitudinal control, in particular, we are concerned with braking in an emergency. We note that traditional cruise controllers for platoons do not guarantee a safe braking in such a case, which requires special attention as detailed next.

## 1.1. Scope and Motivation

The inter-vehicle separations currently employed in platooning are in the range of 5 to 10m. However, further compacting platoons has a positive impact on vehicle throughput and, in addition, wind tunnel experiments have demonstrated that even the lead vehicle experiences benefits when the separations are below 5m. The optimum fuel/energy savings are obtained at separations of around 1m [56] [57]. As a result, in this work, we focus on inter-vehicle separations below 5m, i.e., less than one vehicle length.

On the other hand, at such inter-vehicle separations, it becomes considerably more difficult to guarantee a safe operation, in particular, when braking in an emergency. In such a scenario, the goal is not to simply brake the whole platoon at a deceleration rate that is comfortable for in-vehicle passengers and stop in a long distance, rather the distance to a hazard or other road traffic ahead might be short, thereby, demanding that all vehicles apply their maximum possible brake forces in order to minimize the stopping distance of the platoon and reach a complete standstill. Further, during the whole maneuver it has to be ensured that no intra-platoon collisions happen. The short inter-vehicle distances (below 5m) coupled with heterogeneous braking capabilities of vehicles make such maneuvers extremely dangerous.

So far, classical and modern control techniques have already been used to develop cruise controllers for platoons [75] [15] [85]. These controllers aim to achieve *string stability* [67] [68]. That is, small variations in a platoon lead's velocity and, hence, the corresponding variations in the separation to its immediately following vehicle are guaranteed not to amplify as they propagate towards the tail of the platoon [67] [68].

Unfortunately, ensuring string stability does not guarantee a collision-free braking [8] [9]. Especially during emergency, the vehicles have to decelerate at their maximum capabilities and this implies control systems incur saturation, i.e., the condition where computed output forces exceed those that can be applied by actuators. In addition, vehicles differ in terms of

their type, and/or loading conditions and their resulting maximum deceleration capabilities. As a result, if one vehicle brakes at a deceleration rate, the same rate might not be possible for its immediately leading and/or following vehicles, thereby, potentially leading to collisions depending on the inter-vehicle separation.

Another important factor to be considered during emergency braking are road-profile transitions the vehicles undergo. For example, if a vehicle already braking at its maximum deceleration on a flat road enters a downhill, it cannot negate the effect of grade, which aids vehicle motion. As a result, its deceleration magnitude reduces and a safe brake maneuver can no longer be guaranteed. Therefore, to guarantee safety all the above mentioned factors have to be addressed.

Thus, emergency braking needs to be analyzed, and verified independent of the cruise scenario. Apart from minimizing the stopping distance, fuel/energy savings for all vehicles, and short platoon length are also needed. These can be achieved only by maintaining the inter-vehicle separations below  $5m$ . Such short separations increase the design complexity of brake maneuvers. Hence, in this work, we address emergency braking and propose a cyber-physical approach. The details are presented in the next section.

## 1.2. Contributions

In this work, we consider vehicles with heterogeneous deceleration capabilities (due to different vehicle types and/or loading conditions) in a platoon scenario at inter-vehicle separations below  $5m$  (in order to maximize the aerodynamic benefits and achieve a short platoon length). We address the problem of braking in an emergency, and minimize the stopping distance of the whole platoon. In this direction, the following contributions are made:

- In Chapter 4, initially, we introduce our inter-vehicle communication strategy based on IEEE 802.11p. Then, we assume idealized conditions of braking on a flat road and an instantaneous deceleration tracking by all vehicles, and introduce the intuitive approaches for emergency braking namely *Least Platoon Length* and *Least Stopping Distance*. Their shortcomings are detailed and their advantages are combined into an approach named *Subplatoon*. However, there are certain shortcomings with this approach as well, particularly, in utilizing the maximum deceleration capabilities of vehicles during an emergency. We overcome them in our cyber-physical design named *Space Buffer* which utilizes the inter-vehicle separations and minimizes the stopping distance of the platoon. The separations are comprised of two parts namely *safeguard* and *space buffer*. Safeguard is reserved exclusively for communication loss between vehicles, whereas the space buffer in all the inter-vehicle separations are utilized, and we compute each individual vehicle's reference deceleration that needs to be tracked once emergency braking is initiated. The inputs to all the above mentioned approaches are stopping distances of vehicles from a common cruise velocity (typically around  $100km/h$ ) under idealized conditions as mentioned above.
- In reality, no vehicle can achieve its assigned deceleration instantaneously, and emergency braking might happen on varying road profiles as well. Hence, we consider these realistic conditions in Chapter 5 and introduce brake-by-wire controllers. During emergency braking, these controllers present at each vehicle are responsible for tracking the reference decelerations computed as per our Space-Buffer approach. Since controller related effects like rise and settling time exist in tracking an assigned deceleration, we derive an expression of vehicle stopping distance on a flat road that takes these effects into account (which are neglected by the existing standard expression of stopping distance). Apart from flat roads, the designed brake-by-wire controllers can track their assigned decelerations on uphill road profiles as well.

- The most challenging conditions for emergency braking are presented by downhill road profiles. As a result, some brake-by-wire controllers cannot track their assigned decelerations. This is because they are already decelerating at their maximum limit on a flat road (in order to minimize the overall stopping distance as per our approach). Hence, in a downhill, these controllers cannot negate the effect of grade and, hence, they fail to track their assigned decelerations. As a consequence, the affected vehicles need a longer distance to stop. Therefore, in such a scenario, it cannot be guaranteed that the whole platoon brakes in a safe manner anymore. Clearly, one can design the system for the worst case instead, i.e., considering the steepest possible downhill. However, this is a pessimistic approach with the cost of a longer stopping distance on a flat road. This longer distance entails the risk of colliding with other road traffic ahead, thereby, jeopardizing safety. As a result, in Chapter 6, we rather extend our Space-Buffer approach to compensate for variations from the flat road profile, particularly downhill, by enabling cooperation/coordination among vehicles. The idea is that a vehicle broadcasts a *distress message*, if it is unable to track its assigned deceleration. Other vehicles in the platoon then adapt their decelerations to avoid collisions.
- Finally, in Chapter 7, we first perform a detailed evaluation of the intuitive, Subplatoon, and Space-Buffer approaches under idealized conditions. We demonstrate that our Space-Buffer approach performs best when all the three parameters are considered simultaneously, i.e., achieved aerodynamic benefits, overall platoon length, and stopping distance from a common cruise velocity. Subsequently, we consider realistic conditions of braking and evaluate our controller-based Space-Buffer approach. Even in the most challenging conditions of steep downhill braking, we demonstrate how our approach enables cooperation/coordination among vehicles and ensures no inter-vehicle collisions happen, while simultaneously minimizing the stopping distance. We illustrate all these through detailed simulations involving high-fidelity vehicle models. Towards the end, we also analyze the number of wireless communication packets that can be lost in all the presented approaches without affecting safety.

Even though more work is needed towards a real-world implementation of our Space-Buffer approach, we demonstrate its benefits in this work, especially, the feasibility.

### 1.3. Models and Assumptions

In the following, we present and discuss models and assumptions used as a basis for this work:

- **Category of vehicles.** For simplification, we assume two-axle vehicles, i.e., mostly passenger cars and utility vehicles. The presented work can also be extended to multi-axle vehicles like trucks and truck-trailer combinations, having implications in the design of brake-by-wire controllers, but otherwise none.
- **Maximum deceleration.** A vehicle's loading condition affects its maximum achievable deceleration magnitude. As explained later, this is a function of both the brake-force distribution to the vehicle's front and rear axles (i.e., what percentage of the brake force acts on the front and rear axles) and the weights acting on them. Therefore, we assume that the vehicles are equipped with the necessary sensors that estimate/measure the same.
- **Brake-by-wire systems.** Conventional brake systems are designed for manual operation and typically based on hydraulics. However, for operating in a platoon, brake systems have to be automated making brake-by-wire systems necessary. These are usually of electromagnetic nature and can be activated with a control signal that regulates the brake force.



- **Reference-deceleration tracking.** We assume that there are no quantization errors up to two decimal places in reference deceleration tracking by brake-by-wire controllers. We can later remove this restriction, clearly, resulting in longer stopping distances, however, the proposed approach remains valid.
- **Road-profile transitions/maximum platoon length.** Once an emergency brake maneuver is initiated, we assume that there is at most one road-profile transition, for example, from flat road to downhill or from one grade/slope to another, etc. This is no serious limitation for highways, where road profile changes tend to be rather smooth. However, it implies limiting the maximum allowable length of a platoon, which we further assume to be around  $200m$ .
- **Maximum grade.** For uphill and downhill road profiles, we consider a maximum grade/slope of eight degrees ( $8^\circ$ ), which is in line with the European highway standards [83] and around the globe.
- **Cruise velocity of the platoon.** We consider that, when an emergency brake maneuver is initiated, the velocity of the platoon is around  $100km/h$ . This is a typical speed on highways. Clearly, this speed is common to all vehicles in the platoon. In principle, the maximum allowable cruise velocity can be further increased, however, this changes also the real-time requirements affecting, in particular, the sampling period of the brake-by-wire controller present at each vehicle and the periodicity of wireless messages exchanged between vehicles.
- **Intra-platoon communication.** During emergency braking, critical information has to be exchanged between vehicles in a wireless manner. Hence, platoon vehicles are required to be equipped with transceivers that broadcast and receive information over the allocated frequency band in Europe according to European Telecommunications Standards Institute (ETSI). Clearly, fail-safe behavior must be implemented in case of communication loss,<sup>2</sup> however, this is out of the scope of this work. Finally, based on the the results from [11], we consider a negligible propagation delay of wireless packets (introduced later) within the platoon. This is in line with the selected cruise speed of  $100km/h$  and platoon length of  $200m$ .

## 1.4. Structure of the work

The rest of this work is organized as follows. In the next chapter, we introduce principles and fundamentals of this work. We begin by briefly reviewing the inter-vehicle spacing policies used in platooning. This is then followed by a discussion of wind-tunnel experiments with platoons demonstrating their aerodynamic benefits. Next, the impact of loading conditions on braking dynamics of a vehicle are outlined. We then introduce the existing standard expression of stopping distance, on which all our emergency braking approaches are based. During emergency braking, vehicles are required to track their assigned reference decelerations. Hence, the computations performed by brake-by-wire systems to exert the necessary brake force are also presented in this chapter. For the design of brake-by-wire systems, in particular brake-by-wire controllers, we extract a vehicle model in a state-space representation. Finally, we conclude the chapter by introducing the ongoing standardization of V2V and V2I communication based on IEEE 802.11p. Deviations from the standard and the modifications employed in this work are also detailed.

---

<sup>2</sup>For example, any vehicle in a platoon could initiate an emergency brake maneuver, if a given number of messages from its immediately leading vehicle are lost, in the end, dissolving the platoon for the sake of safety.

In Chapter 3, we review existing works with respect to platooning. We begin by briefly looking at the existing projects which typically deal with longitudinal and lateral control of vehicles in the cruise scenario. We further review relevant works dealing with brake scenarios, which in contrast to the former are less in number. Finally, we conclude by identifying a gap in existing research and explain how our work bridges the same.

In Chapter 4, we begin by introducing our inter-vehicle communication strategy. Then, under idealized conditions of braking, we introduce the intuitive approaches. We then combine these approaches into the Subplatoon approach. Subsequently, we introduce our proposed Space-Buffer approach, which is a cyber-physical design based on provisioning space buffers in between vehicles. Our approach allows balancing the overall stopping distance, platoon length, and aerodynamic benefits as opposed to the other potential approaches.

In Chapter 5, we consider realistic conditions of braking, introduce brake-by-wire controllers and discuss their performance specifications. We also derive an expression of a vehicle's stopping distance on a flat road under controller action.

In Chapter 6, we extend our Space-Buffer approach to compensate for variations from the flat road profile by enabling coordination/cooperation among vehicles in situations of distress, i.e., when certain vehicles are unable to track their reference decelerations, especially in a downhill. All other vehicles then adapt their decelerations to prevent inter-vehicle collisions and, thereby, guarantee a safe brake maneuver.

In Chapter 7, we perform an extensive evaluation of our Space-Buffer approach and present the results. We begin by comparing it with the other approaches and, then, simulate it on different road profiles to demonstrate that the coordination scheme ensures safe braking. To this end, we make use of high-fidelity vehicle models developed in Matlab/Simulink. Finally, chapter 8 concludes this work by identifying possible extensions and future developments.

# Chapter 2.

## Principles and fundamentals

In this chapter, we cover the principles and fundamentals of our approach. In this direction, we first introduce the spacing policies typically used in platoons. Then, the details about aerodynamic force and its magnitude reduction for individual vehicles during platooning are presented. Next, the impact of loading conditions on the braking dynamics of a vehicle are explained. This is followed by the standard expression of stopping distance, which helps us in the design of our Space-Buffer approach. Then, the computations performed by brake-by-wire systems to achieve an assigned deceleration during emergency braking are introduced. Subsequently, for the design of such systems, we model the braking dynamics in a state-space representation. Finally, we outline the existing and ongoing standardization of wireless communication to facilitate information exchange between vehicles.

### 2.1. Platoon spacing policies

In this section, we introduce the spacing policies commonly used in platooning. For ease of explanation, we consider a platoon of 3 vehicles. As explained further, the separations between vehicles can be constant or a function of speed. However, irrespective of the spacing policy used, the individual vehicle controllers have to ensure string stability in the cruise scenario.

#### 2.1.1. Constant spacing policy

In this spacing policy, the separations between vehicles are a constant  $s_c$  [69] as shown in Fig. 2.1. This common inter-vehicle separation would usually be decided by the lead vehicle or even the road infrastructure can recommend this by communicating it through a road side unit (RSU). The individual vehicle controllers are responsible for maintaining the preset separation to their immediate lead vehicle. Any variations in this separation caused due to acceleration/deceleration of the platoon lead or the immediate lead vehicle have to be reduced to zero.

Existing works have used this spacing policy with separations in the range of 5 to 10m [24]. With respect to achieving string stability, critical information like the lead vehicle's velocity are required by all individual vehicle controllers, which is typically conveyed by wireless communication [69]. Relying only on information obtained from in-vehicle sensors does not guarantee string stability [67].



Figure 2.1.: Constant spacing policy

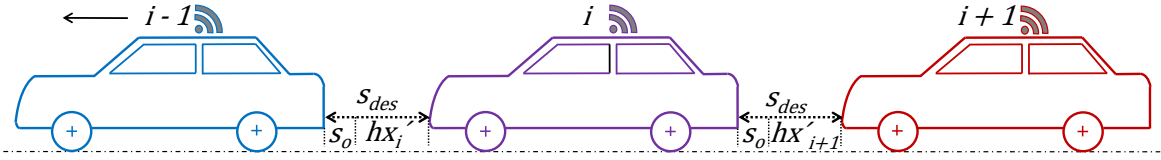


Figure 2.2.: Constant time headway policy

### 2.1.2. Constant time headway policy

In this spacing policy, the inter-vehicle separations are not constant, but a function of platoon cruise velocity. It increases linearly with an increase in velocity. Hence, the desired spacing between vehicles as shown in Fig. 2.2 can be expressed as [32]:

$$s_{des} = s_0 + h\dot{x}, \quad (2.1.1)$$

where  $h$  is referred to as time headway or time gap in seconds and is a constant. It is usually decided by the platoon lead. The platoon cruise velocity in  $m/s$  is denoted by  $\dot{x}$ . The inter-vehicle separation can be further increased through the parameter  $s_0$  which denotes the minimum separation between vehicles in meters (m). Hence,  $s_{des}$  (also in  $m$ ) represents the desired separation between vehicles [32]. For example, if  $h = 1s$  and  $s_0 = 1m$ , then, the inter-vehicle separation would be  $31m$  at a platoon cruise velocity of  $30m/s$  ( $108km/h$ ). This separation reduces to  $16m$  for a cruise velocity of  $15m/s$  ( $54km/h$ ).

Recent works done in [41], [47], and [84] employ time headway below  $1s$ . Apart from platooning, this spacing policy is also used in advanced driver assistance systems (ADAS) like adaptive cruise control (ACC), where a vehicle cruises at a speed set by the driver. If any other vehicle is encountered in its path, a safe distance would be maintained as per this policy [63].

In comparison to constant spacing policy, the achieved fuel/energy savings and vehicle throughput are lesser due to the larger inter-vehicle separations. For ensuring string stability, inter-vehicle communication is not required. Information obtained from local sensors suffices. Thus, this spacing policy is ideal for platoons with a mix of both automated and non-automated vehicles [69].

### 2.1.3. Nonlinear spacing policies

One of the popular nonlinear spacing policy is the variable time headway [32]. In this policy, the time headway is not constant, but a function of the relative velocities between two consecutive vehicles. For example, if a preceding vehicle is traveling faster than a following vehicle, the relative velocity can be considered positive and the time headway can be reduced. On the contrary, if the lead vehicle is traveling slower than its following vehicle, the relative velocity is negative and, in this case, the time headway has to be increased [32].

This spacing policy was introduced in the early stages of vehicle automation where V2V communication was not yet standardized and implemented. Hence, there was a need of a spacing policy that produced small errors by vehicle controllers [32]. However, since the introduction and ongoing standardization of V2V and V2I communication, all works have concentrated on either the constant time headway or the constant spacing policy.

In this thesis, apart from minimizing the stopping distance when braking in an emergency, our goal is to simultaneously achieve optimum fuel/energy savings, and short platoon length. Hence, we employ the constant spacing policy. In particular, our inter-vehicle separations are in the range of  $2$  to  $4m$ . At such short separations, the magnitude of aerodynamic force acting on all vehicles, including the platoon lead would be reduced when compared to operating in isolation. The details of the same would be introduced in the next section.

## 2.2. Aerodynamic effects

In this section, we first introduce factors that influence the magnitude of aerodynamic force acting on a vehicle. Then, the details about magnitude reduction during platoon operation are outlined. Finally, generalizations that can be made for longer platoons are enumerated.

There are a number of forces that oppose the motion of a car. The most prominent ones are the rolling resistance, grade resistance, inertia, and aerodynamic force [48]. The energy required for a passenger car traveling at speeds higher than  $80\text{km/h}$  to overcome the aerodynamic resistance is greater than the energy required to overcome the rolling resistance of tires and resistance in the transmission [53] [48].

There are two sources generating aerodynamic resistance. First, the airflow over the exterior of a vehicle body and, second, the airflow through an engine's radiator system, and vehicle's interior for cooling, heating, and ventilating purposes. Of these two, the former accounts for more than 90% of the total aerodynamic resistance and generates normal pressure and shear stress on the body of a vehicle [48].

The external aerodynamic resistance consists of the following two components: *pressure drag* and *skin friction*. The pressure's normal component on a vehicle body acting against its motion gives rise to pressure drag, whereas the shear stress in the boundary layer adjacent to the external surface of a vehicle body causes skin friction. Of these two, the pressure drag constitutes more than 90% of the total aerodynamic resistance of a typical passenger car. The skin friction becomes prominent only for long vehicles likes buses and tractor-trailer combinations [48].

Overall, the aerodynamic resistance acting on a vehicle is given by the following equation [48]:

$$R_a = \frac{\rho}{2} C_D A_f V_r^2, \quad (2.2.1)$$

where  $\rho$  is the air-mass density in  $\text{kg/m}^3$ ,  $C_D$  is the coefficient of aerodynamic resistance encapsulating all the components mentioned above,  $A_f$  is frontal or projected area of a vehicle in  $\text{m}^2$  along the direction of travel. Finally,  $V_r$  represents a vehicle's speed relative to the wind in  $\text{m/s}$  [48].

An important observation from the above equation is that the aerodynamic resistance is proportional to the square of speed. Thus, if the speed of a vehicle is doubled, there is a fourfold increase in the energy required to overcome the aerodynamic resistance [48].

### 2.2.1. Factors affecting aerodynamic force

It is clear from the above (2.2.1) that even air-mass density influences aerodynamic resistance, apart from a vehicle's velocity, and its design characteristics. The air-mass density is dependent on atmospheric conditions like ambient temperature and altitude. There is a 14% reduction in the aerodynamic resistance when the ambient temperature increases from  $0^\circ\text{C}$  to  $38^\circ\text{C}$ . Further, an increase in altitude of  $1219\text{m}$  will lead to a 17% decrease in aerodynamic resistance. Therefore, to account for these factors, the value of air-mass density is considered as  $1.225\text{kg/m}^3$  in performance calculations [48] and, hence, we use the same in our work as well.

A number of vehicle design and operational factors influence the coefficient of aerodynamic resistance  $C_D$ . In particular, the shape of a vehicle's body including its forebody, afterbody, underbody, wheel wells, drip rails, window recesses, external mirrors, and mud flaps all influence the coefficient of aerodynamic resistance. In addition to the shape, a vehicle's attitude, commonly referred to as the *angle of attack*, which is the angle between a vehicle's longitudinal axis and the ground, and other operational factors like radiator open or blanked, windows open or closed, etc., also affect the coefficient of aerodynamic resistance [48].

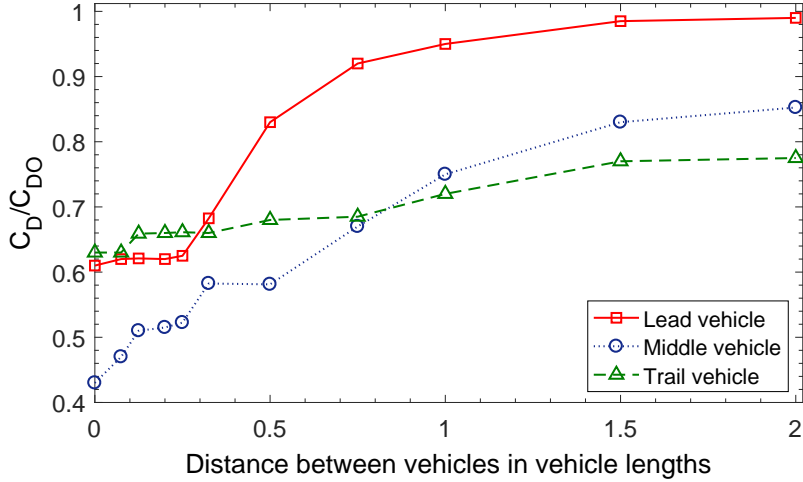


Figure 2.3.: Drag coefficient ratios for three close-following vehicles [57]

The vehicle loading conditions influences both ground clearance, i.e., distance between the vehicle body and ground, and angle of attack. Hence, the value of  $C_D$  is also affected. For passenger cars,  $C_D$ 's value can be obtained from wind-tunnel tests [48]. These values typically lie in the range of 0.311–0.475 and the same is used in our work for simulation.

Finally, the frontal area of a vehicle  $A_f$  can be determined from accurate vehicle drawings. If they are not available, a photograph taken from the front can also be used [48]. Usually for passenger cars,  $A_f$  varies in the 79–84% range of the area calculated from their overall width and height. Therefore, in our work, we consider  $A_f$  to be in the  $2m^2$ – $2.5m^2$  range [48].

### 2.2.2. Aerodynamic effects during platoon operation

A vehicle closely following another vehicle will have reduced magnitude of its  $C_D$  and, hence, experiences reduced aerodynamic force. This is the principle behind existing platoon strategies where several cars or trucks follow a lead vehicle at distances of 5 to 10m. The lead vehicle will usually be a truck so that the following and trail vehicles benefit the most from reduced aerodynamic force [24] [1]. However, at these separations, the lead vehicle is devoid of benefits [56] [57].

The University of California along with the United States Department of Transportation conducted several experiments as part of the California PATH program [56] [57]. These experiments considered platoons with different number of vehicles and demonstrated that even the lead vehicle experiences fuel/energy savings, when the inter-vehicle distances are reduced to less than one vehicle length (5m), i.e., approximately in the range of 1 to 4m.

The ratio of aerodynamic drag coefficient when traveling in a platoon ( $C_D$ ) to the aerodynamic drag coefficient of the same vehicle in isolation ( $C_{D0}$ ) is plotted in Fig. 2.3 for a three-vehicle platoon as a function of vehicle lengths. Here, vehicles are assumed to have the same height [56] [57].

At inter-vehicle distances of 1 vehicle length or greater, the lead vehicle is unaware of the following vehicles and almost has no benefits. The following and trail vehicles experience reduced aerodynamic force up to a distance of 10 vehicle lengths. Since only the following and trail vehicles benefit at such inter-vehicle distances, this is said to be a *weak interaction regime*. The lead vehicle begins to experience significantly less aerodynamic force only when the inter-vehicle distance reduces to less than 1 vehicle length. This is said to be a *strong interaction regime* as the benefits are mutual. In this case, the drag coefficient ratio for the trail vehicle also decreases but not so rapidly — see Fig. 2.3.

In the strong interaction regime, there will be a reduction in the drag coefficient ratio for the lead vehicle up to a spacing of 0.20 vehicle lengths. Further, until zero spacing, it is more or less constant. Interestingly, at 0.35 vehicle lengths, the drag coefficient ratio of the lead is less than that of the trail vehicle and continues to be the same until zero spacing. This counter-intuitive behavior can be attributed to complex aerodynamic interactions [56] [57] that go beyond the scope of this work. We can figuratively say that the following and trail vehicles push the air mass towards the lead vehicle's rear part and, hence, the latter experiences a sort of *tailwind* [56] [57].

The middle or second vehicle's drag coefficient ratio is constituted by two plateau regions — from 0.1 to 0.2 and from 0.3 to 0.5 vehicle lengths. Due to the combined effects stemming from both the lead and trail vehicles, the second vehicle benefits the most and has the lowest drag coefficient ratio [56] [57].

**An example.** To better understand Fig. 2.3, consider a vehicle having a drag coefficient of 0.45 ( $C_{DO}$ ) when traveling in isolation. Now, consider two vehicles of the same height follow this vehicle at a close distance of 0.2 vehicle lengths, i.e., 1m. As per Fig. 2.3, at such a distance, the value of  $C_D/C_{DO}$  is 0.62 for the lead vehicle. This results in its new drag coefficient to be  $0.62 \times 0.45 = 0.279$ . When these values for  $C_D$  are substituted in (2.2.1), we find a 38% reduction in the magnitude of aerodynamic force during platoon operation assuming, the velocity is constant in both the cases.

Due to reduced aerodynamic force, the fuel consumption also reduces when traveling in a platoon. The California PATH program [56] considered two-, three-, and four-vehicle platoons at different inter-vehicle separations of 0.6 to 1.2 vehicle lengths. Fuel/energy savings were logged for each configuration. In the two-vehicle platoon case, the average fuel savings at 0.6 vehicle lengths (approximately 3m) was observed to be much greater than the average savings for the same two-vehicle platoon at a spacing of 1.2 vehicle lengths (approximately 6m). Increasing the number of vehicles in the platoon, increased the overall average fuel savings with more savings at shorter inter-vehicle separations. Particularly, at separations of 0.6 vehicle lengths, the average fuel savings for two-, three-, and four-vehicle platoons were 5.5%, 7.5%, and 8.5% respectively. The following vehicles, i.e., in between the lead and trail vehicles, exhibited the most savings of around 10%, where as the trail vehicle, i.e., the last vehicle in the platoon, around 7%, and the lead vehicle between 3 to 4%. [56].

Based on these aforementioned factors, there are some generalizations that can be made for platoons with more than 3 vehicles. These are as follows [57]:

- The drag-coefficient ratio for a lead vehicle and for each of the subsequent vehicles up to the  $n^{\text{th}}$  is independent of the number of vehicles given that there are at least  $n+1$  vehicles.
- The vehicles in between the lead and trail vehicles of a platoon experience the least drag coefficients and, thereby, have the most fuel/energy savings.
- Adding vehicles to a platoon reduces the average drag-coefficient ratio for the whole platoon. However, this asymptotically approaches a value of around 0.5 as per Fig. 2.3, considering that inter-vehicle separations are reduced to zero, which is not achievable in practice.
- As the inter-vehicle distances vary, the trail vehicle will experience the least variation in its drag-coefficient ratio.

In this work, we consider a maximum of 20 vehicles operating in platoons. Note that even though more than 20 vehicles can be studied and analyzed theoretically, from the perspective of real-world implementation, too many vehicles cannot be part of a platoon due to

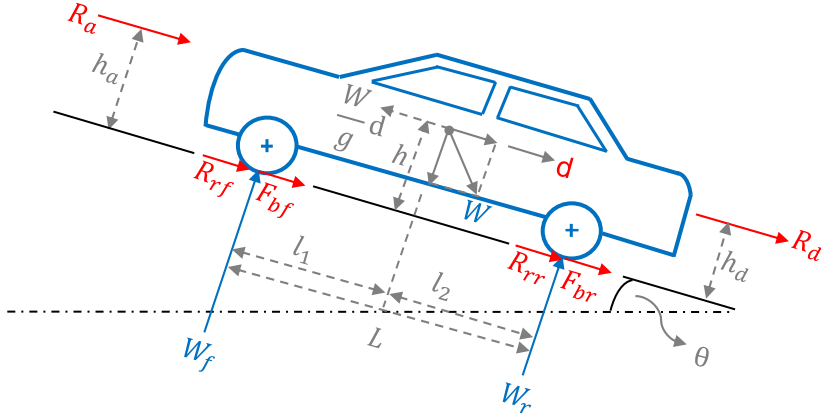


Figure 2.4.: Forces on a two-axle vehicle during braking [48]

infrastructure issues. Finally, it is important to note that aerodynamic force opposes vehicle motion, and its magnitude is reduced during platooning. This naturally leads to a brake system performing more work to bring the vehicle to a complete standstill during brake maneuvers. Hence, braking in a platoon results in a longer stopping distance, when compared to braking in isolation.

Further, when designing brake maneuvers, the heterogeneous deceleration capabilities of platoon vehicles have to be considered. If not, inter-vehicle collisions happen. The factors causing these non-homogeneous deceleration capabilities of vehicles are explained in the next section.

## 2.3. Braking dynamics

In this section, we first look at the forces acting on a two-axle vehicle during braking. Then, the impact of loading conditions on maximum achievable deceleration magnitude is outlined. Subsequently, we introduce the standard expression of stopping distance. This is followed by the calculations performed by a brake-by-wire system for achieving a desired deceleration during emergency braking. Finally, for designing the critical part of such systems, i.e., brake-by-wire controllers, we model the braking dynamics in a state-space representation. These controllers are present at each vehicle and ensure safe emergency braking.

### 2.3.1. Forces during braking

The forces acting on a two-axle vehicle during braking are shown in Fig. 2.4 [48]. The rolling resistances at the front and rear axles are denoted as  $R_{rf}$  and  $R_{rr}$  respectively in Newtons (N).  $R_a$  is the aerodynamic resistance also in N, as represented by (2.2.1). It is acting at a height  $h_a$  in meters (m) from the road surface. The forces in N generated by a vehicle's brake system acting at its front and rear axles are denoted as  $F_{bf}$  and  $F_{br}$  respectively. The weights acting on the front and rear axles in N are denoted as  $W_f$  and  $W_r$  respectively. The draw-bar load or trailer (if any) denoted as  $R_d$  is also in N. It is acting at a height  $h_d$  (in m) from the road surface [48].

The linear deceleration of a vehicle along the longitudinal axis is denoted as  $d$  in  $m/s^2$ . Similarly, the acceleration due to gravity also in  $m/s^2$  is denoted as  $g$ . The vehicle's center of gravity is at a height  $h$  in m from the road surface. Its distance in m from the centers of front and rear axles are  $l_1$  and  $l_2$  respectively. The total wheel base combining both  $l_1$  and  $l_2$  also in m is denoted as  $L$ . Finally, the road on which the vehicle is traveling makes an angle  $\theta$  in degrees with the horizontal [48].



The rolling, aerodynamic, and uphill grade resistances oppose the motion of a vehicle and aid as additional forces during braking. However, the force generated by a vehicle's brake system acting at the tire-road interface is the major decelerating force. Thus, the total resultant force acting on a decelerating vehicle can be expressed as [48]:

$$F_{total} = F_b + f_r W \cos(\theta) + R_a \pm W \sin(\theta), \quad (2.3.1)$$

where  $F_{total}$  is the resultant total force in  $N$ . The brake forces generated by a vehicle's brake system acting at the front and rear axles, previously denoted as  $F_{bf}$  and  $F_{br}$  respectively are combined into one resultant total force  $F_b$  also in  $N$ .  $f_r$  is the coefficient of rolling resistance, and  $W$  is the vehicle's weight ( $W_f + W_r$ ) in  $N$  [48].

The rolling resistances at the front and rear axles previously denoted as  $R_{rf}$  and  $R_{rr}$  respectively are a function of the coefficient of rolling resistance  $f_r$ , vehicle weight  $W$ , and road angle  $\theta$ . As a result,  $f_r W \cos(\theta)$  represents the combined rolling resistance. With respect to the grade resistance  $W \sin(\theta)$ , it is important to note that the positive term has to be used when the vehicle is on an uphill. In a downhill, the negative term has to be used [48].

Assuming, no trailers are being towed, the magnitude of draw-bar load  $R_d$  (see again Fig. 2.4) is 0 and, hence, it does not appear in the equation. Finally, even though there is transmission resistance, its contribution to overall braking is extremely small and neglected in (2.3.1).

### 2.3.2. The impact of vehicle loading conditions

Even though passenger cars belong to the same performance category and are equipped with similarly performing brake systems (to a great extent), their braking capacities will differ because of their loading conditions. The loading conditions are a function of number of occupants in a car, additional loads that are being carried, their distances from a vehicle's center of gravity and, hence, the forces they exert on the front and rear axles.

Similar to the weight transfer from the front to rear axle during acceleration, there is also a weight transfer due to inertia from the rear to the front during braking. That is why passengers of a car experience being pushed backwards when a car accelerates, and thrown forwards when a car decelerates. Therefore, the weights acting on the front and rear axles respectively during braking are expressed as [48]:

$$W_f = \frac{1}{L} [Wl_2 + h(F_b + f_r W)], \quad (2.3.2)$$

and

$$W_r = \frac{1}{L} [Wl_1 - h(F_b + f_r W)]. \quad (2.3.3)$$

The maximum brake forces sustained by the front and rear axle wheels are a function of the coefficient of road adhesion  $\mu$ , and the weight acting on that axle. These maximum forces for front and rear axles respectively are expressed as [48]:

$$F_{bfmax} = \mu W_f, \quad (2.3.4)$$

and

$$F_{brmax} = \mu W_r, \quad (2.3.5)$$

where  $W_f$  and  $W_r$  are as represented by (2.3.2) and (2.3.3) respectively.

An important aspect of the above two equations is that as long as the brake force supplied to an axle is less than the product of coefficient of road adhesion  $\mu$  and the weight on that axle, the corresponding wheels do not lock. When the brake force equals this product, the wheels are at the point of locking. If the wheels of both the front and rear axles are at

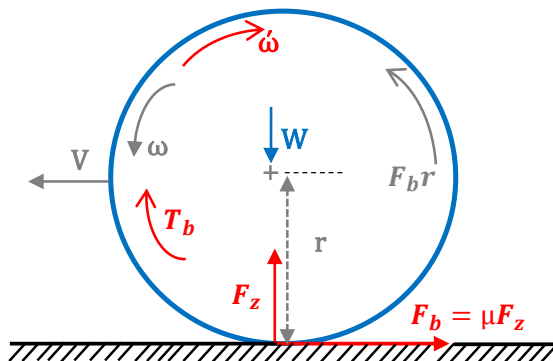


Figure 2.5.: Forces and moments acting on a wheel during braking [48]

the point of locking simultaneously, the maximum deceleration magnitude of a vehicle is achieved. However, when the magnitude of brake force at any axle exceeds this product, the corresponding wheels get locked. In other words, locked wheels of any axle indicate that the magnitude of brake force distributed to that axle is more than that it can handle [48].

The reason for wheels locking can be better understood by specifically looking at the forces and moments acting on a single wheel during braking as shown in Fig. 2.5. Assume that  $F_b$  denotes the brake force at this wheel, developed at the road-tire contact patch when a brake torque  $T_b$  is applied. About the tire center, this brake force has a moment  $T_t$ . Its direction is opposite to that of the applied brake torque  $T_b$ . Thus, the tire's angular deceleration  $\dot{\omega}$  is caused by the difference between  $T_t$  and  $T_b$ . It is expressed as [48]:

$$\dot{\omega} = \frac{T_t - T_b}{I_w} = \frac{F_b r - T_b}{I_w}, \quad (2.3.6)$$

where the mass moment of inertia of the tire about its center is denoted as  $I_w$ , and  $r$  represents the radius of the tire. The tire accelerates when the difference between  $F_b r$  and  $T_b$  is positive. On the contrary, it decelerates when this difference is negative [48].

Apart from the tire's angular deceleration, the brake force  $F_b$  also causes the linear deceleration of the tire center  $d_c$  and is expressed as [48]:

$$d_c = \frac{F_b}{\frac{W}{g}}, \quad (2.3.7)$$

where  $W$  denotes the weight on the wheel. Therefore, a tire gets locked when the magnitude of brake torque  $T_b$  is large and, hence, the angular deceleration  $\dot{\omega}$  is high. Note that a locked tire implies its angular velocity  $\omega$  is zero, but not its linear velocity [48].

Hence, brake force distributed to locked wheels at any axle have no effect on braking and the vehicle slows down only with the help of sliding resistance between the skidding tires and the road. In order to prevent wheels locking, brake force distribution to the axles must be in proportion to that of their normal loads. This distribution can in fact be computed as follows [48]:

$$\frac{K_{bf}}{K_{br}} = \frac{F_{bfmax}}{F_{brmax}} = \frac{l_2 + h(\mu + f_r)}{l_1 - h(\mu + f_r)}, \quad (2.3.8)$$

where the proportions of total brake force on the front and rear axles are represented by  $K_{bf}$  and  $K_{br}$  respectively.

**An example.** Consider a vehicle whose loading conditions on the front and rear axles are 32% and 68% respectively (when at rest). The ratio of the height of center of gravity from

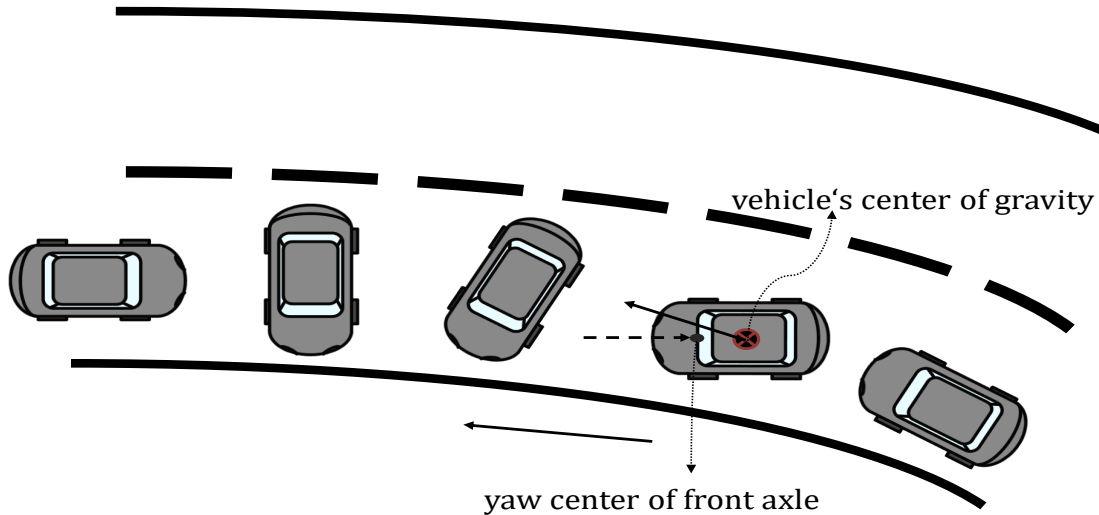


Figure 2.6.: Impact of rear wheels locking [48]

the ground to the wheel base  $\frac{l}{L}$  is 0.18. The ratio of the distance of center of gravity from the midpoint of rear axle to the wheel base denoted as  $\frac{l_2}{L}$  is 0.32. Similarly, with respect to the front axle,  $\frac{l_1}{L}$  is 0.68. Substituting these values in (2.3.8) and considering the coefficient of road adhesion  $\mu$  as 0.85 and the coefficient of rolling resistance as 0.015, the maximum deceleration magnitude would be achieved only when 47% of the generated brake force is distributed to the front axle and the remaining 53% to the rear axle [48]. Note that this brake-force distribution applies only to this particular loading condition. For other loading conditions, the optimum brake-force distribution has to be computed accordingly.

A vehicle's brake-force distribution to the axles is a difficult proportion to arrive at as both the loaded and unloaded conditions have to be considered. Once this distribution is fixed, based on the loading conditions, a vehicle may or may not achieve its maximum deceleration magnitude during braking. Further, the wheels may get locked due to the aforementioned factors [48].

The scenario of wheels locking is extremely dangerous as it leads to catastrophic events. The locking of rear wheels result in the loss of directional stability. This is because their capability to resist lateral motion is reduced to zero. Therefore, if side wind or road camber or centrifugal force initiate a slight lateral movement, a yawing moment about the yaw center of the front axle will be developed due to the inertial force. Then, the moment arm of the inertial force increases as the yaw motion progresses further resulting in an increase in yaw acceleration. Therefore, the rear end of the vehicle swings around  $90^\circ$ , moment arm gradually decreases, and this eventually leads to the vehicle rotating  $180^\circ$  with the rear end as shown in Fig. 2.6 [48]. This is particularly more dangerous on icy roads as the available friction is low and the rate at which a vehicle's kinetic energy dissipates is very slow [48].

Alternatively, if the front tires lock, a vehicle loses directional control and any steering inputs from the driver have no effect on the wheels. The vehicle then skids in the direction of the locked wheels. However, when the front tires lock, a driver can momentarily release the brakes partially or completely and this would help in regaining vehicle control as the brake force would be reduced or nullified. The same is not possible when the rear wheels lock and no amount of expertise can restabilize the vehicle [48].

As a result, incorporating these factors and scenarios, regulations in many European countries require the front wheels to lock up before the rear wheels [48]. Modern technologies like

antilock brake system (ABS) [66] [54] can detect and prevent locking of wheels and, thus, are integrated into brake systems.

Even under optimal distribution of the brake force to the axles, there exists a limit to the magnitude of maximum achievable deceleration. This is bounded by the coefficient of road adhesion  $\mu$  [16]. This is because the interaction between a vehicle and the road happens through the contact patch of the tires. As a result, the maximum achievable deceleration magnitude when normalized as  $g$  (acceleration due to gravity) will not exceed  $\mu$ . This implies that on dry asphalt surfaces where the coefficient of adhesion is 0.85, the maximum achievable magnitude is  $0.85g$ . However, for snowy surfaces, this value drastically reduces to a magnitude of  $0.2g$  [48].

In summary, loading conditions and the fixed brake-force distribution affect a vehicle's maximum achievable deceleration magnitude. Therefore, when designing emergency brake maneuvers, the heterogeneous deceleration capabilities of vehicles in the platoon have to be considered. In this direction, stopping distances of all vehicles from a common cruise velocity are required. There exists a standard expression that computes this and the same is presented in the next section.

### 2.3.3. Stopping distance

In this section, we introduce the standard expression for computing the stopping distance of a vehicle. The stopping distance  $S$  (provided the wheels do not lock) is a function of various parameters as [48]:

$$S = \frac{\gamma_m W}{2gC_A} \ln \left( 1 + \frac{C_A V_{init}^2}{\eta_b \mu W + f_r W \cos(\theta) \pm W \sin(\theta)} \right). \quad (2.3.9)$$

In (2.3.9),  $W$  is the vehicle's weight in Newtons ( $N$ ),  $g$  denotes the acceleration due to gravity in  $m/s^2$ ,  $C_A$  is the aerodynamic constant as shown in (2.3.10),  $V_{init}$  is the initial speed of the vehicle in  $m/s$ ,  $\eta_b$  is the braking efficiency as per (2.3.11),  $\mu$  is the coefficient of road adhesion,  $f_r$  is the coefficient of rolling resistance, and  $\theta$  is the road angle or inclination in degrees ( $W \sin(\theta)$  takes a positive sign in an uphill and a negative sign in a downhill). The moment of inertia of the rotating parts involved in braking is denoted as  $\gamma_m$  and termed *equivalent mass factor*. It has a value of 1.03 to 1.05 for passenger cars. This factor indicates that a brake system has to decelerate a mass slightly more than the vehicle's mass (due to rotating parts) [48]. In addition, we have [48]:

$$C_A = \frac{\rho}{2} C_D A_f, \quad (2.3.10)$$

and

$$\eta_b = \frac{(\frac{d}{g})}{\mu}, \quad (2.3.11)$$

where  $\rho$ ,  $C_D$ , and  $A_f$  are as per (2.2.1), and  $d$  is the achieved deceleration in  $m/s^2$  (cannot exceed a magnitude of  $0.85g$ ) [48].

Clearly, the stopping distance will be longer in case of heavy vehicles and lower deceleration magnitudes. Further, the achieved stopping distance by braking at maximum possible deceleration magnitude would yield different stopping distances on a complete uphill, flat, and downhill road profiles. This is because the effect of grade force in a downhill cannot be negated due to actuator saturation and, hence, the deceleration would be of lesser magnitude than that achieved on flat and uphill road profiles.

On the contrary, in an uphill, the deceleration magnitude would be greater than that achieved on flat and downhill road profiles. Hence, braking on complete uphill and downhill road profiles of maximum steepness yield the best and worst stopping distances of a vehicle

respectively. Therefore, when designing platoon brake maneuvers, the impact of these road profile changes on the achievable deceleration magnitudes have to be accounted for as well.

Note that a vehicle's stopping distance on a flat road computed using (2.3.9) would be shorter than that achieved in reality. This is because the time taken for brake activation is not included, i.e., after the brake pedal activation, there is some dead time before the brake pressure builds and reaches the actuators and this leads to the vehicle traveling a few meters (depending on its velocity) [48].

Additionally, this standard expression assumes instantaneous deceleration. In reality, after the dead time elapses and the brake pressure reaches the actuators, a controller regulates the brake force and gradually tracks a reference deceleration. Even though the vehicle is decelerating in this phase, the magnitude is not equal to the steady state value leading to a longer stopping distance. Therefore, due to these factors, we can conclude that the value computed by (2.3.9), for example, on a flat road ( $\theta = 0$ ) provides a stopping distance that a vehicle can never achieve in reality.

In our work, we consider braking on a flat road and instantaneous deceleration tracking as idealized conditions. Then, under these conditions in Chapter 4, we introduce our approaches for emergency braking. Later in Chapter 5, we consider realistic conditions of braking and derive an expression that computes a vehicle's stopping distance incorporating the above neglected factors.

Once emergency braking is initiated, all vehicles of a platoon are required to brake at their assigned decelerations. This deceleration can be vehicle-specific or common to all and is decided as per a chosen braking approach (introduced later). The brake-by-wire system present at each vehicle perform certain computations and apply the necessary brake force. In the next section, we outline these performed computations.

#### 2.3.4. Brake-by-wire systems

Conventional brake systems use hydraulics to transport the pressure generated by brake pedal to brake actuators. They are popular, but suitable only for manual driving. When operating in platoons, due to short inter-vehicle separations, control systems perform the necessary maneuvers. This implies that there is a need to command and control the brake actuators. Thus, brake-by-wire systems are needed rather than traditional brake systems. Apart from automation and control, the other advantage with these systems is the drastic reduction of dead time or transport delay of brake pressure.

There are two categories of brake-by-wire systems namely *electro-hydraulic brake* and *electro-mechanical brake* [89]. In the former, the hydraulic pressure is generated by a master cylinder and transported to brake actuators using hydraulic lines very similar to traditional brake systems. However, the cylinder is controlled through an electric motor. In the latter, hydraulics is completely eliminated and the entire system including the brake actuators are electrically controlled [89].

Irrespective of the category of brake-by-wire system used, the following computations are performed once emergency braking is initiated. These are necessary to determine the brake force needed to decelerate a vehicle at an assigned rate. Recall that apart from the force generated by a brake system, there are additional forces that aid braking. Therefore, all these forces have to be accounted for in the computations. In this direction, we begin by using Newton's second law of motion as below:

$$F_{total} = m \cdot d, \quad (2.3.12)$$

where  $F_{total}$  represents the resultant force in Newtons (N),  $m$  represents the mass in kilograms (kg), and  $d$  represents the desired deceleration in  $m/s^2$ . Substituting the above in equation (2.3.1) we get:

$$F_{total} = F_b + f_r W \cos(\theta) + R_a \pm W \sin(\theta) = m \cdot d. \quad (2.3.13)$$

The mass of a vehicle can be replaced as below:

$$F_{total} = F_b + f_r W \cos(\theta) + R_a \pm W \sin(\theta) = \frac{W}{g} d. \quad (2.3.14)$$

Thus, the resultant deceleration (normalized by  $g$ ) can be obtained as [48]:

$$\frac{F_b + f_r W \cos(\theta) + R_a \pm W \sin(\theta)}{W} = \frac{d}{g}. \quad (2.3.15)$$

Therefore, to achieve a required deceleration, a brake-by-wire system has to account for factors like road angle, aerodynamic force, grade resistance and, then, exert the required brake force  $F_b$ . Along with this, the weight and brake force distribution on/to the front and rear axles together with the magnitude of maximum possible brake force need to be known. Modern vehicles are already equipped with sensors that can measure the same [48] [76] [81]. Additionally, the variation in aerodynamic force can be kept minimal by maintaining the inter-vehicle separations (almost) constant.

Now that the computations performed by a brake-by-wire system are outlined, next, for the design of controller in these systems we need a model of the vehicle's braking dynamics. This can be obtained from the forces acting on a two-axle vehicle as shown in Fig. 2.4. Thus, our next section will focus on extracting this model.

### 2.3.5. A vehicle model in state-space representation

In this section, we model the braking dynamics of a vehicle using state-space representation. For this, we first consider all the forces acting on a two-axle vehicle as shown in Fig. 2.4. Then, we gradually refine and simplify our model so that it is suitable for brake-by-wire controller design.

The aerodynamic, rolling, and grade resistances aid the vehicle during braking. As shown in (2.3.1), the rolling and grade resistances are a function of vehicle weight  $W$ , and road angle  $\theta$ . A vehicle's weight remains constant and, hence, based only on the road grade, the combined magnitude of these two forces acting on a vehicle varies.

In particular, the variation in the magnitude of rolling resistance as a function of road angle  $\theta$  is extremely small. As mentioned before, we consider maximum road grade of  $8^\circ$ . That is,  $\cos(8^\circ)$  is 0.99 and, for flat roads with  $\theta=0$ ,  $\cos(0^\circ)$  is 1. Thus, during the whole brake maneuver, regardless of road profile changes a vehicle undergoes, the rolling resistance remains almost constant. It can be approximated as  $f_r W_i$ , where  $f_r$  is the coefficient of rolling resistance, the vehicle's weight is again denoted as  $W$  and the subscript  $i$  denotes the vehicle's position in a platoon of  $n$  vehicles ( $1 \leq i \leq n$ ).

On the contrary, the grade force  $W_i \sin(\theta)$  can either aid braking (in an uphill) or oppose it (in a downhill). However, in the case of flat roads,  $\theta=0$  and, hence,  $\sin(0^\circ)$  is 0. Thus, the magnitude of grade force is also zero. Therefore, depending on the road profile a vehicle is currently in, the grade force acting on it can either aid or oppose braking or be nonexistent. Hence, in our vehicle model, we consider the grade force as a disturbance.

Unlike the rolling and grade resistances, the aerodynamic resistance is dependent on the vehicle  $i$ 's drag coefficient and varies quadratically with its velocity as [48]:

$$R_{a_i} = C_{A_i} \cdot V_i^2, \quad (2.3.16)$$

where  $R_{a_i}$  represents the aerodynamic resistance in Newtons (N) acting on the vehicle  $i$ . Similarly, the vehicle  $i$ 's velocity in  $m/s$  is represented as  $V_i$ . The vehicle's aerodynamic constant  $C_{A_i}$  is given by [48]:

$$C_{A_i} = \frac{\rho}{2} C_{D_i} A_{f_i}, \quad (2.3.17)$$

where  $\rho$ ,  $C_{D_i}$ , and  $A_{f_i}$  are as per (2.2.1).

We intend to use linear control theory for the design of our brake-by-wire controllers. To this end, we neglect the aerodynamic force as per (2.3.16), i.e., we disregard the only nonlinear component in our model. This results in the computation of a longer stopping distance with some degree of pessimism, however, we guarantee safety by the proposed analysis.

Considering all these factors, we model only the force generated by a brake system and the grade force (as disturbance).<sup>1</sup> The input brake force exhibits a linear behavior, i.e., increasing the brake force increases the magnitude of deceleration (until a maximum limit is reached at saturation). Further, the achieved deceleration is independent of time. Thus, our model constitutes a linear time invariant (LTI) system, for which we derive the following state-space representation:<sup>2</sup>

$$\dot{x}_i = 0 \cdot x_i + \frac{1}{\gamma_m \cdot m_i} \cdot u_i + z_i, \quad (2.3.18)$$

and

$$y_i = 1 \cdot x_i, \quad (2.3.19)$$

where the only state is the vehicle  $i$ 's velocity in  $m/s$  represented as  $x_i$ . Similarly, its deceleration in  $m/s^2$  is denoted as  $\dot{x}_i$ , and its mass in kilograms ( $kg$ ) is  $m_i$ . The controlled input  $u_i$  is the brake force in Newtons ( $N$ ), and the disturbance (grade force) acting on the vehicle also in  $N$  is  $z_i$ .

Note that (2.3.18) states Newton's second law, i.e., the deceleration is equal to the (input) brake force  $u_i$  divided by the mass times the equivalent mass factor  $\gamma_m$ . Since the disturbance  $z_i$  (i.e., grade force in our case) affects the resultant deceleration, it is also present in the equation.

Clearly, a brake-by-wire controller requires a vehicle's resultant deceleration for reference tracking instead of its velocity. The rate of change of velocity is acceleration/deceleration. Therefore, by differentiating the output velocity from our state-space model, we can obtain the vehicle's deceleration. In reality, it is the contrary, i.e., vehicles are equipped with accelerometers which directly measure a vehicle's acceleration/deceleration and, then, using standard algorithms, the velocity would be estimated [26].

Note that a brake-by-wire controller cannot track an assigned deceleration instantaneously. Therefore, we use this extracted vehicle model, and later in Chapter 5 we introduce performance specifications of brake-by-wire controllers, and derive an expression of vehicle stopping distance on a flat road under controller action. By considering the controller related effects, we address one of the realistic conditions of braking, i.e., non-instantaneous reference deceleration tracking.

Finally, in order to guarantee a collision-free emergency braking, apart from decelerating at an assigned rate, all vehicles of a platoon are also required to periodically exchange critical information. This can be achieved through V2V communication. To facilitate this, there is an ongoing standardization at both regional and international levels. The details are introduced in the next section.

---

<sup>1</sup>The rolling resistance could also have been modeled as a state. However, neither does it have any dynamics, nor does it depend on the input brake force. Further, from Newton's second law of motion, its contribution to overall braking, is always  $f_r W_i / (W_i / g) = 0.147 m/s^2$  (assuming  $f_r = 0.015$  and  $g = 9.8 m/s^2$ ). This is extremely small and, hence, neglected.

<sup>2</sup>The standard state-space representation of an LTI system is of the form  $\dot{x}_i = Ax_i + Bu_i + z_i$  and  $y_i = Cx_i + Du_i$ , where  $A$ ,  $B$ ,  $C$ , and  $D$  are the system, input, output, and feedforward matrices respectively. The input vector is denoted as  $u_i$ ,  $x_i$  is the state vector,  $y_i$  is the output vector, and  $z_i$  is the disturbance vector. However, note that we have one-element vectors  $x_i$ ,  $u_i$ , and  $z_i$ . As a result, matrices  $A$ ,  $B$ ,  $C$ , and  $D$  become scalars. Further, to be consistent with the standard representation, we explicitly make the output  $y_i$  equal to our only state  $x_i$ .

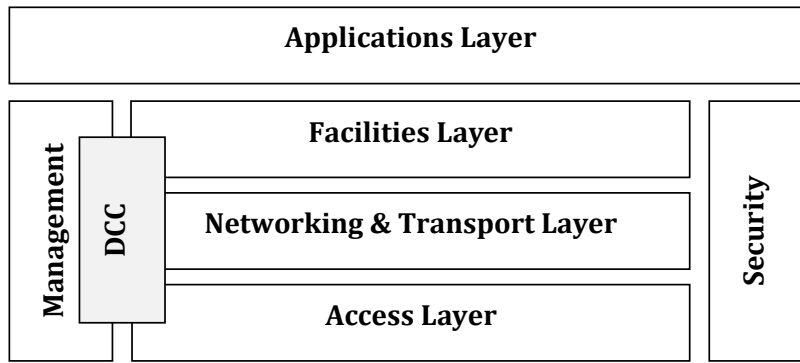


Figure 2.7.: ITS reference model [29]

## 2.4. Vehicle-to-vehicle communication (V2V)

Modern vehicles are equipped with sensors like radar, lidar, camera, and so on. However, they have limitations with respect to the area that they can scan. For example, a radar can scan the area in front of a vehicle and determine the velocity and current distance of only the vehicle(s) in front. This obtained information is not shared with other neighboring/following vehicles. If there are actions of undetected traffic that affects the vehicle, for example, an abrupt brake maneuver, its detection would be very late and may lead to vehicular collisions, thus impacting traffic safety.

On the contrary, if the actions of undetected traffic are communicated through wireless messages, the appropriate warnings can be displayed to the driver through ADAS leading to appropriate actions being performed well in advance. Thus, traffic safety can be ensured.

In this regard, through information and communication technologies, systems are developed to enable transportation of goods and humans by efficient and safe use of transport infrastructure and means like cars, planes, ships, trains, and so on. These systems are collectively termed intelligent transport systems (ITS) [33]. They are based on V2V and V2I communication comprising of *vehicle domain* and *infrastructure domain* [45].

The vehicle domain comprises hardware and software present in each vehicle where the ITS applications would be deployed. The architecture is based on international organization for standardization's (ISO) open system interconnection (OSI) reference model and is shown in Fig. 2.7 [29] [45]. The OSI layers — Datalink and Physical are grouped into *Access layer*. Similarly, Transport and Network layers are grouped into *Networking and Transport*, whereas Presentation and Session layers in the OSI model are grouped into *Facilities layer*. The *Applications* layer constitutes applications related to road safety and traffic efficiency. They can communicate with other ITS applications with the support of the other layers. A dedicated short-range communication technology based on IEEE 802.11p is used. Apart from these layers, management and security related services, along with decentralized congestion control (DCC) methods for balancing the network load are also included in the reference architecture [33]. Therefore, a vehicle equipped with this reference architecture is collectively termed *ITS vehicle station (IVS)* [45] [35].

On the other hand, the infrastructure domain comprises mainly of RSUs. They can communicate with an IVS by broadcasting critical information. Additionally, their aim is to provide connectivity from vehicles to back-end services. Typically, the information broadcast by RSUs would be managed by *ITS central stations (ICS)* [45].

ITS are standardized at both regional and international levels. For instance, in the USA it is performed by IEEE 1609 [2], whereas in Europe, it is done by ETSI [3]. As part of V2V and V2I communication (combined together as V2X), particularly for the exchange of messages



V2X Network Header		V2X Message Payload	
Network Layer Data		Facility Layer Data	
		Generic Information	Concrete Message Information
Sender's ID, position, speed, direction, timestamp etc.	Addressing details for distribution and forwarding algorithms	CauseCode, ActionId, cancellationFlag, generationTime, validityDuration	<ul style="list-style-type: none"> <li>• Cooperative Awareness Message (CAM)</li> <li>• Decentralized Environmental Notification Message (DENM)</li> </ul>

Figure 2.8.: General V2X message format [45]. Apart from V2X payload, every message also includes information for network and facility layer. For example, Sender's ID, speed, position, direction, timestamp and so on are part of the Network layer along with addressing details for forwarding of messages. Messages can be associated to respective applications through CauseCode, whereas different subsequent messages of the same event are referenced through ActionId [45].

related to traffic safety and efficiency, and service announcements, ETSI has specified four types of messages namely [45]:

- **Cooperative awareness message (CAM):** These are periodically sent by all vehicles, RSUs, and even by infrastructure equipments like road signs, traffic lights, barriers, and so on. These messages support several ITS applications. They comprise status and attribute information of the ITS station. For example, a vehicle includes the time, its position, motion state, dimensions, its type, and so on. The receiving ITS station is then aware of the presence of the transmitting ITS station. Based on the position, if a vehicle is too close, the receiving ITS station displays a warning to the driver to initiate appropriate actions [36].
- **Decentralized environmental notification message (DENM):** These are event triggered messages and would alert road users of a detected event. For example, road hazard or certain traffic condition's type and location are communicated through these messages. They are shared to all affected vehicles that are located in a geographical location. The receiving IVSs process and display appropriate messages to the driver. The DENM can be repeated and persists until the event is present [37].
- **Signal phase and timing message (SPAT):** These messages are broadcast by RSUs to indicate the remaining time of green light phase at a road intersection so that traffic flow is optimized [45].
- **Service announcement message (SAM):** RSUs can advertise the services they offer through broadcasting this type of message [45].

The general format of these messages is illustrated in Fig. 2.8 [45]. Apart from SAM, all the other messages are sent on the allocated three channels in Europe — IEEE channel 176, 178, and 180 — as shown in Fig. 2.9 [29]. These are reserved exclusively for safety related messages. The differences between USA and Europe standardizations with respect to the allocation of channels can also be noted.

IEEE Channel	172	174	176	178	180	182	184
U.S. allocation	Critical Safety of Life	Service Channel (SCH)	SCH	Control Channel (CCH)	SCH	SCH	Hi-Power Public Safety
European allocation	SCH	SCH	SCH	SCH	CCH	SCH	SCH
Center frequency	5.860	5.870	5.880	5.890	5.900	5.910	5.920

Figure 2.9.: Channel allocations in US and Europe [29]. In Europe, channel numbers 176, 178, and 180 are reserved for messages (apart from SAM). Particularly, CAMs and DENMs are sent over channel number 180.

Over the allocated control channel (CCH) in Europe, the two prominent message categories sent are the periodic status update CAM and the event triggered DENM. These play a critical part in the operation of platoons as well. Particularly, CAMs can be used for vehicle control, both during the cruise and brake scenarios, whereas DENMs can be used to initiate brake maneuvers [13] [14].

The medium access control (MAC) algorithm deployed in IEEE 802.11p is termed *enhanced distributed coordination access* (EDCA). As per this, every node in the ITS first checks if the channel is free during a short time period — *arbitration interframe space* (AIFS) (there are different values of AIFS for different priority of messages as shown in Table 2.1). If the channel is free, then the node transmits. Otherwise, it chooses a random back-off integer value from the contention window (CW) range  $[0, CW_{min}]$  for that message priority. Then, only when the channel is sensed free during certain time periods referred to as *slot time* ( $13\mu s$  for a  $10MHz$  channel), this value is decremented. Once the value reaches zero, the node transmits without any further delay. If there are other transmissions simultaneously, packet losses and distortions happen. As no acknowledgments are present, the transmitting node is unaware about the same [38]. For these reasons, ETSI recommends a channel utilization of only 25% or less [34].

The recommended update frequency of CAM and DENM along with the random nature of the 802.11p MAC protocol does not provide the necessary delay bounds for time-critical traffic, for example, inter-vehicle communication in platoons [49] [71] [13]. Hence, one way to shorten the delay is to reduce the update frequency of CAMs as part of the DCC algorithm [34], but this affects a platoon’s safety. Therefore, works done in [12] [80] [58] [50] and [14] have proposed protocols that either use the available bandwidth at the control channel, or use the other available channels (apart from CCH). Hence, in the former approaches, the protocol has to work on top of IEEE 802.11p, whereas in the latter, a separate transceiver

Table 2.1.: Access category (AC) priorities [38]

AC Priority	$CW_{min}$	$CW_{max}$	AIFS ( $\mu s$ )
1	3	7	58
2	7	15	71
3	15	1023	110
4	15	1023	149

is required to listen to other channels. However, this extra cost is justified by the resulting fuel/energy savings from platooning [14].

With respect to the update frequency of messages, truck manufacturers propose a faster update frequency of  $50\text{Hz}$  for CAMs [10], i.e., one CAM every  $20\text{ms}$ , as opposed to the standard's recommendation of  $10\text{Hz}$  ( $100\text{ms}$ ) [36]. Hence, in this work, we follow the truck manufacturers recommendation for both CAMs and DENMs and deviate from the standard. We also assume that a suitable protocol exists that provides the necessary communication delay bounds, especially, for platoons operating at speeds of around  $100\text{km/h}$  and at separations below  $5\text{m}$ . Our intra-platoon communication strategy with these modifications is introduced in detail in Chapter 4.

Thus, V2V communication constitutes the backbone of platoon operation. It is also required in making any new vehicle to join an existing platoon, as well as an existing vehicle to leave a platoon. As mentioned before, vehicles operating in a platoon should know their maximum achievable deceleration magnitude and, hence, the resulting stopping distance. Therefore, any new vehicle joining has to communicate this information to a platoon leader. Then, the platoon lead, based on braking capacities and stopping distances of existing and new vehicles, computes decelerations to be achieved by all vehicles (as per a braking approach) during emergency situations. Then, the same is communicated to all vehicles. Further, once the new vehicle is induced into the platoon, it has to broadcast critical information periodically both during cruise and brake scenarios.<sup>3</sup>

## 2.5. Summary

From the principles and fundamentals introduced in this chapter, we can conclude that cooperative driving or platoons are interesting because they result in fuel/energy savings. More the number of vehicles and shorter the separations, the greater the achieved savings. These savings are optimum when the platoon lead also experiences benefits. This can only happen when the inter-vehicle separations are in the range of 1 to  $4\text{m}$ . Hence, for operating at such distances, the constant spacing policy is preferred over the constant time headway policy.

However, operating at separations below  $5\text{m}$  makes emergency brake maneuvers extremely dangerous. This is mainly due to different vehicle types and their heterogeneous loading conditions resulting in nonhomogeneous maximum achievable deceleration magnitudes. Therefore, this nonhomogeneity should be considered when braking a platoon to complete standstill in the shortest possible distance. Further, the variations in road profiles during braking have to be accounted for as well. If neglected, certain vehicles cannot track their assigned reference decelerations, for example, due to braking in or after entering a steep downhill, potentially leading to vehicular collisions. Thus, to ensure a safe and collision-free emergency braking, coordination among vehicles is required. This can be accomplished through the exchange of wireless messages based on IEEE 802.11p.

---

<sup>3</sup>An example algorithm for inducing a new vehicle into a platoon can be found in the appendix.



# Chapter 3.

## Related work

In this chapter, we review the research done so far with respect to platooning. First, we begin with existing platooning projects and, then, we look at works addressing platoon coordination and formation. Next, works related to the cruise scenario, i.e., longitudinal and lateral control of vehicles, are discussed. Finally, we consider the brake scenario and review existing works. We conclude by identifying a gap in research and explain how our work bridges the same.

### 3.1. Overview of platooning systems

There are many variations of platooning based on goals, implementation, types of vehicles participating, infrastructural requirements, level of automation of longitudinal and lateral control, and so on. Based on these parameters the following platooning projects exist [23]:

**PATH:** The University of California along with the United States Department of Transportation worked in a joint-venture project named PATH [56] [57]. The initial goal of PATH was to increase the capacity of highways and, thereby, decrease traffic congestion, fuel consumption, pollution, and accidents. The study showed that the capacity of passenger-car lanes on highways can be safely increased by a factor of two to three, if vehicles operate in platoons of up to 10 vehicles [23] [56] [57].

PATH demonstrated a platoon operation of 8 vehicles as early as 1997. The longitudinal control was accomplished through radar, while the lateral control through magnetometer sensors. Magnetic markers embedded in the center of the lane at every  $1.2m$  of the test track assisted the vehicles in keeping the lane. To facilitate coordination among vehicles, a radio communication system was used [64]. Later in 1999, suitable changes were made to these vehicles in order to measure their fuel consumption during platooning [56] [57].

Experiments were performed with platoons of 2-, 3-, and 4-vehicles. For these configurations, fuel savings were logged at different inter-vehicle separations of 3-, 4-, 5-, and 6-meters. It was found that the average fuel savings increases with an increase in the number of vehicles and more savings are achieved at shorter separations. Overall, based on various factors, an individual vehicle's fuel savings were observed to be in the 0 – 10% range [56] [57].

More recently, the focus in PATH has shifted to platoons of heavy-duty trucks like tractor-trailer combinations. Similar to passenger-car platoons, the inter-vehicle separations considered are 3- and 4-meters [23].

**CHAUFFEUR I & II:** While PATH initially concentrated on passenger vehicles, the European Project CHAUFFEUR I [43] considered two heavy-duty trucks for automated vehicle following. This application termed *electronic tow bar* involved a manually driven lead truck. The following truck's control was automated by obtaining critical information from the lead vehicle through a bidirectional V2V communication system over a  $2.4GHz$  microwave channel [43].

In addition to the wireless communication, particularly, for the following vehicle's longitudinal control, its relative position was obtained through an image processing system. A

special pattern of infrared lights at the back of the lead vehicle aids this system to determine the current distance [43].

With respect to lateral control, unlike PATH, no changes to the road infrastructure were performed. The tests were carried out at inter-vehicle separation of  $6m$  [43]. As part of CHAUFFEUR II [20], the aim was to extend the electronic tow bar application to follow any truck. Also, a demonstration of a three-truck platoon was performed. Suitable changes to vehicle control architectures from CHAUFFEUR I were performed. In particular, the operating frequency for V2V communication was shifted from the initial  $2.4GHz$  to  $5.8GHz$  [20].

**SARTRE:** It is a more recent FP7 project, whose aim is to develop solutions that enable vehicles to join and drive in platoons on public motorways without making changes to the existing road infrastructure. In SARTRE, the lead vehicle is a manually driven truck, whereas the following vehicles can either be trucks or passenger cars. These vehicles are automatically maneuvered by longitudinal and lateral control systems [23].

To enable coordination among vehicles and, thereby, implement platoons in a safe manner, V2V communication along with local sensors in each vehicle are used. The V2V communication is based on ITS-G5. The lead vehicle's local signals like speed, acceleration/deceleration, etc., sampled through its sensors are shared among the following vehicles, which are then used as inputs to the control algorithms. Therefore, the control of the following vehicles' is done by their respective local systems, sensors, and actuators based on information from the lead vehicle [23].

The main goal of control systems in the following vehicles is to ensure that the preset distance to the immediate lead vehicle is maintained such that no external vehicles can interfere with the platoon. Further, the path and trajectory of the lead vehicle are also tracked. In case of emergency scenarios like evasive braking or loss of wireless communication, these systems can take over vehicle control completely and maneuver them independently [23].

SARTRE demonstrated the operation of a 5-vehicle platoon on public roads near Barcelona, Spain in May 2012 [23]. A prototype of the V2V communication system demonstrated that the rear placement of antenna enables a better reach of the lead vehicle's information to all following vehicles, especially, for distances over  $70m$  [22].

**Grand cooperative driving challenge (GCDC):** The rise of cost-effective and reliable communication systems have driven the development of cooperative driving systems. As part of 2011 GCDC competition, multi-vendor vehicles of both passenger and heavy-duty truck types participated in cooperative driving. Both urban and highway scenarios were dealt in this competition. Using information about surrounding environment, each vehicle performs its longitudinal control such that the distance to its immediate lead vehicle is maintained [23].

Based on V2V and V2I communication along with sensor fusion technologies and control, GCDC's main goal was to fast track the development and demonstration of platooning or cooperative driving systems. The participating teams used different sensor technologies and the inter-vehicle communication was based on IEEE 802.11p and communication access of land mobiles (ISO CALM) fast protocol [23]. The latter is concerned with IPv6 networking between ITS stations communicating over the global internet [7].

**SCANIA-platooning:** Even heavy-duty vehicle manufacturers like SCANIA have shown interest in platooning. Their main intention is to reduce fuel consumption and, hence, fleet management costs. One of their projects termed *Distributed Control of a Heavy Duty Vehicle Platoon*, partly funded by the Swedish government is in collaboration with KTH Sweden. Its other project termed *iQFleet* also funded by the Swedish government is a collaboration between VTI (Swedish National Road and Transport Research Institute), Trafikverket (The Swedish Transport Administration) and KTH Sweden [23].

While the former project aims at efficient control of a single truck with emphasis on safety, in the latter, platooning is one of the topics researched. As a result, the focus is primarily on platoon control with respect to road infrastructure, topology, and other road users. The emphasis is particularly on the development of strategies and architectures to support and route platoons in an optimal way [23].

Road tests were performed by transporting goods between two manufacturing plants in different Swedish cities. During the first phase, professional truck drivers used ACC for platooning. Since the measurements were radar based, time headway of 2 to 3s were used. In the second phase, V2V communication was used to enable shorter separations. These separations would be further reduced in the later phases until truck drivers are comfortable with the distances [23].

**KONVOI:** The inter-vehicle distances maintained during truck platooning have to be comfortable for the drivers and this indeed is one of the most significant factors in acceptance of platooning systems. One project that addresses such criteria is the German national project KONVOI started in 2005. Apart from driver acceptance, this project also studies the economic and legal implementation of platoons along with its impact on traffic flow and environment. In 2009, the project demonstrated the safe operation of four heavy trucks in real traffic with inter-vehicle separations of 10m. Apart from V2V and V2I communication, sensors like mono-camera, radar, and lidar were employed in the trucks. The lead truck was manually driven by a professional driver with support from ACC and lane departure warning (LDW) systems [4].

**Energy ITS:** Apart from research in the European and North-American continents, a significant project in the Asian continent is Energy ITS started in 2008 by the Japanese ministry of economy, trade and industry. Its aims are fuel/energy savings and prevention of global warming through the use of ITS technologies. The project also aims at mitigating the lack of skilled drivers. With respect to tests conducted, three automated trucks operated at speeds of around 80km/h with inter-vehicle distances of 10m. The reduction in energy consumption was observed to be about 15%. Lateral control was achieved by lane marker detection through computer vision, whereas longitudinal control was accomplished through V2V communication in conjunction with radar and lidar [23].

## 3.2. Vehicle coordination for platoon formation

Even though vehicles of both passenger and heavy-duty types are considered for platooning, more research has been done in the context of heavy-duty vehicles [86] [9] [51] [18] [59] [39] [65]. The reason for this is the significant fuel/energy savings and the associated cost benefits for truck operators. Therefore, there is a need to coordinate the movement of trucks such that they form platoons when traveling along their planned route to destination. In this section, we review works that address coordination of trucks for platoon formation.

The problem of truck coordination is mainly characterized by the absence of a central database to locate heavy-duty vehicles' current position and their final destination. Additionally, a global coordinator for recommending routes for platooning opportunities is also missing. Even if such a system with all the information is available, the fuel-optimal routing problem becomes NP-hard in nature even for small road networks [46].

Hence, a distributed platoon coordination framework was proposed in [46]. Virtual controllers placed at major road intersections are part of this distributed network. These controllers adjust slightly the speeds of approaching heavy-duty vehicles and, thus, help in coordinating platoon formation. It is important to note that only when the resulting fuel/energy

savings from platooning are greater than the cost of adjusting speeds, these controllers propose a velocity adjustment to the approaching heavy-duty trucks [46].

Apart from this distributed network, a system that centrally coordinates the formation of truck platoons was proposed in [79]. Through V2I communication, trucks connect to this system and, in turn, the system helps to dynamically form platoons by computing/providing routes and speed profiles. For this computation, constraints like speed limits, destination, arrival deadline, and driver rest periods are considered [79].

Even though works based on distributed and central architectures have been proposed, as of now, a commercial platooning system is still absent [52]. This leads to a very low number of trucks participating in spontaneous platooning. The truck drivers usually rely on in-vehicle systems like ACC or drive manually behind each other. The inter-vehicle distances in such cases are usually large and, hence, the achieved fuel/energy savings are also less. This in fact, was shown by the work done in [52] where a digital road network and vehicle probe data were analyzed. To increase truck coordination possibilities, [52] proposes three schemes namely *catch up*, *departure*, and *transport* [52].

In the catch up mechanism, the follower vehicle drives faster, usually around  $15\text{km/h}$  and catches up with a lead vehicle and continues before splitting up at its destination. In the departure mechanism, a truck's departure time is adjusted such that a platoon can be formed. Finally, in the transport mechanism, roads segments were considered over a time period, and platooning possibilities through possible transport rescheduling were analyzed [52].

In comparison to spontaneous platooning, coordination of truck movement yields more fuel/energy savings. This was shown in [78]. Hence, the problem of coordination of a large number of trucks was studied. Based on a first-order fuel model, pairwise fuel-optimal plans are initially derived for two vehicles. Then, these pairwise plans for all trucks are input to a clustering algorithm that determines the coordination leaders for different clusters [78].

More recently, the EU project COMPANION [72] aims at a system development for the creation, coordination, and operation of platoons. Further, the end user acceptance, legal, as well as standardization issues are also addressed. The inputs into this system are logistics data, and environmental factors like traffic data and weather information. The truck drivers would be assisted in joining and leaving a platoon through on-board and off-board systems [72].

In this work, our emphasis is on the design of emergency brake maneuvers. Hence, we consider that vehicles have already coordinated their movement and are operating in platoons.

### 3.3. The platoon cruise scenario

Once a platoon is formed, there are two critical scenarios to be considered during operation namely cruise and brake. In this section, we review works that address the cruise scenario, where each vehicle has to maintain a preset distance (as per a spacing policy) and an appropriate alignment to its immediate lead vehicle and travel at a constant velocity. The longitudinal and lateral control systems present at each vehicle are responsible for meeting these objectives.

Any vehicle can easily maintain the necessary distance to its immediate lead, if the lead vehicle is operating at a constant velocity. However, if the immediate or platoon lead is accelerating or decelerating, there would be variations in the inter-vehicle separations. An important property that describes the propagation of these separation errors along the platoon is termed *string stability* [67] [68].

According to this, inter-vehicle separation errors between any two vehicles should not amplify as they propagate along the upstream of vehicles [67] [68]. For example, if there are variations in inter-vehicle separation of 3<sup>rd</sup> and 4<sup>th</sup> vehicle, it should not amplify into



large inter-vehicle separation errors between 6<sup>th</sup> and 7<sup>th</sup> vehicle, and further until the end of platoon.

Failing to achieve string stability will result in large inter-vehicle separations and, thus, inter-vehicle collisions [63]. Therefore, controllers have to suppress the magnitude of separation errors as they propagate. In this direction, they can either rely on in-vehicle sensors like radar or utilize V2V communication to obtain the necessary information [63].

As mentioned before, if only in-vehicle sensors are used, string stability can be guaranteed only through the constant time headway policy [67]. On the other hand, if V2V communication is used, both constant spacing and constant time headway policies can achieve string stability [63].

The central focus of all works related to the cruise scenario is to achieve string stability. In this regard, classical control design techniques from the literature have been proposed [86], [9], and [51]. Apart from standard techniques, formal methods and *symbolic models* [15] are also used. A decentralized symbolic control with application to heavy-duty vehicle platooning was proposed in [15]. The individual vehicle dynamics can be abstractly described using symbolic models. Each symbol in a symbolic model denotes an aggregation of continuous states. This formal design technique is helpful in addressing system specifications provided through temporal logic or automata, which are hard to implement using classical control design techniques [15].

Regardless of the control design technique chosen, the contents of information exchanged through wireless communication plays a significant role in achieving string stability. In this direction, the work done in [44] studies the stability and robustness of platoons with large number of vehicles to external disturbances. Specifically, two decentralized control architectures, namely, *predecessor following* and *symmetric bidirectional*, were compared. Further, both classes of linear and nonlinear vehicle controllers were considered [44].

In predecessor following architectures, every vehicle's control action would be dependent only on the information from its immediate lead vehicle, whereas in symmetric bidirectional architectures, it depends on the information from both its immediate lead and trail vehicles. The information from both vehicles are weighed equally. The design guidelines from this study state that symmetric bidirectional architectures have a much better robustness to external velocity disturbances in comparison to predecessor following architectures. However, if there are cost constraints due to the need of additional sensors to process information from both front and rear vehicles, the study recommends predecessor following architectures. Further, with these architectures, it is better to choose nonlinear control design techniques over linear ones for vehicle maneuvers [44].

Once a controller is developed, string stability can be achieved with the help of critical information exchanged over the control channel in the 5.9GHz band. Since non-platooning applications also use the same allocated control channel, there is no guarantee that the periodically exchanged critical information would reach all vehicles successfully. Packet losses and distortions therefore impact safe cruise operation. Hence, control design should also incorporate such limitations.

Specifically, to address congestion and reduce the network load, work done in [75] proposes a nonlinear event-triggered controller. As per this, every vehicle's controller decides when to transmit its state information based on a trigger rule as opposed to time-triggered communication. Thus, this controller fares better in comparison to its time-triggered counterpart, which transmits periodically irrespective of a change in the vehicle's state [75].

Even in cases of lightly loaded networks and successful transmissions, vehicles towards the end of the platoon might be outside the reach of the lead vehicle. Hence, packet re-transmissions need to be performed by intermediate vehicles. This implies latencies and communication delays and, thus, impacts string stability. These effects were studied in [88]. The mentioned work found that a platoon is string stable only when all its individual ve-

hicle controllers perform their actions simultaneously. This implies that all vehicles should experience the same delay in both the immediate and platoon lead vehicles' information. Particularly, the delay with respect to the immediate lead must be small [88].

Apart from longitudinal control, string stability is also considered from the perspective of lateral control. If this is not ensured, the vehicle may enter adjacent lane or drive off the roadway [77]. This may lead to accidents or severe injuries to passengers, and other road users. Few works address this aspect because the turns on highways are not as significant as in urban scenarios. This leads to steering inputs of lesser magnitude. The works done in [77] and [39] with respect to lateral string stability are the most prominent.

Lateral string stability was achieved in [77] using only onboard sensors like camera or radar, and relying on V2V communication to obtain the needed information from the vehicle in front. The lateral control of a single heavy-duty vehicle was performed in [39] using the approach of model predictive control (MPC). Preview information like curvature of the road was used for vehicle maneuvers [77].

Recall that the core objectives of platoon cruise scenario — velocity and distance control, and string stability — closely match that of advanced driver assistance systems like ACC. Therefore, to accomplish these objectives it is not always necessary that completely new architectures be developed. Hence, there are also works that rely on extending ACC with V2V communication so that it is feasible for platoon cruise operation. The advantages of doing the same were shown in [21] and [70]. These systems are termed cooperative ACC (CACC).

Since the only architectural changes are addition of wireless communication, there are works that have already implemented and tested the same. The notable ones are [41], [47], and [84]. An important result from these works is that the time headway value can be reduced to below 1s, resulting in increased vehicle throughput, and more fuel/energy savings in comparison to using only ACC [41] [47] [84].

Even though all existing works in the cruise scenario focus on ensuring string stability, it is important to note that this property has no relevance during braking. In other words, ensuring string stability does not guarantee safe and collision-free brake maneuvers [8] [9]. Especially during emergency, the velocity of vehicles are drastically reduced and, additionally, the maximum possible brake forces are applied by all vehicle controllers in order to minimize the stopping distance of the platoon. This implies controllers incur saturation as there is a limit to the brake force that can be generated and the corresponding deceleration that can be achieved. Further, heterogeneous deceleration capabilities of vehicles have to be considered. Therefore, there is a need to address and design emergency brake maneuvers separately, independent of the cruise scenario.

Since string stability has no relevance during braking, we do not consider the same in this work. Our only assumption with respect to the cruise scenario is that all vehicles are cruising at a common velocity before emergency braking is initiated.

### 3.4. The platoon brake scenario

In this section, we review works that address the platoon brake scenario. In comparison to cruise, they are less in number. Towards the end of this section, we identify a gap in existing research and explain how our work bridges the same.

The work on platoon brake scenario began as early as 2001, where the benefits of vehicle coordination were studied in [87]. The aim was to reduce the probability of inter-vehicular collisions, their expected number, and the relative velocities at impact. Constant spacing policy was used and the inter-vehicle separations were in the range of 1 to 4m. The study concluded that, through coordination among vehicles, the above mentioned parameters' values can be significantly reduced in comparison to the uncoordinated case [87].

Another work that supports the need for coordination among vehicles during braking is [25]. The safety of platoons was evaluated with a stochastic model. The computation of average number of collisions that occur in a platoon along with the probability of different methods of collision occurrence were computed by the model. The study proposes a fast dissemination of warning messages through the use of V2V communication, especially, during emergency. Further, even if warning messages reach all the concerned vehicles, the variation in drivers' reaction time may still cause vehicular collisions. Thus, the study concludes that cooperative/chain collision avoidance (CCA) techniques can eliminate the same and the braking of all vehicles has to be initiated simultaneously [25].

Coordination among vehicles can be achieved through cooperative autonomous control (CAC). The work done in [90] proposes a braking control protocol based on CAC. As per this, information from neighboring vehicles obtained through V2V communication is utilized and all vehicles decelerate to a target stopping position without collisions [90].

The work done in [74] demonstrated that coordination achieved through synchronized braking can avoid rear-end collisions even when short inter-vehicle separations of  $8m$  are used in a platoon. As per [74], once a hazard is detected, the lead vehicle does not brake immediately, rather it repeatedly broadcasts DENMs and after a preset waiting time, it brakes together with all the following vehicles at a high deceleration rate<sup>1</sup> of  $12m/s^2$ . Considering interference from network traffic generated by non-platooning vehicles the study recommends a minimum waiting time of  $100ms$  after a hazard is detected so that the DENMs reach all the vehicles [74].

Since the platoon lead is not decelerating during the waiting time, the stopping distance is longer. To minimize this, as per [73], the platoon lead broadcasts a DENM and decelerates at a low magnitude of  $2m/s^2$ . All the following vehicles with the exception of the trail decelerate at the same magnitude upon receiving the DENM. However, the trail decelerates at a higher rate of  $8m/s^2$  upon DENM reception and broadcasts its acknowledgment. Upon receiving this acknowledgment, its immediately leading vehicle switches from the deceleration of  $2m/s^2$  to  $8m/s^2$  and in turn broadcasts its acknowledgment and so on. Thus, this process continues and all vehicles towards the lead sequentially switch from the lower to higher deceleration magnitude upon reception of acknowledgment from their respective immediately following vehicles [73].

Apart from vehicle coordination, the inter-vehicle distances during platooning also impact the safety of brake maneuvers. Hence, optimal control and game theory were used in [18] to determine the minimum possible safe separation in a heavy-duty vehicle platoon. This separation is a function of several factors like vehicles' relative velocities, their braking capabilities, and their positions in a platoon. A two-truck platoon was simulated to be operating both in cruise and brake scenarios. Additionally, both homogeneous and heterogeneous vehicle masses were considered. The study showed that when operating at cruise speeds of around  $25m/s$  ( $90km/h$ ), an inter-vehicle separation greater than or equal to  $2m$  is safe. Further, if such short separations are used, it is preferred to have the better braking vehicle as the trail [18].

Similar to cruise scenario, V2V communication is also critical during brake maneuvers. The brake actions of a platoon lead are broadcast and, hence, the associated communication delay may affect safety. Thus, there exists a limit on the maximum possible delay. The same was studied in [19]. As per this study, the maximum tolerable communication delay between two similarly braking vehicles is given by their inter-vehicle separation divided by their velocity (before braking) [19].

---

<sup>1</sup>Recall that the maximum achievable deceleration is limited by the coefficient of road adhesion. On dry asphalt surfaces this is around  $0.85g$  ( $8.33m/s^2$ ) [48]. As a result, decelerations greater than this magnitude are not achievable in practice.

Another work that considers communication latency is [55]. Additionally, this work also considers the dependence of platoon safety on the contents of wireless message, their structure, and reliability. For safe platoon braking, the study outlines the necessity of including brake command from the lead in the wireless message, rather than just relying on speed and distance information from radar and information from neighboring vehicles [55].

An important factor that affects communication delay is wireless network performance. The platoon control from the perspective of control and network performance together was considered in [40]. The worst-case upper bounds on inter-vehicle distances subject to network performance metrics like packet losses were derived. The results recommend short inter-vehicle spacings of less than  $3m$  for 8-vehicle platoon, if the network is reliable. However, in case of a non-reliable network, either a limit has to be imposed on the number of vehicles or the maximum jerk, i.e., rate of change of deceleration, of vehicles has to be restricted to  $4m/s^2$  [40].

Finally, even the impact of control system failures and the effects of drivers' reaction times on manual braking were studied in [65]. A two-truck platoon was considered and the study concluded that the following vehicle had to brake at a higher deceleration magnitude than the lead to avoid collisions in scenarios of control system failures [65].

Even though all the aforementioned works consider the aspects of safe brake maneuvers in terms of vehicle coordination, inter-vehicle separation, and communication delays, it is easy to note that there are no works specifically addressing emergency brake maneuvers with heterogeneous deceleration capabilities of vehicles. The reason could be that tests are performed in controlled environments with homogeneous vehicles and, since there are no external traffic, these situations may not arise.

However, in the direction towards implementing platoons in real traffic, and further towards autonomous driving, external (non-platooning) traffic does coexist with such vehicle arrangements. Then, emergency brake maneuvers will be more common due to traffic jams, accidents, construction work/obstacles on a highway, human errors (in non-automated vehicles), and so on. Therefore, there is a need to design safe emergency brake maneuvers.

As explained before, the loading conditions of a vehicle affect its maximum achievable deceleration. Depending on the types of vehicles participating in a platoon, their individual braking capacities will be nonhomogeneous and differ drastically. For example, a small passenger car may brake better in comparison to a heavily loaded utility vehicle. This implies that the former can come to a complete standstill in a much shorter distance than the latter. Hence, these factors have to be accounted for when designing such maneuvers.

In addition, road profile transitions the vehicles undergo during braking impact their maximum achievable deceleration magnitude, i.e., a vehicle already applying its maximum brake force will have its deceleration magnitude reduced if it enters a downhill. Road conditions like wet/snow/glaze/oil also impact the achieved deceleration as the vehicles' tires cannot grip the surface. In such situations, coordination among vehicles becomes extremely important to prevent collisions and guarantee a safe brake maneuver.

Thus, there is a need of an emergency brake maneuver/scheme/approach that takes into account all these aforementioned factors, achieves coordination among vehicles, and accomplishes a safe and collision-free braking while simultaneously minimizing the stopping distance of the platoon. Thus, we bridge this existing gap in the current research through this work. We propose a cyber-physical design named Space Buffer and demonstrate its benefits, especially, its feasibility. Our approach can also be easily extended to the much less stringent case of non-emergency braking in platoons.

## Chapter 4.

# Braking under idealized conditions

In this chapter, initially, we introduce our inter-vehicle communication strategy common to all the presented approaches. Then, we look into the two intuitive approaches for emergency braking. Subsequently, based on these approaches, we introduce the Subplatoon approach. Finally, our Space-Buffer approach is detailed. All these approaches are based on the stopping distances of vehicles computed as per Section 2.3.3. For this computation, we assume that emergency braking happens on a flat road, and all vehicles achieve their required deceleration instantaneously. These two assumptions constitute our *idealized conditions*. Since in reality, this would never be the case, the brake-by-wire controller introduced in the next chapter accounts for realistic conditions and changing road profiles.

### 4.1. Intra-platoon communication

Our intra-platoon communication strategy is common to all the emergency braking approaches presented further and comprises three types of wireless messages namely *live signal*, *brake command*, and *distress message* as shown in Fig. 4.1. These are sent over the frequency band allocated in Europe by the ETSI [35]. Note that the focus of this section is not on the structure or format of these messages, rather on their contents that are disseminated for achieving vehicle coordination as explained below.

The live signal can be mapped to a CAM [36] based on IEEE 802.11p standard. However, we deviate from the standard's recommendation of a  $100ms$  transmission period [36] and choose a period of  $20ms$  (to account for speeds of around  $100km/h$ ). Our choice is based on the observations by truck manufacturers as mentioned in [62].

Live signals are broadcast both during brake and cruise scenarios from every vehicle  $i$ , where  $i$  is an index representing a vehicle's position in platoon, i.e.,  $1 \leq i < n$ , and  $n$  is the last vehicle (which does not need to send a live signal). Note that even though the live signals from a vehicle are received by all its surrounding vehicles, they are processed only by the immediately following vehicle. To this end, a live signal must include the index of the vehicle from which it proceeds and every vehicle must know its immediately leading vehicle in the platoon.

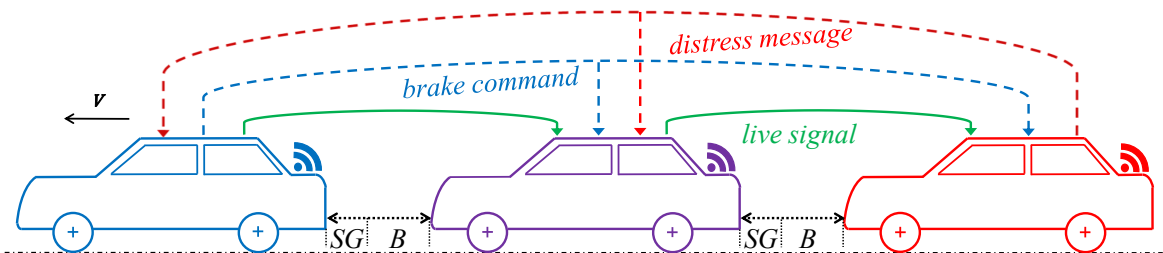


Figure 4.1.: Intra-platoon communication: live signal, brake command, and distress message

For the sake of braking, in addition, a vehicle  $i$ 's live signal must include its deceleration  $d_i$ , its velocity  $V_i$ , its position  $P_i$  in  $m$  (relative to the lead vehicle's position), and the time  $t_i$  at which  $d_i$ ,  $V_i$ , and  $P_i$  were measured. These information can be easily obtained by a vehicle's local sensors. For example, a combination of global positioning system (GPS) and inertial measurement unit (IMU) can be used for high-accuracy absolute positioning (i.e., coordinates) out of which a relative position can be derived or radar/lidar sensors can be used (may be, also together with an IMU) for relative positioning. Further details are, however, out of the scope of this work.

With respect to the Space-Buffer approach, the inter-vehicle separations are comprised of two parts namely *safeguard* (SG) and *space buffer* (B) as shown in Fig. 4.1. As presented later, only the space buffer is utilized during emergency braking. Therefore, apart from the aforementioned deceleration, velocity, position, and its index, a vehicle  $i$  also appends the minimum remaining space buffer (up to its position in the platoon) to its live signal. To explain how this works, let  $B_i$  denote the remaining space buffer between vehicles  $i - 1$  and  $i$ , i.e., how much of the original  $B$  remains at the point in time of sending the live signal:

$$B_i = P_i - \left[ P_{i-1} + \left( V_{i-1}(t_i - t_{i-1}) - \frac{1}{2}|d_{i-1}|(t_i - t_{i-1})^2 \right) \right] - SG, \quad (4.1.1)$$

where  $t_i$  is the time at which  $P_i$  was measured,  $t_{i-1}$  is the time at which  $d_{i-1}$ ,  $V_{i-1}$ , and  $P_{i-1}$  were measured for  $1 \leq i < n$ , and  $SG$  is the aforementioned safeguard between any two vehicles. Clearly, (4.1.1) is valid as long as the deceleration  $d_{i-1}$  remains constant in  $(t_{i-1}, t_i)$ . This can only happen when the vehicle is either decelerating at a constant assigned rate or it is saturated at a lower magnitude, for example, by decelerating in a steep downhill (which is a realistic condition). For this reason, vehicle  $i - 1$  has to send an asynchronous live signal (i.e., independent of the  $20ms$  period) to  $i$  after its brake-by-wire controller settles at the desired deceleration or saturates at a lower magnitude.<sup>1</sup>

Once  $B_i$  is computed, vehicle  $i$  determines the minimum remaining space buffer given by:

$$B_i = \min (B_{i-1}, B_i) \quad (4.1.2)$$

that is, the minimum between the minimum remaining space buffer as per its immediately leading vehicle  $i - 1$  (sent within vehicle  $i - 1$ 's live signal) and its own remaining space buffer as per (4.1.1) is chosen and included in its live signal.

Apart from disseminating the crucial information mentioned above, live signals help in detecting packet losses as well and, thereby, implementing fail-safe mechanisms. If a given number of live signal updates are lost in a row, the affected vehicle dissolves the platoon by assuming the worst case. That is, the affected vehicle assumes that its leading vehicles are already braking and performs a (decentralized) emergency brake maneuver by broadcasting a brake command (explained next). As a consequence, all its following vehicles begin to brake and the platoon dissolves completely. However, this is supposed to be an extreme exception when, for example, communication is lost completely.

Meanwhile, the brake command can be sent over a DENM [37] and is typically broadcast by the platoon lead (with the exception described above) to initiate an emergency brake maneuver. For safety reasons, a brake command has to be replicated over the live signal until complete standstill.

Once a brake command is broadcast by the platoon lead, all the following vehicles including the lead will begin braking simultaneously  $20ms$  later. This is done in accordance with our Space-Buffer approach. Note that our approach can also be easily extended to the case of non-simultaneous braking, where the lead begins braking immediately. However, this  $20ms$

<sup>1</sup>In reality, deceleration tracking by brake-by-wire controllers is not instantaneous, rather it tracks the assigned deceleration with a delay. Further details about the brake-by-wire controllers as well as the reason for their saturation in certain road profiles are presented in Chapter 5.

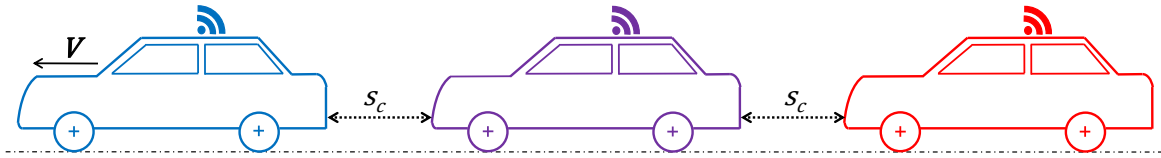


Figure 4.2.: Least Platoon Length: The inter-vehicle separations are a constant. During an emergency, all vehicles brake at the deceleration rate of the weakest vehicle.

delay has a negligible impact (of at most  $0.6m$ , assuming platoon cruise velocity of  $30m/s$ ) on the overall stopping distance [30].

During emergency braking, a distress message (also a DENM) is broadcast by any vehicle that is unable to track its assigned deceleration, for example, when it enters a downhill (realistic condition). The purpose is to inform all other vehicles to adapt their originally assigned decelerations. Hence, after a distress message broadcast, all other vehicles perform computations based on distress message's contents (introduced later) and begin simultaneously tracking their respective new decelerations  $20ms$  later. The distressed vehicle continues sending distress messages (every  $20ms$ ) until this is acknowledged by its immediately leading vehicle over the live signal. In turn, this latter requires an acknowledgment from its immediately leading vehicle and so on up to reaching the platoon lead.

Note that there can be cascaded distress messages from the same or different vehicles, e.g., when changing from one downhill to a steeper one. Simultaneous distress messages are less probable, but also possible, if two or more identical vehicles incur a distress situation. In this case, the vehicle being more *distressed*, i.e., the vehicle that has the maximum deviation from its assigned deceleration, must be considered for further computations simply disregarding all others.

Finally, it is important to note that we do not consider propagation delays for any of these messages. Further, we assume that all vehicles are within the reach of the platoon lead (in case of brake command broadcast) as well as the trail vehicle (in case of distress message broadcast). These assumptions are based on the field trials done in [11], where vehicles within  $300m$  range of the transmitter receive a broadcast message with 100% probability and almost instantly (as mentioned before, we restrict our platoon length to  $200m$ ).

## 4.2. Intuitive approaches

Now that the common inter-vehicle communication strategy is introduced, in this section, we look at the intuitive approaches for emergency braking, and identify their advantages and disadvantages.

### 4.2.1. Least Platoon Length

In this approach, whole platoon brakes as the *weakest* vehicle, i.e., the vehicle that has the lowest deceleration magnitude and, therefore, the longest stopping distance. Since this lowest deceleration magnitude can be achieved by all other vehicles, a safe and collision-free brake maneuver results. However, the resulting stopping distance of the platoon is dictated only by the weakest vehicle. This implies that the platoon can come to a complete standstill in a short distance, if the weakest vehicle's deceleration magnitude is close to the maximum possible ( $0.85g$ ). On the contrary, if its magnitude is low, it would lead to a very long stopping distance. In the latter scenario, this approach becomes undesirable for emergency braking. The other disadvantage is that none of the other vehicles' much greater deceleration capabilities are utilized.

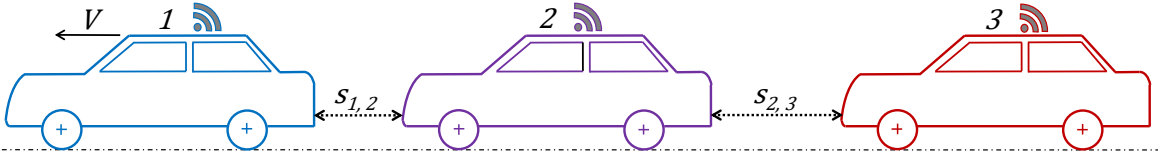


Figure 4.3.: Least Stopping Distance: Vehicles are sorted as per their increasing stopping distances, where 1 represents the vehicle with the shortest stopping distance followed by the vehicle with the second best stopping distance and so on till the last vehicle which brakes the worst. The inter-vehicle separations are not constant, but vary as a function of the difference in stopping distances of two consecutive vehicles. During an emergency, all vehicles brake at their respective maximum deceleration capacities.

However, there are a couple of advantages associated with respect to achieved fuel/energy savings, and overall platoon length, due to the constant separations  $s_c$  as shown in Fig. 4.2. For example, the inter-vehicle separations can just be  $1m$ , as the fuel/energy savings are optimum at this separation [56] [57]. This also leads to the shortest platoon length and, thus, other road users can also coexist leading to much better utilization of the road infrastructure.

Finally, since every vehicle brakes at the rate of the weakest vehicle, any new vehicle joining the platoon can easily be appended to the end. In the other approaches that would be introduced further, this would not be the case.

**An example.** Consider a vehicle which can brake at a maximum deceleration magnitude of  $0.7g$  (i.e.,  $0.7 \times 9.8m/s^2 = 6.8m/s^2$ ). Now, a trail vehicle intends to form a platoon and follows up to maintain a distance of  $1m$ . Even though this trail vehicle is of same height and performance category as that of the lead vehicle, it is differently loaded and, as a result, its maximum achievable deceleration magnitude is  $0.6g$  (i.e.,  $0.6 \times 9.8m/s^2 = 5.8m/s^2$ ). Since the trail vehicle is the weakest of the two in terms of decelerating, once the platoon is formed and an emergency brake maneuver is initiated, the deceleration rate of the platoon will not exceed  $0.6g$ . The lead vehicle calculates and exerts the necessary brake force such that its deceleration is  $0.6g$  (even though it is capable of decelerating at more than  $0.6g$ ).

Now, consider a third vehicle that joins this two-vehicle platoon, and it can achieve a maximum deceleration of only  $0.55g$ , the deceleration of the whole platoon is now restricted to  $0.55g$ . However, if this vehicle is capable of decelerating by more than  $0.6g$ , it is required to decelerate at only  $0.6g$  as per this approach.

#### 4.2.2. Least Stopping Distance

In contrast to Least Platoon Length, the Least Stopping Distance approach achieves optimum stopping distance by allowing the vehicle with the strongest deceleration and, thereby, the shortest stopping distance to lead the platoon. This is then followed by the vehicle with the second best stopping distance, and so on until reaching the last vehicle which brakes the worst. Since the best braking vehicle in a particular set of vehicles leads the platoon, the optimum stopping distance results.

However, the inter-vehicle separations are not constant like in Least Platoon Length, but these vary as a function of the difference in stopping distances between consecutive vehicles as shown in Fig. 4.3, where vehicle 1 represents the best decelerating vehicle and vehicle  $n$  represents the vehicle with the least deceleration capability. The greater the difference in deceleration magnitudes of two consecutive vehicles, the greater their separations will be. Thus, the achieved fuel/energy savings are also less and a longer platoon results.



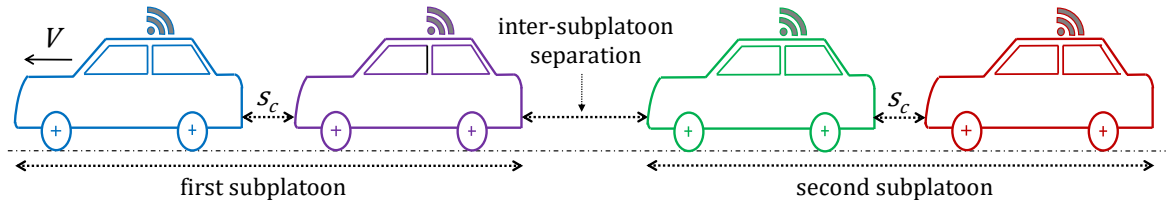


Figure 4.4.: Subplatoon: Vehicles are clustered into 2 subplatoons, where the inter-vehicle separations in the subplatoons are a constant. However, the inter-subplatoon separation varies as a function of the difference in stopping distances of the chosen first subplatoon lead and the worst braking vehicle.

Finally, it is important to note that this approach needs the best braking vehicle in a particular set of vehicles to lead the platoon and the following vehicles are sorted as per their increasing stopping distances. Hence, if any new vehicle intends to be a part of an existing platoon, it has to join in at the appropriate position, which can be between existing vehicles or at the end. It can also become the lead depending on its deceleration capability and the capabilities of existing vehicles.

**An example.** Consider a vehicle with a maximum achievable deceleration of  $0.7035g$ . It can achieve a stopping distance of  $69.57m$  (as per (2.3.9)) from a cruise velocity  $V_{init}$ . Now, another vehicle intends to form a platoon with this existing vehicle and is capable of decelerating at a maximum of  $0.7786g$ . It needs a stopping distance of  $63.37m$  from the same cruise velocity. Since the former vehicle is the weakest in terms of braking, the latter overtakes the former during platoon formation and becomes the lead. The difference in their stopping distances is  $6.2m$  and, hence, the following vehicle has to maintain a separation greater than this.

Now, if a third vehicle intends to join this two-vehicle platoon and can achieve a stopping distance of  $78.20m$  by decelerating at a maximum of  $0.6193g$ , it can join in as the last vehicle. This should maintain a separation greater than  $8.63m$  ( $78.20 - 69.57$ ) to the second vehicle. Clearly, the inter-vehicle separations are varying and this leads to lesser fuel/energy savings and a longer platoon. Particularly, the platoon lead in this example does not have any fuel/energy savings as the separation with its immediately following vehicle is greater than  $5m$  [56] [57].

Note that the third vehicle has a lesser deceleration capability than the existing first and second vehicles and, hence, it was easily appended behind the second vehicle. If its deceleration capability was much better or in between the existing vehicles, it would have become the platoon lead or joined in between the two respectively. Then, the inter-vehicle separations would have been adapted accordingly.

### 4.3. Subplatoon approach

Clearly, we would like to have a platoon with the highest possible aerodynamic benefits, the shortest possible length, and the shortest possible stopping distance. To this end, we introduce our Subplatoon approach, which is a hybrid solution based on the previously mentioned intuitive approaches. The goal is to maintain inter-vehicle separations constant like in Least Platoon Length and, at the same time, minimize the stopping distance.

The overall platoon is divided into 2 subplatoons as shown in Fig. 4.4. The first subplatoon consists of all vehicles that can brake at a higher or same deceleration magnitude as that of the platoon lead, and the second subplatoon consists of all vehicles that decelerate at a lesser

magnitude than the platoon lead. As for Least Platoon Length, the second subplatoon brakes at the rate of the weakest vehicle.

The inter-vehicle separations in each subplatoon are a constant similar to Least Platoon Length, whereas the inter-subplatoon separation is a function of the difference in stopping distances between the first subplatoon lead and the weakest vehicle. Even though this is clearly more than the constant separations in each subplatoon, the fuel/energy savings are considerably better than the Least Stopping Distance approach.

**An example.** Consider 1, 2, 3, ...  $n$  vehicles as part of a platoon. Assuming vehicle 1 has the shortest and vehicle  $n$  has the longest stopping distance, the first subplatoon lead will be vehicle  $x$  that achieves stopping distance, platoon length, and aerodynamic benefits as close as possible to their respective optimum values. As shown in Fig. 4.4, the first subplatoon consists of all vehicles capable of braking at deceleration magnitudes that are same as or higher than the lead, i.e.,  $x, 1, 2, \dots, x-1$ . The second subplatoon can be led by any vehicle that has a lesser deceleration magnitude than  $x$ , i.e.,  $n, n-1, n-2, \dots, x+1$ . However, this subplatoon has to brake at the rate of the weakest vehicle. Hence, the brake-by-wire systems have to be configured such that all vehicles brake as  $n$  in the second and as  $x$  in the first subplatoon respectively.

Note that Least Stopping Distance is a special case of the Subplatoon approach, where there is exactly one vehicle per subplatoon, i.e., a total of  $n$  sub platoons. There can be any number of sub platoons between 2 and  $n$ . However, for a chosen lead vehicle  $x$ , it is easy to see that there cannot be any configuration with more than two sub platoons that yields a lesser length for the whole platoon. This is because the stopping distance of the first subplatoon is determined by  $x$  and that of the last subplatoon by  $n$ . Independent of the number of sub platoons we have, the sum of their inter-subplatoon separations cannot be less than the difference in stopping distances between  $x$  and  $n$ . On the other hand, having more than two sub platoons might negatively impact aerodynamic benefits, since the inter-subplatoon separations are usually large as already discussed.

With respect to any new vehicle joining an existing platoon, it can either join in the first or second subplatoon based on whether its maximum deceleration magnitude is equal to or greater than that of first subplatoon lead or less than that respectively. However, once the subplatoon to join is determined, it is not necessary to join in at a particular position like in the Least Stopping Distance approach. Hence, it can be easily appended towards the end of the respective subplatoon.

Any new vehicle joining can also become the first subplatoon lead, if the combined aerodynamic savings, platoon length, and stopping distance achieved are greater than the currently achieved values. In such a scenario, the inter-subplatoon separation has to be adapted accordingly.

One major drawback associated with the Subplatoon approach is the large inter-subplatoon separation. Since it is greater than the intra-subplatoon separations, other road users may drive into this larger gap. Then, once emergency brake maneuver is initiated, the lead of the second subplatoon needs this large separation and closes up to the last vehicle of the first subplatoon. The existence of other road users will lead to vehicular collisions.

Finally, even though the Subplatoon approach achieves stopping distances better than Least Platoon Length, the braking capacities of all vehicles apart from the first subplatoon lead and the weakest vehicle are not used optimally. Hence, there is a need to further minimize the achieved stopping distance such that it is closer to the value achieved with the Least Stopping Distance approach. Towards this direction, we introduce our Space-Buffer approach in the next section.

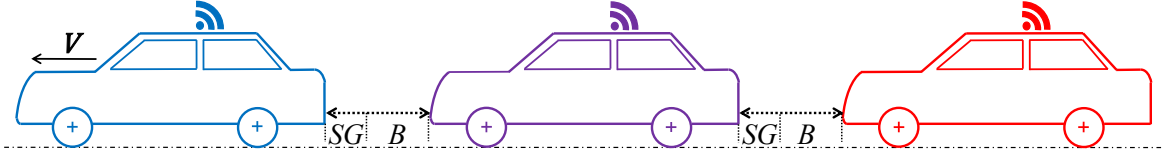


Figure 4.5.: Space Buffer: Vehicles are sorted as per their increasing stopping distances. However, the inter-vehicle separations are a constant comprising of  $SG$  and  $B$ , where  $SG$  is reserved exclusively for communication loss and only  $B$  is utilized during emergency braking.

## 4.4. Space-Buffer approach

In this section, we introduce our Space-Buffer approach. Initially, we present the computations performed to obtain individual vehicle decelerations that need to be tracked once emergency braking is initiated. Since the inter-vehicle separations are utilized to achieve a short stopping distance, subsequently we prove that our approach results in a safe brake maneuver.

### 4.4.1. Space buffer computations

In this section, we introduce the computations performed in our Space-Buffer approach to arrive at individual vehicle decelerations to be tracked once emergency braking is initiated. Similar to Least Platoon Length, inter-vehicle separations are the same for all vehicles and kept constant. However, as mentioned before, these separations now consist of two parts namely safeguard ( $SG$ ) and space buffer ( $B$ ) as shown in Fig. 4.5. The  $SG$  accounts for eventual communication loss between vehicles, whereas the space buffer in all the inter-vehicle separations are utilized during emergency braking.

As a result of constant separations, this approach also has a reduced overall platoon length and high aerodynamic benefits. The difference to Least Platoon Length is that vehicles in this approach make use of the space buffer contained in the inter-vehicle separations to allow for a shorter stopping distance of the whole platoon. In other words, the lead vehicle is allowed to brake at a higher deceleration magnitude than the following vehicles.

As with Least Stopping Distance, let us again assume that vehicles are sorted in the order of increasing stopping distances. That is, for the stopping distances of any two vehicles  $i$  and  $j$  denoted by  $S_i$  and  $S_j$  respectively, it holds that  $S_i \leq S_j$  if  $i < j$  holds.<sup>2</sup>

Now, for each vehicle, if we utilize the space buffers contained in all the inter-vehicle separations towards the lead and subtract them from the corresponding vehicle's stopping distance, there exists a vehicle for which this value will be the maximum. This approach then allows for an overall stopping distance given by:

$$S_{SB} = \max_{1 \leq j \leq n} (S_j - (j - 1)B), \quad (4.4.1)$$

where  $B$  is again the space buffer,  $n$  is the number of vehicles in the platoon and — by the assumed order — the index of the vehicle with the lowest deceleration magnitude and, hence, the longest stopping distance, and  $j$  is an index representing the vehicle's position from the lead. Clearly,  $B$  must be less than or equal to the chosen inter-vehicle separation. Later, in our experiments we assign  $B$  a value of  $1m$ ,  $2m$ , and  $3m$ , and choose  $SG$  as  $1m$ , thereby, resulting in total inter-vehicle separations of  $2m$ ,  $3m$ , and  $4m$  respectively.

<sup>2</sup>This is not an absolutely necessary condition, however, if vehicles are not in this order, the resulting decelerations might not lead to an optimum stopping distance.

Let us assume that  $S_j - (j - 1)B$  is maximum for  $j = x$ . Now,  $S_{SB} = S_x - (x - 1)B$ . So we allow the lead vehicle to have a stopping distance equal to  $S_{SB}$  that is  $(x - 1)B$  shorter than that of vehicle  $x$  in the platoon. In other words, we make use of all space buffers between the lead and the vehicle  $x$  to compensate for the difference in stopping distances in the worst case, i.e.,  $S_x - S_{SB}$ .

The next step is to configure the brake-by-wire systems of all vehicles to guarantee that no collisions occur. To this end, we make use of (2.3.9) for each vehicle  $i$  in the platoon:

$$S_{SB} + (i - 1)B = K_1 \ln \left( 1 + \frac{K_2}{\eta_b \mu W + K_3} \right), \quad (4.4.2)$$

i.e., we make the stopping distance of vehicle  $i$  equal to the selected stopping distance of the lead (i.e.,  $S_{SB}$ ) plus all space buffers in between the lead and vehicle  $i$ , where  $i$  is also a vehicle index starting from the lead. For simplicity, we have made following replacements  $K_1 = \frac{\gamma_m W}{2gC_A}$ ,  $K_2 = C_A V_{init}^2$ , and  $K_3 = f_r W$  ( $\theta = 0$ ). Next, we need to solve for  $\eta_b$ , i.e., the braking efficiency of vehicle  $i$ , so we proceed as follows:

$$e^{\frac{S_{SB} + (i-1)B}{K_1}} = 1 + \frac{K_2}{\eta_b \mu W + K_3}, \quad (4.4.3)$$

and then,

$$\eta_b = \frac{\left( \frac{K_2}{\left( e^{\frac{S_{SB} + (i-1)B}{K_1}} - 1 \right)} - K_3 \right)}{\mu W}. \quad (4.4.4)$$

Finally, we can use (2.3.11) to compute the necessary deceleration  $d$  of vehicle  $i$  and (2.3.15) to compute the necessary brake force  $F_b$  to be exerted.

**An example.** Consider a four-vehicle platoon where vehicles are arranged as per their increasing stopping distances. Assume these are 65, 70, 75, and 80m respectively by decelerating at their maximum capability from a common initial velocity  $V_{init}$ . Now, calculating  $S_j - (j - 1)B$  for each vehicle, where  $B$  is chosen to be 3m results in 65, 67, 69, and 71m respectively. Since 71m is the maximum, this constitutes  $S_{SB}$ . Therefore, the individual stopping distances to be achieved by these 4 vehicles once emergency braking begins are 71, 74, 77, and 80m respectively. It can easily be observed that even though the separations are constant like in Least Platoon Length, the lead vehicle brakes at a higher deceleration magnitude than the weakest vehicle and brakes within a distance that is 9m shorter in this case. Further, by considering the shortest stopping distances of all vehicles and then performing the space buffer computations, there is an efficient use of deceleration capabilities of all vehicles.

The performed computations to arrive at the individual vehicle decelerations consider the space buffers in inter-vehicle separations that are embedded between vehicles. Thus, after an emergency brake maneuver is initiated, all the vehicles gradually utilize the space buffer contained in the separation to their respective immediately leading vehicles and at complete standstill, all inter-vehicle separations would be reduced to only the  $SG$ . Therefore, it is necessary to ensure that the displacements of any two consecutive vehicles during braking guarantees safety, i.e., no inter-vehicle collisions happen. A mathematical proof of the same is presented next.

#### 4.4.2. Proving collision-free brake maneuvers

Now, we present a mathematical proof of collision-free braking when utilizing the space buffers. For ease of exposition, we rely on the displacement formula given below for the  $i^{\text{th}}$

vehicle in our approach. Note that in contrast to (2.3.9), this does not consider any forces apart from those exerted by a vehicle's brakes, which results in a longer stopping distance:

$$S_i = V_{init}t - \frac{1}{2}d_i t^2, \quad (4.4.5)$$

where  $S_i$  represents the displacement or stopping distance in  $m$ ,  $V_{init}$  represents the initial velocity in  $m/s$  when braking is initiated. The time in seconds ( $s$ ) required to achieve standstill is represented by  $t$ , and  $d_i$  denotes the deceleration in  $m/s^2$ . Since we consider deceleration, a minus sign exists in the equation.

Note that vehicle  $i$  comes to standstill after some time  $t = \frac{V_{init}}{d_i}$  and that its  $S_i = S_{SB} + (i - 1)B$ , where  $B$  is the space buffer. Substituting these in (4.4.5) and rearranging, we obtain:

$$d_i = \frac{V_{init}^2}{2[S_{SB} + (i - 1)B]}. \quad (4.4.6)$$

Similarly, the difference in deceleration magnitudes between any two consecutive vehicles,  $i$  and  $i + 1$ , denoted by  $\Delta d_{i,i+1}$ , is given by:

$$\Delta d_{i,i+1} = \frac{V_{init}^2}{2} \left[ \frac{B}{[S_{SB} + (i - 1)B](S_{SB} + iB)} \right]. \quad (4.4.7)$$

Now, the time required for vehicle  $i + 1$  to fully consume the space buffer to vehicle  $i$  can be obtained by substituting  $\Delta d_{i,i+1}$  in (4.4.5) and solving for  $t$ :

$$t = \frac{V_{init} + \sqrt{V_{init}^2 - (2 \cdot \Delta d_{i,i+1} \cdot B)}}{\Delta d_{i,i+1}}. \quad (4.4.8)$$

A collision-free braking exists between any two consecutive vehicles  $i$  and  $i + 1$  provided the time required to consume the space buffer  $B$  between them is greater than or equal to the time required to stop the  $(i + 1)^{th}$  vehicle. Therefore,

$$\frac{V_{init}}{d_i} \leq \frac{V_{init} + \sqrt{V_{init}^2 - (2 \cdot \Delta d_{i,i+1} \cdot B)}}{\Delta d_{i,i+1}} \quad (4.4.9)$$

has to be ensured, i.e., the  $(i + 1)^{th}$  vehicle should stop before it consumes its space buffer to the  $i^{th}$  vehicle.  $B$  is lesser when compared to  $S_{SB}$  and  $V_{init}$ . For example,  $3m$ ,  $62m$  and  $30m/s$  respectively. When these values are substituted in (4.4.7), it results in  $\Delta d_{i,i+1} < 1$  and, hence,  $\frac{\Delta d_{i,i+1}}{d_i} < 1$ . With this, (4.4.9) holds, if the following holds:

$$V_{init}^2 \geq 2 \cdot \Delta d_{i,i+1} \cdot B, \quad (4.4.10)$$

i.e., the term under the square root should be zero or greater than zero.

The largest value of  $\Delta d_{i,i+1}$  results when the denominator's value in (4.4.7) is the smallest. This happens when  $i = 1$ . Substituting this value of  $i$  in (4.4.7) and in turn replacing  $\Delta d_{i,i+1}$  in (4.4.10),

$$1 \geq \frac{B^2}{S_{SB}^2 + (S_{SB} \cdot B)}, \quad (4.4.11)$$

is required. Rearranging (4.4.11) leads to:

$$S_{SB}^2 + (S_{SB} \cdot B) \geq B^2. \quad (4.4.12)$$

Since  $B < S_{SB}$ , it is clear that,

$$\left( \frac{S_{SB}^2}{B} + S_{SB} \right) \geq B. \quad (4.4.13)$$

This proves that vehicle  $i + 1$  stops before fully consuming its space buffer  $B$  to its immediately leading vehicle, independent of the value of  $i$ .

## 4.5. Parameters for comparison of the approaches

Now that the approaches for emergency braking are presented, in this section, we introduce the parameters based on which these approaches will be compared. Later in Chapter 7, a detailed evaluation will be performed.

The parameters for comparison are achieved aerodynamic benefits, overall platoon length, and stopping distance from a common cruise velocity. Since the chosen inter-vehicle separations in all the approaches affect these parameters, we fix a value for the same, particularly, for the separations in Least Platoon Length and within the two sub platoons. Additionally, the  $1m$   $SG$  introduced in our Space-Buffer approach to account for eventual communication loss is now extended to all the other approaches. Thus, in the chosen inter-vehicle separations, the  $SG$  is also included.

In Least Platoon Length, the inter-vehicle separations are as short as  $SG$  ( $1m$ ), i.e., accounting only for packet losses. Clearly, this leads to optimum fuel/energy savings and overall platoon length. In the Least Stopping Distance approach, as mentioned before, the separations are a function of the difference in stopping distances of two consecutive vehicles. Further, this separation is increased by the one meter  $SG$ . The varying inter-vehicle separations lead to lesser fuel/energy savings and longer platoons. However, optimum stopping distance would be achieved by this approach.

Similar to Least Platoon Length, in the Subplatoon approach, the inter-vehicle separations are just the  $1m$   $SG$  within the two sub platoons. However, the inter-subplatoon operation is the difference between the stopping distances of the weakest vehicle and the chosen first subplatoon lead plus  $SG$ . Even though fuel/energy savings and platoon length are optimum for each of the two sub platoons, their combined savings and overall platoon length are not optimum because of the larger inter-subplatoon separation (as shown in detail in Chapter 7).

Finally, with respect to the Space-Buffer approach, as mentioned before, we choose a value of 1-, 2-, and 3-meters for  $B$  and appending the  $1m$   $SG$  results in inter-vehicle separations of 2-, 3-, and 4-meters respectively. Note that only when the separations are below  $5m$ , a platoon lead has aerodynamic benefits [56] [57]. As a result, we restrict the maximum value of  $B$  to  $3m$ .

In Chapter 7, we simulate platoons of 20 vehicles and compare these approaches. Further, the impact of braking capabilities of vehicles on these aforementioned parameters are also analyzed. Additionally, we address communication loss between vehicles and obtain a threshold on the number of packets that can be safely lost in all the approaches.

## 4.6. Key findings

In this chapter, we assume idealized conditions of braking on a flat road and an instantaneous deceleration tracking. Initially, we presented the intra-platoon communication strategy common to all the approaches. The necessary changes in comparison to the ETSI standard was also detailed. Then, the intuitive (Least Platoon Length and Least Stopping Distance) and Subplatoon approaches for emergency braking were introduced. Their shortcomings were detailed and then these were dealt within our Space-Buffer approach.

The intuitive approaches achieve optimum fuel/energy savings and overall platoon length (in Least Platoon Length), and optimum stopping distance (in Least Stopping Distance). Hence, they provide the optimum values against which the performance of the Subplatoon and Space-Buffer approaches can be measured. For the real world implementation, it is desirable to have an approach that minimizes the stopping distance, and simultaneously achieves aerodynamic benefits and short platoon length.

In this direction, the Subplatoon approach achieves optimum fuel/energy savings and sub-platoon lengths only within the two sub platoons. However, the achieved stopping distance is

suboptimal as the braking capacities of vehicles apart from the first subplatoon lead and the weakest vehicle are not fully utilized. The other disadvantage with this approach is the large inter-subplatoon separation. Other non-platooning vehicles may drive into this gap causing inter-vehicle collisions when emergency braking is initiated.

In our Space-Buffer approach, the (shortest) stopping distances of all vehicles are first considered and, then, depending on the value of  $B$ , i.e., the space buffers, the individual vehicle decelerations are computed. This leads to a much better utilization of all vehicles' deceleration capacities and, hence, stopping distances are shorter and close to the optimum (as shown in detail in Chapter 7). Further, the inter-vehicle separations are constant and in the range of 2 to  $4m$ . Thus, both aerodynamic benefits and shorter platoons result.

Therefore, for these reasons, we develop a brake-by-wire controller for the Space-Buffer approach (rather than the Subplatoon approach). This controller is required at each vehicle to track the assigned reference deceleration. Additionally, these controllers account for realistic conditions of braking, i.e., changing road profiles, and controller-related effects in tracking the assigned deceleration. The details of the same are presented in the next chapter.





# Chapter 5.

## Considering realistic brake conditions

In this chapter, we consider realistic conditions of braking, i.e., changing road profiles and non-instantaneous reference deceleration tracking, and introduce brake-by-wire controllers. During emergency braking, these controllers present at each vehicle are responsible for decelerating at an assigned reference computed using our Space-Buffer approach. As presented in the previous chapter, for computing these reference decelerations, we require the stopping distances of all platoon vehicles. Even though a standard expression as per (2.3.9) exists, we do not rely on the same as explained next. Then, through further sections, we derive a controller-based expression of vehicle stopping distance on a flat road. The resulting values of all vehicles are used in our space buffer computations.

### 5.1. Controller-based stopping distance

A vehicle's stopping distance computed as per (2.3.9) and used under idealized conditions is not precise enough as it does not account for the following factors:

**Brake activation time:** Even though brake-by-wire systems use electrical signals for control and automation, they still rely on mechanical and hydraulic components for the transportation of brake pressure to the wheels as in electro-hydraulic brakes [89]. Even though hydraulic components are completely eliminated in electro-mechanical brakes [89], the electrical components involved do have some lag, for example, due to the inertia of motors in cylinders and brake calipers. As a result, from the point in time of brake pedal activation, until the brake pressure builds and reaches the wheels, there is a non-negligible dead time in these systems.<sup>1</sup> This results in a vehicle traveling few meters (depending on its cruise velocity) before actually starting to decelerate [48].

**Non-instantaneous deceleration tracking:** After the brake pressure reaches the actuators, (2.3.9) assumes that the magnitude of brake force is instantly equal to the magnitude needed in order to achieve an assigned reference deceleration. In other words, instantaneous tracking of reference deceleration is assumed. However, in reality, brake-by-wire controllers regulate the brake force such that the reference deceleration is gradually tracked over time. Thus, this time-varying brake force has to be accounted for.<sup>2</sup> The controller's performance is then characterized by the non-negligible rise and settling time resulting in the vehicle traveling few meters. Note that during this transient, a vehicle is still decelerating, but not at the assigned reference. Only after the settling time has elapsed, the vehicle decelerates at the assigned reference.

The first factor can indeed be approximated by a few meters and added to the value computed as per (2.3.9). Nevertheless, approximating the latter is not straightforward. This is

---

<sup>1</sup>Even though non-negligible, the dead time is much lesser when compared to traditional brake systems.

<sup>2</sup>Variations in the brake force will be negligible in the steady states, but considerably large at transients.

because the vehicle masses, and their individual reference decelerations as per our Space-Buffer approach would be different. As a result, even though the performance criteria (introduced later) are same for all brake-by-wire controllers, these different vehicle specific properties, and assigned decelerations lead to non-homogeneous controller gains and, therefore, distances covered by vehicles in platoon would be different.

If the inter-vehicle separations were indeed large, even this second factor can be approximated. However, the inter-vehicle separations in this thesis are below  $5m$ . Further, our Space-Buffer approach utilizes the space buffers in the inter-vehicle separations during emergency braking. All these factors necessitate the precise computation of a vehicle's stopping distance under its controller's action, as opposed to approximation. Hence, our aim is to derive a controller-based expression of stopping distance.

## 5.2. Brake-by-wire performance specifications

In this section, we introduce the performance specifications that are to be achieved by all brake-by-wire controllers. From these homogeneous specifications, it can be ensured that the behavior of all controllers are the same. For example, if the specification concerning settling time is met, it can be ensured that after an emergency brake maneuver is initiated, and the settling time has elapsed, all vehicles are decelerating at their assigned references.

Considering the mechanical and hydraulic, and/or electrical components of a brake-by-wire system, their associated lag, limitations with respect to the magnitude of the brake force generation, and the implications of braking at short inter-vehicle separations, the specifications in Table 5.1 are chosen.

As per our Space-Buffer approach, once emergency braking is initiated, the vehicles will either operate close to or at their maximum deceleration magnitudes. Therefore, it is important to design the individual control systems such that no overshoot is produced during reference tracking. If this design criteria is forgone and a controller tracks a reference deceleration as quickly as possible, for example, enforcing an overshoot, saturation effects may occur at the actuators. This leads to the controller's output response being discontinuous.<sup>3</sup> Then, the characterization of such a response as an expression becomes hard and complex.

As mentioned before, there is a dead time involved after brake pedal activation. Once this dead time elapses, and the brake pressure reaches the actuators, every individual controller should decelerate at its assigned reference from  $400ms$  onwards.

<sup>3</sup>Generally, if an assigned reference deceleration is well within a vehicle's maximum limit, the controller can be designed to produce an overshoot. Then, the only constraint is that the produced overshoot should also remain within the vehicle's maximum limit. However, this is never the case when braking in an emergency, since controllers work at or close to saturation.

Table 5.1.: Controller design specifications

Specifications	Value	Description
Overshoot	0%	The deceleration magnitude (expressed as a percentage) during the transient that exceeds the steady-state value.
Settling time	$\leq 400ms$	Time required to achieve a deceleration that remains within $\pm 2\%$ of reference.
Steady-state error	$\approx 0\%$	The difference between reference and achieved deceleration in the steady state.
Feedback delay	$20ms$	Delay incurred in the feedback loop.

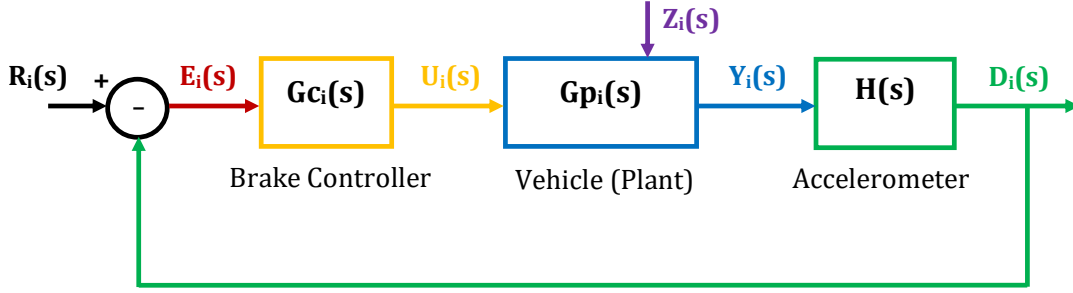


Figure 5.1.: Closed-loop control system

In addition, we consider the controller to have a feedback delay of  $20ms$  due to data processing by sensor and the path taken by the data to traverse back to the controller, i.e., a change in the controlled brake force produces a change in deceleration, which would be sensed and communicated back to the controller  $20ms$  later.

Finally, it is absolutely necessary that every controller track its assigned reference deceleration in the steady state with zero or negligible steady-state error. This is extremely important as all vehicles are braking at very short separations. Failing to meet this requirement causes the steady state error to accumulate over time leading to either collisions with an immediately leading or trail vehicle. This primary collision can then trigger secondary collisions leading to catastrophic events and endangering lives of in-vehicle passengers and other road users.

The aforementioned performance specifications can be met using any of the control design techniques. In fact, the control design technique need not be the same for all controllers. For example, techniques based on optimal control like linear quadratic regulator (LQR) or MPC can be used. Another example can be the popular proportional integral derivative (PID) technique. Regardless of the design technique chosen, the controller based expression of stopping distance that we derive in the next section will still be valid. The only requirement is that the controller's transfer function has to be obtained.

In our work, for designing brake-by-wire controllers we choose the PID technique. The reason is due to its ease of design and wide acceptance. Therefore, the proportional, integral, and derivative gains have to be appropriately tuned for meeting the performance specifications. The gain values can be easily obtained through standard techniques like Pole Placement or Root Locus [60]. Since these are state of the art, we would not emphasize on it here.<sup>4</sup>

### 5.3. Deriving the controller-based stopping distance

In this section, we derive a controller-based expression of stopping distance. To begin with, we first convert the car model in state-space form represented by (2.3.18) and (2.3.19) into a transfer function  $G_{p_i}(s)$ . Then, a transfer function of the PID controller  $G_{c_i}(s)$  is also obtained. Recall that the output of the state-space model is vehicle's velocity. Hence, we need to differentiate it and obtain the deceleration for reference tracking. Therefore, an accelerometer's transfer function is also obtained and we denote it as  $H(s)$ .

We now reduce the closed-loop system shown in Fig. 5.1 into a single-input/single-output system as shown in Fig. 5.2, where the input is vehicle  $i$ 's reference deceleration  $R_i(s)$  and the output is its achieved deceleration  $D_i(s)$ .<sup>5</sup> In Fig. 5.1,  $E_i(s)$  is the error signal, i.e.,  $R_i(s) - D_i(s)$ ,  $U_i(s)$  is the controlled brake force,  $Y_i(s)$  is the vehicle's velocity, and  $Z_i(s)$

<sup>4</sup>Nevertheless, in the appendix, we outline the steps we performed for control design.

<sup>5</sup>In order to distinguish signals in the time and frequency domain, we use uppercase for signals in the frequency domain  $s$  and explicitly mention (s).

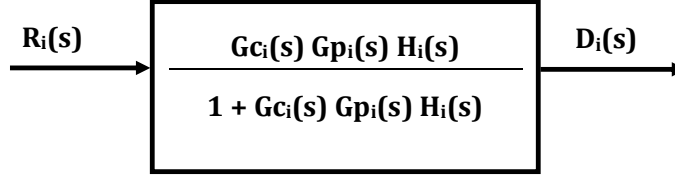


Figure 5.2.: Single-input/single-output system

is the disturbance grade force. Now, assuming no disturbances ( $Z_i(s) = 0$ , i.e.,  $\theta = 0$ ), the transfer function of this overall system with closed-loop feedback is represented by  $G_i(s)$  and expressed as:

$$G_i(s) = \frac{Gc_i(s)Gp_i(s)H(s)}{1 + Gc_i(s)Gp_i(s)H(s)}. \quad (5.3.1)$$

Multiplying  $R_i(s)$  with the above overall system transfer function  $G_i(s)$  produces an output (achieved deceleration)  $D_i(s)$ , which can be obtained by first decomposing this product, i.e., a 4<sup>th</sup> order transfer function into partial fractions as:

$$D_i(s) = R_i(s)G_i(s) = \frac{R_1}{s - p_1} + \frac{R_2}{s - p_2} + \frac{R_3}{s - p_3} + \frac{R_4}{s - p_4}, \quad (5.3.2)$$

where  $R_1$  to  $R_4$  are the residues and  $p_1$  to  $p_4$  are the poles. Then, applying inverse Laplace transform for (5.3.2), we obtain an expression of the output deceleration in time domain  $t$  as:

$$d_i(t) = R_1e^{p_1t} + R_2e^{p_2t} + R_3e^{p_3t} + R_4e^{p_4t}, \quad (5.3.3)$$

where  $d_i(t)$  represents the vehicle  $i$ 's deceleration at time  $t$ . Since deceleration is the rate of change of velocity, integrating (5.3.3) results in the expression of velocity  $v_i(t)$  as:

$$\int d_i(t) dt = v_i(t) = \frac{R_1e^{p_1t}}{p_1} + \frac{R_2e^{p_2t}}{p_2} + \frac{R_3e^{p_3t}}{p_3} + \frac{R_4e^{p_4t}}{p_4} + V_{init} + C_1, \quad (5.3.4)$$

where  $V_{init} + C_1$  is a constant of integration with  $V_{init}$  representing the initial velocity in  $m/s$  at the moment of braking. Thus,  $C_1$  is chosen such that  $v_i(t) = V_{init}$  at time  $t = 0$ , i.e., when braking begins (5.3.4) should be equal to  $V_{init}$ . Therefore, we substitute  $t = 0$  and choose  $C_1 = -\left(\frac{R_1}{p_1} + \frac{R_2}{p_2} + \frac{R_3}{p_3} + \frac{R_4}{p_4}\right)$ .

Now, velocity is the rate of change of position, thus, integrating (5.3.4) yields the expression of vehicle stopping distance  $s_i(t)$  as:

$$\int v_i(t) dt = s_i(t) = \frac{R_1e^{p_1t}}{p_1^2} + \frac{R_2e^{p_2t}}{p_2^2} + \frac{R_3e^{p_3t}}{p_3^2} + \frac{R_4e^{p_4t}}{p_4^2} + V_{init}t + C_1t + S_{init} + C_2, \quad (5.3.5)$$

where  $S_{init} + C_2$  is a second constant of integration with  $S_{init}$  being the vehicle's position in  $m$  at the moment of braking. Similar to before,  $C_2$  is chosen such that (5.3.5) is equal to  $S_{init}$  at  $t = 0$ . Hence, we substitute  $t = 0$  and choose  $C_2 = -\left(\frac{R_1}{p_1^2} + \frac{R_2}{p_2^2} + \frac{R_3}{p_3^2} + \frac{R_4}{p_4^2}\right)$ . Note that since we are interested in the vehicle's stopping distance and not in its absolute position, we assume  $S_{init} = 0$ , i.e., we *measure* the vehicle's (longitudinal) displacement relative to  $S_{init}$ .

In order to compute a vehicle's stopping distance as per (5.3.5), apart from the residues, poles, and the initial velocity, the time  $t$  is also required. Since  $t$  is present in the exponent terms of (5.3.4), we can express it as a polynomial through Taylor series and then obtain an expression of  $t$ , which in turn has to be substituted in (5.3.5).

Alternatively, we can also compute the value of  $t$  numerically. For the sake of simplicity, we choose the numerical option. In this direction, we begin by substituting  $t = 0$  in (5.3.4),

### 5.3. Deriving the controller-based stopping distance

and incrementing in steps of sampling time of the controller, we iterate until the value of this expression is zero or less than zero. In other words, at time  $t=0$  when braking begins, the vehicle would be at the platoon cruise velocity  $V_{init}$ , and after some time its velocity reaches zero, i.e., standstill. This value of  $t$  would be the stopping time of the vehicle, which when substituted in (5.3.5) yields the stopping distance.

**An example:** Consider a vehicle with mass  $m = 3265\text{kg}$ . Due to its loading conditions and considering  $\gamma_m = 1.05$ , its maximum achievable deceleration magnitude is  $d = 4.76\text{m/s}^2$ . Similarly,  $V_{init} = 30\text{m/s}$ ,  $A_f = 2.02\text{m}^2$ ,  $C_A = 0.315$ ,  $\rho = 1.225\text{kg/m}^3$ ,  $g = 9.8\text{m/s}^2$ ,  $f_r = 0.015$ , and  $\mu = 0.85$ . In addition, we assume a *dead time* of  $0.1\text{s}$  to activate the brakes, hence, the vehicle travels  $3\text{m}$  ( $30 \cdot 0.1$ ) before beginning to decelerate. Substituting these parameters in (2.3.9), and appending the dead time, yields a stopping distance of  $93.71\text{m}$  considering a constant deceleration by neglecting all controller-related effects.

Now, using the same parameters, we obtain the vehicle's transfer function and design a PID-based brake-by-wire controller (using Matlab/Simulink) to meet the performance specifications of Table 5.1. The resulting integral gain  $K_i = 34282.5$ , whereas both the proportional and derivative gains are 0. Therefore,  $G_{c_i}(s) = \frac{K_i}{s}$ , while  $H(s)$  was chosen as  $\frac{s}{s+1}$ .

For the decomposition as per (5.3.2), the poles and residues are  $[-10, -1, 0, 0]$  and  $[4.77, 0, -4.77, 0]$  respectively and we obtain (5.3.3) using the inverse Laplace transform. However, for these residues and poles (5.3.3) simplifies to  $(d_i(t))$  has a negative value after  $t = 0$ ):

$$d_i(t) = R_1 e^{p_1 t} + R_3. \quad (5.3.6)$$

Integrating (5.3.6), we derive a corresponding expression of velocity as:

$$\int d_i(t) dt = v_i(t) = \frac{R_1 e^{p_1 t}}{p_1} + R_3 t + V_{init} + C_1, \quad (5.3.7)$$

which we numerically solve to obtain the stopping time  $t = 6.4\text{s}$ . Note that  $C_1 = 0.477$ . Integrating (5.3.7) results in:

$$\int v_i(t) dt = s_i(t) = \frac{R_1 e^{p_1 t}}{p_1^2} + \frac{R_3 t^2}{2} + V_{init} t + C_1 t + C_2 + S_{init}, \quad (5.3.8)$$

where  $C_2 = 0.0477$ . Substituting  $t = 6.4\text{s}$  and  $S_{init} = 0$  in (5.3.8) yields the brake-by-wire stopping distance of  $97.32\text{m}$ . That is, after the dead time elapses and the brake force reaches the actuators, the vehicle needs  $6.4\text{s}$  to reach a standstill under controller action, thereby, covering a distance of  $97.32\text{m}$ . If we also include the dead time of brake activation ( $0.1\text{s}$ ) and the distance traveled in that time ( $3\text{m}$ ), it results in an overall stopping time and distance of  $6.5\text{s}$  and  $100.32\text{m}$  respectively.

The braking dynamics of a vehicle (i.e., all the forces shown in Fig. 2.4) along with its brake-by-wire controller was modeled and simulated in Matlab/Simulink. The resulting brake-by-wire stopping distance was  $100.28\text{m}$  (from  $V_{init} = 30\text{m/s}$ ), which is similar to the analytically computed value from this example. Table 5.2 shows the analytically computed values of vehicle position as per (5.3.8) in comparison to the actual values during simulation. Note that in contrast to our analytical (LTI) model, the performed simulation considers both aerodynamic and rolling resistances which are nonlinear.<sup>6</sup> The performance specifications achieved by the brake-by-wire controller can also be verified in Fig 5.3.

<sup>6</sup>These forces were not included in our LTI car model. Their magnitudes are  $C_A V_{init}^2$  and  $f_r W \cos(\theta)$  respectively (as per (2.3.9)).

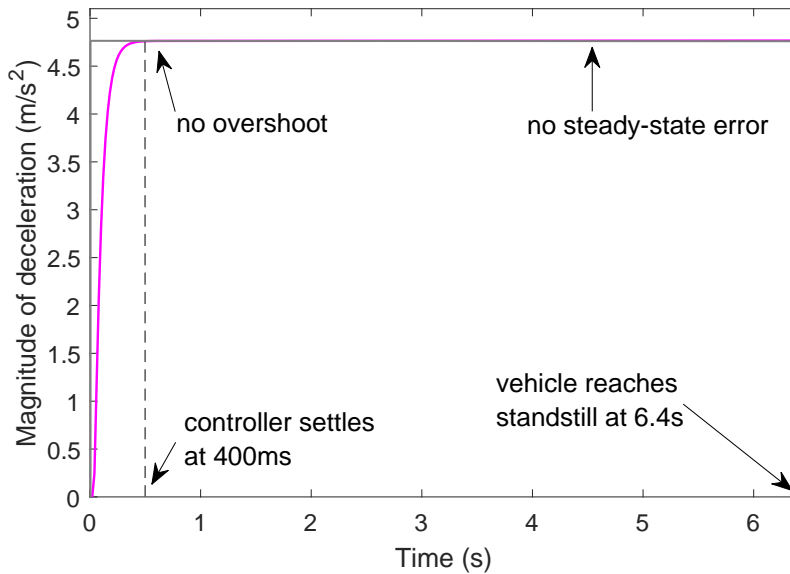


Figure 5.3.: Reference deceleration tracking by an example vehicle. After the brake’s dead time elapses, the reference deceleration magnitude changes (from 0 to  $4.76m/s^2$ ) at time 0 and the controller begins tracking the same.

### 5.4. The controller-based Space-Buffer approach

Once the individual brake-by-wire controllers are designed for all the vehicles to meet the aforementioned performance specifications, our aim is to compute the shortest possible stopping distance of each vehicle from a common platoon cruise velocity ( $V_{init}$ ) under the action of its controller using (5.3.5). For this computation, we assume no disturbances for the entire brake maneuver. In other words, for each vehicle decelerating at its limit under the action of its brake-by-wire controller, we compute its shortest stopping distance on a flat road.

Once these are computed for all the platoon vehicles, the same would be used in our space buffer computations as shown in Section 4.4.1 to obtain each individual vehicle’s deceleration magnitude. Thus, the procedure remains the same, and only the stopping distances obtained from (5.3.5) are used rather than (2.3.9).

Thus, one of the realistic conditions — non-instantaneous deceleration tracking — has been addressed. We now address the other realistic condition, i.e., changing road profiles. However, we first have to ensure that the ordering of vehicles on both uphill and downhill

Table 5.2.: Computed and simulated vehicle positions. After actuators’ dead time elapses, the time is counted. However, the positions here do include the distance traveled due to dead time.

Time (in s)	Position computation as per (5.3.5) (in m)	Position in simulation (in m)
1	30.53	30.52
2	53.95	53.93
3	72.59	72.56
4	86.47	86.43
5	95.58	95.54
6.4	100.32	100.28

road profiles remain the same as that on a flat road. If this is not case, the space buffer computations would be incorrect. This is discussed in the next section.

#### 5.4.1. The ordering of vehicles

Similar to Least Stopping Distance, our Space-Buffer approach also requires that vehicles be sorted as per their increasing stopping distances. Under one of the idealized conditions of completely flat road, one can determine the order and make any new vehicle to join in at the appropriate position in a platoon. However, under realistic conditions, particularly, changing road profiles ( $\theta \neq 0$ ), stopping distance among other factors is also a function of vehicle weight and this implies grade resistance ( $W \sin(\theta)$ ) would be nonhomogeneous on platoon vehicles. Hence, we have to ensure that vehicle order remains the same irrespective of the road profile. In other words, an ordering of vehicles, for example, on a flat road should remain the same both on complete downhill and uphill road profiles (realistic conditions).

On the contrary, if vehicle ordering is not the same, there would be incorrect space buffer computations potentially leading to stopping distances that cannot be achieved by vehicles because their ordering is different on different road profiles. Then, vehicles need to be re-arranged for every road profile change a platoon undergoes, which is clearly cumbersome. However, we reason that this would never be the case.

Incorporating all the forces acting on a vehicle, the deceleration achieved by any vehicle (normalized as  $g$ ) is represented by (2.3.15). Substituting for the aerodynamic resistance  $R_a$  as per (2.2.1), and replacing  $W$  by  $m \cdot g$ , this equation can be rewritten as:

$$\frac{F_b + (f_r \cdot m \cdot g \cdot \cos(\theta)) + C_A V^2 \pm (m \cdot g \cdot \sin(\theta))}{m} = d, \quad (5.4.1)$$

where  $C_A$  is as per (2.3.17). According to Newton's second law of motion, the summation of the individual contribution from each of these forces constitutes the overall vehicle deceleration  $d$ . Thus, splitting them up into fractions leads to:

$$\frac{F_b}{m} + (f_r \cdot g \cdot \cos(\theta)) + \frac{C_A V^2}{m} \pm (g \cdot \sin(\theta)) = d. \quad (5.4.2)$$

The contribution from the first term would be a constant provided the brake force  $F_b$  is constant. With respect to the second term, as previously mentioned, we consider the variation of road angle  $\theta$  to be from  $0^\circ$  to  $8^\circ$ . Hence,  $\cos(\theta)$  is almost constant, as it varies only from 1 to 0.99. Therefore, the second term's contribution is also a constant  $0.147m/s^2$  (assuming  $f_r = 0.015$  and  $g = 9.8m/s^2$ ). The contribution from aerodynamic force is dependent only on individual vehicle's velocity  $V$  and  $C_A$ , and not on  $\theta$ .

Finally, the contribution from the fourth term would also be a constant provided  $\theta$  remains constant, which is the case in complete uphill and downhill. Therefore, the resulting offset deceleration  $g \cdot \sin(\theta)$ , due to the grade resistance can be negated by vehicles by generating more brake force. However, this might not be possible for all vehicles, especially the ones towards the end of a platoon. This is because they are required to brake at their maximum possible brake forces even on a flat road (to minimize the overall stopping distance). Hence, when they undergo a road profile change, they simply cannot counter the effect of (disturbance) grade force and, thereby, fail to track their respective assigned decelerations.

However, all the other vehicles are not braking at their maximum deceleration magnitudes and, hence, they can generate further additional brake force to counter the disturbance effect. Therefore, it is clear that individual vehicle weights do not impact vehicle ordering on uphill and downhill road profiles and, hence, the order of vehicles on a flat road according to their stopping distances remains the same.

### 5.4.2. Considering uphill road profiles

Now that vehicle ordering remains the same for all road profiles has been established, we now consider changing road profiles, particularly uphill, and discuss whether any changes are required in our controller-based Space-Buffer approach.

The resulting decelerations computed for a flat road under controller action can be tracked by all controllers even on uphill road profiles. In fact, a brake-by-wire controller has to apply a lesser brake force than that applied on a flat road. This is because the (disturbance) grade force aids braking. Further, if a vehicle undergoes a road profile change from a flat road to an uphill, it is absolutely necessary that the controller continues to track its assigned reference deceleration, even though it might be able to decelerate at a higher rate. This is important because the following vehicles may still be on a flat road and decelerating at a magnitude greater than the assigned one might result in collisions from behind.

However, it must be ensured that the grade force magnitude is not such that a controller has to accelerate instead of braking in order to track its assigned reference deceleration. If accelerating is required, the delay in transitioning from braking to accelerating caused mainly due to engine dynamics and controller switching might result in inter-vehicle collisions. However, it can be mathematically proven that this situation never arises.

**Theorem 1.** *Let us consider that during a brake maneuver, a vehicle undergoes a road profile change and enters an uphill. In this case, the vehicle's brake-by-wire controller will never have to accelerate in order to track its assigned reference deceleration.*

*Proof.* As previously mentioned, a vehicle's maximum brake force magnitude cannot exceed the product of coefficient of road adhesion  $\mu$  and vehicle weight  $W$ :

$$F_{b_{max}} = \mu W. \quad (5.4.3)$$

Replacing  $W$  by  $m \cdot g$ , where  $m$  denotes the vehicle's mass, and  $g$  is the acceleration due to gravity, and using Newton's second law of motion, the corresponding maximum deceleration magnitude that would be achievable by brake force alone will be  $\mu \cdot g$  (under optimal brake-force distribution). The coefficient of road adhesion is usually around 0.85 for dry asphalt surfaces. As a result, the maximum achievable deceleration magnitude is  $0.85g$ .

Therefore, during braking, a controller has to accelerate on an uphill, only when the deceleration magnitude achieved through the disturbance grade force  $W \sin(\theta)$  alone is greater than  $0.85g$ . However, assuming maximum road grade of  $8^\circ$ , the resulting maximum possible deceleration magnitude is only around  $\frac{m \cdot g \cdot \sin(8^\circ)}{m} = 0.14g$ . Since  $0.14g < 0.85g$ , a controller never accelerates on an uphill. It only regulates the brake force magnitude and continues tracking its reference deceleration.  $\square$

In conclusion, our controller-based space buffer computations performed for flat roads need no changes for uphill road profiles. In the next section, we consider downhill road profiles and discuss whether any modifications are necessary.

### 5.4.3. Considering downhill road profiles

So far, we considered that vehicles brake on a flat road (i.e.,  $\theta = 0$ ) and designed brake-by-wire controllers as explained above. These controllers will track their assigned decelerations on an uphill too. If vehicles enter a downhill, the brake-by-wire controllers still attempt to compensate the (disturbing) grade force by applying a greater brake force. Now, if the necessary increase in brake force does not exceed the maximum possible, our brake-by-wire controllers will be able to maintain the desired deceleration they were designed for. Hence, the vehicles' stopping distances continue to be those of the flat road, i.e., the whole platoon can safely brake in the downhill too.



On the other hand, if the required increase in brake force exceeds the maximum possible by any vehicle, e.g., in a pronounced downhill, the corresponding brake-by-wire controller saturates and will be unable to reach its desired deceleration, yielding a longer stopping distance for the affected vehicle. As a result, it cannot be guaranteed that the whole platoon brakes in a safe manner anymore. We refer to this as a *distress situation*. Recall that vehicles are sorted in the order of increasing stopping distances. Therefore, this situation is common in vehicles towards the end of a platoon as proven next.

Note that vehicles in the platoons middle can be under distress (without the trail vehicles being affected) only in case of anomalies such as snow/oil/glaze on the road. However, we restrict our discussion to distress arising due to changing road profiles, particularly, when entering a downhill as mentioned above.

**Theorem 2.** *Let us assume that  $n$  vehicles in a platoon are sorted (starting from the lead) in the order of their increasing stopping distances on a flat road. As a result, when braking in a downhill of constant grade  $\theta$ , if any vehicle  $i$  incurs distress, i.e., it is unable to track its assigned deceleration from the flat road, every vehicle  $j$  following  $i$  with  $i < j \leq n$  will also be under distress.*

*Proof.* The sum of all the forces acting on a two-axle vehicle results in an overall deceleration  $d$  in a downhill — note that we only include indexes where necessary to distinguish between different vehicles. As per (5.4.2), the resultant deceleration is given by:

$$\frac{F_b}{m} + (f_r \cdot g \cdot \cos(\theta)) + \frac{C_A V^2}{m} \pm (g \cdot \sin(\theta)) = d, \quad (5.4.4)$$

where  $V$  is the vehicle's velocity at an arbitrary point in the downhill. On a flat road, i.e., for  $\theta = 0$ ,  $\frac{F_{b,i}}{m_i} + \frac{C_{A,i} V_i^2}{m_i} \geq \frac{F_{b,j}}{m_j} + \frac{C_{A,j} V_j^2}{m_j}$  holds for all vehicles with  $i < j \leq n$ . (Note again that  $f_r \cdot g \cdot \cos(\theta)$  is the same for all vehicles in the downhill, since  $\theta$  is assumed to be constant.) That is, vehicles are sorted in the order of their increasing stopping distances and, hence, vehicle  $i$  decelerates at a rate that is higher than or equal to that of vehicle  $j$ .

On the other hand, the term  $g \cdot \sin(\theta)$  starts playing a role. However, since  $\theta$  is constant, this term is again independent of the vehicle in question and, hence, the above inequality remains valid. In other words, if the better-braking vehicle  $i$  is under distress in the downhill, any worse-braking vehicle  $j$  will also be under distress, which proves this theorem.  $\square$

**Corollary 1.** *If the whole platoon is in a downhill and multiple vehicles are under distress, the last vehicle in the platoon, i.e., the trail, is the most distressed one, deviating the most from braking on a flat road.*

Hence, in distress situations, it is extremely important that the same is communicated to all other vehicles through a distress message broadcast. Then, all the other vehicles perform certain computations based on information contained in the distress message, and arrive at their respective new decelerations that have to be tracked in order to ensure a safe brake maneuver. This entire cooperative/coordination scheme among vehicles in distress situations is detailed in the next chapter.

## 5.5. Key findings

In this chapter, we considered realistic conditions of braking — changing road profiles and non-instantaneous deceleration tracking — and reasoned why the stopping distance values computed as per the standard expression (i.e., Eq. (2.3.9)) cannot be used in our space buffer computations. To address this shortcoming, we introduced brake-by-wire controllers based

on certain performance specifications. Once emergency braking is initiated, these controllers present at each vehicle track an assigned deceleration computed as per our approach.

To address controller-related effects and, thereby, non-instantaneous deceleration tracking, we derived an expression that computes a vehicle's stopping distance under controller action. Through an example, we demonstrated how this analytically computed value matches that of our highly accurate simulation. Hence, the resulting stopping distances of all vehicles from this controller expression have to be used in the space buffer computations, rather than relying on the standard expression of stopping distance.

To address the other realistic condition of changing road profiles, we initially proved that vehicle ordering, for example on a flat road, remains the same on all other road profiles as well. Further, we considered uphill road profiles and discussed how the space buffer computations done for a flat road still remain valid. However, in a downhill, some vehicles, particularly, towards the end of a platoon are unable to track their respective reference decelerations due to their actuators' saturation. In such situations, to avoid inter-vehicle collisions they broadcast distress messages and a coordination scheme is required among vehicles to ensure collision-free brake maneuvers. This cooperative/coordination scheme is discussed in detail in the next chapter.

## Chapter 6.

# Engineering a cooperative behavior

Since we minimize the stopping distance on a flat road, some of the vehicles, particularly towards the end of the platoon, work already very close to their maximum achievable decelerations. It may thus occur that one such vehicles is unable to keep track with the others, for example, if the platoon enters a downhill, broadcasting a distress message. The required cooperative behavior in such a situation is the focus of this chapter.

In a distress situation, the necessary actions to be performed by the vehicles can be separated into two different categories. The first category comprises vehicle(s) that cannot track their assigned reference deceleration(s), which are henceforth referred to as *distressed vehicle(s)*. Note that in case of more than one vehicle in distress, the most distressed vehicle has to be considered simply disregarding all others. The other category includes all the less or non-distressed vehicles that can no longer continue braking at their originally assigned decelerations and have to adapt them according to the most distressed vehicle.

### 6.1. Actions by distressed vehicles

Every vehicle in the platoon checks for its current deceleration after the settling time has elapsed (400ms as per our specifications), and if there is an error with respect to its assigned deceleration, it broadcasts a distress message as detailed below. Recall that, independent of whether a distress message is sent or not, every vehicle has to send an *asynchronous* live signal to its immediately following vehicle (with an update of its deceleration, speed, and position) as mentioned in Section 4.1.

The contents of the distress message are the distressed vehicle's index  $dis$  (based on which the most distressed vehicle can be identified as per Corollary 1, i.e., the vehicle with the greatest index in  $1 \leq dis \leq n$ ), the minimum remaining space buffer  $B_{min}$  and the maximum stopping distance  $S_{max}$  that results from vehicle  $dis$  being under distress.

Based on the information provided in the live signal from its immediately leading vehicle, a distressed vehicle can compute  $B_{dis}$  as per (4.1.1).  $B_{min}$  is then computed as follows:

$$B_{min} = B_{dis} - \left( V_{dis} - (V_{dis-1} - |d_{dis-1}| \cdot (t_{dis} - t_{dis-1})) \cdot 0.02 - \frac{1}{2} \cdot (|d_{dis-1}| - |d_{dis}|) \cdot 0.02^2 \right), \quad (6.1.1)$$

that is,  $B_{dis}$  minus the expected amount of space buffer that is consumed between vehicles  $dis$  and  $dis-1$  in 20ms. This is because other vehicles start adapting to the distress situation with a delay of 20ms, i.e., one sample period, which needs to be accounted for as explained later in more detail. Note that vehicle  $dis-1$ 's speed is given by  $V_{dis-1} - |d_{dis-1}| \cdot (t_{dis} - t_{dis-1})$ , at time  $t_{dis}$ , at which vehicle  $dis$  computes  $B_{min}$ . Further,  $B_{min}$  is a conservative measure that considers the minimum remaining space buffer up to vehicle  $dis$ , which might not necessarily

be between  $dis - 1$  and  $dis$ ,<sup>1</sup> and reduces it by the greatest possible amount that results from  $dis$  being the most distressed vehicle — see again Theorem 2 and its corollary.

Finally, the stopping distance (or final position at standstill) of the vehicle  $dis$  denoted as  $S_{dis}$  is computed using (2.3.9). It should be noted that (5.3.5) is not valid when the controller is saturated and, hence, unable to track its assigned deceleration. However, since its (saturated) deceleration remains constant, we can still use the standard expression of (2.3.9) to compute its stopping distance. Then, from  $S_{dis}$ , we calculate  $S_{max}$  as:

$$S_{max} = S_{dis} - \left( V_{dis} \cdot 0.02 - \frac{1}{2} \cdot |d_{dis}| \cdot 0.02^2 \right), \quad (6.1.2)$$

that is,  $S_{dis}$  is reduced during the  $20ms$  delay required by other vehicles to start adapting to the distress situation and this is considered by  $S_{max}$ .

Note that apart from multiple vehicles broadcasting their distress messages, cascaded distress messages from the same vehicle are also possible. This might happen when a vehicle that had previously broadcast a distress message has entered another downhill that is much steeper. For example, when the vehicle was initially distressed due to a  $4^\circ$  downhill and, it then entered a much steeper downhill of  $8^\circ$ . In such a scenario, the vehicle is more distressed in the steeper downhill and, hence, its stopping distance will be longer. Therefore, the vehicle has to broadcast a separate distress message with the updated information.

On the contrary, if a previously distressed vehicle enters a flat road (instead of entering a steeper downhill), it can broadcast a *de-distress message* indicating that it is no longer distressed. All the other vehicles can then switch back to tracking their originally assigned decelerations (computed for a flat road) and the overall stopping distance of the platoon can be reduced.

## 6.2. Actions by less or non-distressed vehicles

Once a distress message is broadcast at  $t_{dis}$ , all vehicles receive it almost instantaneously (recall that we assume a negligible propagation delay). The above mentioned contents of the distress message are processed by all less or non-distressed vehicles that need to start adapting by computing their new deceleration values within a  $20ms$  delay (i.e., one sample period) and begin tracking the same.

Considering  $S_{max}$  and  $B_{min}$  from the distress message, a vehicle  $i$  with  $1 \leq i < dis$  first computes a stopping distance  $S_i^{new}$  in  $m$  that has to be covered from the point in time of beginning to track its new deceleration:

$$S_i^{new} = S_{max} - (dis - i)B_{min}. \quad (6.2.1)$$

Let us first assume an instantaneous deceleration switching. As a result, we can compute the constant deceleration  $d_i^{new}$  that brings the vehicle to standstill in a distance  $S_i^{new}$ :

$$V_i^2 + 2|d_i^{new}|S_i^{new} = 0, \quad (6.2.2)$$

where  $V_i$  is vehicle  $i$ 's velocity at  $t_{dis} + 0.02$ , i.e., the point in time of starting to track its new deceleration, which is an amount  $|d_i| \cdot 0.02$  smaller than the speed at  $t_{dis}$ . In other words, from receiving the distress message until switching to the new deceleration  $d_i^{new}$ , vehicle  $i$  continues braking at its originally assigned deceleration  $d_i$  for the duration of  $20ms$ .

---

<sup>1</sup>However, it is always the distressed vehicles that use up more space buffer to their immediately leading vehicles in comparison to the non-distressed vehicles. This is because the distressed vehicles are decelerating at a lesser magnitude than their assigned ones. As a consequence, they are closer to their respective immediately leading vehicles, thereby, consuming more space buffer.

However, the brake-by-wire controller cannot switch instantaneously to  $d_i^{new}$ , but it rather undergoes a transition until it settles after 400ms as per our specifications. We need to consider this additional trajectory to avoid collisions in the transition from one deceleration to another. To this end, we proceed similar to before letting  $\Delta D_i(s)$  denote the difference between  $|d_i|$  and  $|d_i^{new}|$  in the frequency domain  $s$  with  $|d_i| > |d_i^{new}|$ .

Multiplying  $\Delta D_i(s)$  with the closed-loop transfer function of (5.3.1), the expression of the output, i.e., the transition from one deceleration to the other, can be obtained by decomposing into partial fractions similar to (5.3.2). Applying the inverse Laplace transform, we obtain an expression in the time domain  $t$  denoted by  $\Delta d_i(t)$ .

On the other hand, the vehicle is undergoing a transition from its current to the new deceleration. Hence, the current deceleration's expression  $d_i(t)$  and the deceleration difference's expression  $\Delta d_i(t)$  need to be superposed from  $t \geq t_{dis} + 0.02$  onwards. This is possible for a LTI system like ours [60]:

$$\begin{aligned} d_i(t) + \Delta d_i(t) = & R_1 e^{p_1 t} + R_2 e^{p_2 t} + R_3 e^{p_3 t} + R_4 e^{p_4 t} + \tilde{R}_1 e^{p_1(t-(t_{dis}+0.02))} \\ & + \tilde{R}_2 e^{p_2(t-(t_{dis}+0.02))} + \tilde{R}_3 e^{p_3(t-(t_{dis}+0.02))} + \tilde{R}_4 e^{p_4(t-(t_{dis}+0.02))}. \end{aligned} \quad (6.2.3)$$

Although it is not evident from (6.2.3), note that the expression of  $\Delta d_i(t)$  represents the decrease in deceleration, i.e., it diminishes function  $d_i(t)$ 's value from the initial  $d_i$  at  $t_{dis} + 0.02$  to  $d_i^{new}$  at  $t_{dis} + 0.42$  (from which it remains constant). Integrating (6.2.3), we obtain the expression of velocity as:

$$\begin{aligned} v_i(t) + \Delta v_i(t) = & \frac{R_1 e^{p_1 t}}{p_1} + \frac{R_2 e^{p_2 t}}{p_2} + \frac{R_3 e^{p_3 t}}{p_3} + \frac{R_4 e^{p_4 t}}{p_4} + \frac{\tilde{R}_1 e^{p_1(t-(t_{dis}+0.02))}}{p_1} + \frac{\tilde{R}_2 e^{p_2(t-(t_{dis}+0.02))}}{p_2} \\ & + \frac{\tilde{R}_3 e^{p_3(t-(t_{dis}+0.02))}}{p_3} + \frac{\tilde{R}_4 e^{p_4(t-(t_{dis}+0.02))}}{p_4} + V_i + C_3, \end{aligned} \quad (6.2.4)$$

where  $V_i + C_3$  is an integration constant similar to before and  $V_i$  is again the vehicle  $i$ 's speed at time  $t_{dis} + 0.02$ . Further, integrating (6.2.4), we obtain the expression of distance as:

$$\begin{aligned} s_i(t) + \Delta s_i(t) = & \frac{R_1 e^{p_1 t}}{p_1^2} + \frac{R_2 e^{p_2 t}}{p_2^2} + \frac{R_3 e^{p_3 t}}{p_3^2} + \frac{R_4 e^{p_4 t}}{p_4^2} + \frac{\tilde{R}_1 e^{p_1(t-(t_{dis}+0.02))}}{p_1^2} + \frac{\tilde{R}_2 e^{p_2(t-(t_{dis}+0.02))}}{p_2^2} \\ & + \frac{\tilde{R}_3 e^{p_3(t-(t_{dis}+0.02))}}{p_3^2} + \frac{\tilde{R}_4 e^{p_4(t-(t_{dis}+0.02))}}{p_4^2} + V_i t + C_3 t + S_i + C_4, \end{aligned} \quad (6.2.5)$$

where again  $S_i + C_4$  is a constant of integration with  $S_i$  representing vehicle  $i$ 's position in  $m$  at  $t_{dis} + 0.02$  relative to its position at the moment of braking.

Now, vehicle  $i$  has to cover a distance of  $S_i^{new}$  from time  $t_{dis} + 0.02$  until it reaches standstill. If we calculate the time at which the vehicle reaches standstill and evaluate (6.2.5) between the two limits, the distance covered can be obtained. The time to reach standstill when transitioning to  $d_i^{new}$  can either be obtained analytically from (6.2.4) or computed numerically. For the sake of simplicity, we opt to use the numerical approach.

In this direction, we begin by substituting  $t = t_{dis} + 0.02$  in (6.2.4) and iterate in steps of 20ms, i.e., the brake-by-wire controller's sampling time, until the value of (6.2.4) becomes zero (or slightly less than zero). In other words, at time  $t_{dis} + 0.02$ , the vehicle  $i$ 's velocity is equal to  $V_i$  and as time increases the velocity gradually approaches and becomes zero (or slightly less than zero). This stopping time and  $t_{dis} + 0.02$  when substituted as the limits in (6.2.5) yield the stopping distance covered by the vehicle.

However, the distance covered will always be less than the required  $S_i^{new}$ , since transitioning from  $|d_i|$  to settling at  $|d_i^{new}|$  yields a trajectory that is shorter than that intended with the constant  $|d_i^{new}|$ , i.e., the vehicle continues braking at a higher magnitude than the intended new one for some time.

In order to make vehicle  $i$  cover a distance of  $S_i^{new}$ , we have to reduce the magnitude of  $d_i^{new}$ , i.e., the vehicle has to transition to a deceleration that is of a lower magnitude than  $|d_i^{new}|$ . For simplicity, we again opt for the numerical approach. Hence, we reduce the magnitude of  $d_i^{new}$  in steps of 0.01.<sup>2</sup> Let  $|d_{i,k}^{new}|$  denote the reduced magnitude where  $k$  is the iteration and takes a value  $\{1, 2, 3, \dots\}$ . Then, we compute the difference between  $|d_i|$  and  $|d_{i,k}^{new}|$  in the frequency domain  $s$ , multiply the difference with the closed-loop transfer function of (5.3.1) and obtain the corresponding residues as per (5.3.2).

Through inverse Laplace transform, we obtain the deceleration transition's expression in the time domain and, similar to before using (6.2.4) and (6.2.5) respectively, we compute the new stopping time of the vehicle and the corresponding distance covered. Let  $S_{i,k}^{new}$  denote the distance covered with the corresponding reduced magnitude of deceleration. If  $S_{i,k}^{new} \geq S_i^{new}$  we stop the numerical iteration and the vehicle transitions to the corresponding  $d_{i,k}^{new}$  rather than to the initially computed  $d_i^{new}$ . On the contrary, if  $S_{i,k}^{new} < S_i^{new}$ , we repeat the process by reducing the magnitude from the previous iteration until  $S_{i,k}^{new} \geq S_i^{new}$ .

Note that even though the computations are iterative, the numerical solution space to be explored to arrive at the deceleration value is bounded between  $|d_i^{new}|$  and a value close to  $|d_{dis}|$ . This is because any of the less or non-distressed vehicles will never decelerate at a magnitude that is much less than that of the most distressed vehicle. As a result, the numerical solution can be computed well within 20ms (as shown later with an example).

Finally, it is not possible for all the less or non-distressed vehicles to cover a distance of exactly  $S_i^{new}$ . There will be minor differences between the achieved stopping distance  $S_{i,k}^{new}$  and the required  $S_i^{new}$ . This is because we iteratively reduce the deceleration value in steps of 0.01 (until  $S_{i,k}^{new} \geq S_i^{new}$ ) and, hence, quantization error might be incurred.

**An example.** Consider a 10-vehicle platoon with  $2m$  ( $B = 1m$ ) inter-vehicle separations on a downhill slope of  $4^\circ$ . Assume that the last 2 vehicles are unable to track their respective reference decelerations due to their actuators' saturation. As per Theorem 2 and the corollary, the last vehicle is the most distressed. As a result, its distress message broadcast after 400ms of initiating an emergency brake maneuver is considered by all other vehicles. This distress message has all the necessary details. For example, assume  $S_{max}$  is 95.42m, and  $B_{min}$  is 0.99m (from the initial 1m). Note that there is a difference of only 0.01m due to downhill grade of only  $4^\circ$  and early broadcast of distress message (i.e., after 400ms). For road profiles steeper than  $4^\circ$  or if distress situation arises much later, i.e., braking on flat road and then entering a downhill, more space buffer will be consumed and, hence,  $B_{min}$  would be lesser.

All the other vehicles process data in the distress message and adapt their decelerations. As an example, we consider the computations done by the 8<sup>th</sup> vehicle in the platoon. This vehicle has to achieve  $S_i^{new}$  of 93.44m from time 420ms (20ms after distress message broadcast) onwards and, as a result, the corresponding  $|d_i^{new}|$  is  $4.37m/s^2$ . The vehicle has to switch from its current deceleration  $|d_i|$  of  $4.82m/s^2$  to  $|d_i^{new}|$ . This difference of  $0.45m/s^2$  corresponds to  $\Delta d_i$ . From (6.2.4), the vehicle reaches standstill at time 6.96s after it begins transitioning to the new deceleration magnitude of  $4.37m/s^2$  at time 420ms. Substituting these two time limits in (6.2.5) yields a shorter stopping distance of 93.15m rather than the required 93.44m.

Hence, we reduce the magnitude of  $|d_i^{new}|$  from  $4.37m/s^2$  to  $4.36m/s^2$  as explained above. This new magnitude  $|d_{i,1}^{new}|$  produces a corresponding  $S_{i,1}^{new}$  of 93.36m. Since  $S_{i,1}^{new} < S_i^{new}$ , we proceed further and reduce the magnitude to  $4.35m/s^2$ . This new magnitude  $|d_{i,2}^{new}|$  produces a corresponding  $S_{i,2}^{new}$  of 93.56m. Since  $S_{i,2}^{new} > S_i^{new}$ , we stop the numerical computations. Therefore, the vehicle switches to a deceleration magnitude of  $4.35m/s^2$  (from the originally assigned magnitude of  $4.82m/s^2$ ) such that collisions are avoided and a safe brake maneuver is guaranteed. Note that the vehicle covers a stopping distance that is only 0.12m (93.56m –

<sup>2</sup>Recall that as per our assumptions our brake-by-wire controllers can track a deceleration accurately up to two-decimal places. Hence, the value of 0.01 is chosen.

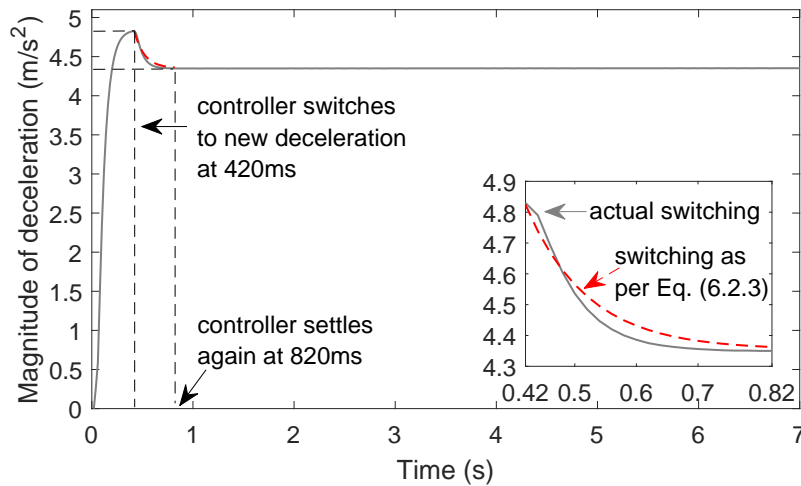


Figure 6.1.: Vehicle 8’s deceleration switching from a  $4.82m/s^2$  to a  $4.35m/s^2$  magnitude during a distress situation

93.44m) longer than the required value and the corresponding deceleration magnitude was computed with just two iterations.

The above such computations are performed similarly at each individual vehicle requiring only two iterations as for the shown case. Similar to the 8<sup>th</sup> vehicle, all up to the 7<sup>th</sup> vehicle cover distances that are longer than their intended ones by 0.02m, 0.03m, 0.16m, 0.12m, 0.04m, 0.04, and 0.15m respectively. Also, the 9<sup>th</sup> vehicle covers a distance that is 0.12m longer than intended. Note that this difference in the resulting stopping distance has to be compensated by the safeguard (*SG*). However, this is not much and only varies from 1cm between the lead and its immediately following vehicle to 13cm between the 2<sup>nd</sup> and 3<sup>rd</sup> vehicle.

The actual deceleration transition by the 8<sup>th</sup> vehicle (as simulated in Matlab/Simulink) and its analytically computed counterpart as per (6.2.3) can be seen in Fig. 6.1. Note again that the controller settles much faster in simulation than the analytically computed trajectory. This is because in the simulation the non-linear aerodynamic and rolling resistances are also acting on the vehicle, whereas the analytical expression considers that only the brake force is acting on the vehicle.

### 6.3. Key findings

In this chapter, we considered the other realistic condition of braking, i.e., changing road profiles, in detail. Particularly, we dealt with downhill road profiles which present the most challenging conditions for emergency braking. In a downhill, the decelerations computed for a flat road cannot be tracked by all vehicles. This situation is common in vehicles that are present towards the end of a platoon. We refer to such situations as distress.

In a distress situation, the actions to be performed by distressed vehicles were outlined. They simply broadcast distress messages which contain crucial information required by the non-distressed vehicles, who no longer can continue braking at their previous assigned decelerations and, hence, have to adapt them. In case of multiple vehicles in distress, the most distressed vehicle’s message is considered by all the other vehicles, including the one whose distress message was broadcast, but not considered due to the presence of the most distressed vehicle.

The distress message contents are processed and all the necessary computations performed within 20ms to arrive at the new deceleration to be tracked were detailed. Hence, after a dis-

distress message broadcast, all the vehicles begin simultaneously tracking their new decelerations  $20ms$  later.

Thus, through the coordination scheme introduced in this chapter, we ensure that inter-vehicle collisions are avoided in distress situations and the whole platoon brakes in a safe manner, while simultaneously minimizing the overall stopping distance. In the next chapter, we perform a detailed evaluation of our Space-Buffer approach and demonstrate that this coordination among vehicles guarantees safe braking.



# Chapter 7.

## Evaluation and simulation

In this chapter, we present an extensive evaluation of our Space-Buffer approach. To begin with, we study the impact of platoon braking on stopping distance. Then, we assume idealized conditions of braking and compare the performance of our Space-Buffer approach with the intuitive approaches — Least Platoon Length and Least Stopping Distance — and the Subplatoon approach. Subsequently, we consider realistic conditions of braking and simulate the platoon to brake on different road profiles. Finally, we address packet losses and analyze the number of packets that can be safely lost in all of the approaches.

### 7.1. The impact of platoon braking on stopping distance

In this section, we simulate a 3-vehicle platoon and demonstrate the impact on the stopping distance when braking in a platoon. We use the intuitive Least Platoon Length as the emergency braking approach in this example. The lead vehicle can decelerate at a maximum of  $0.7g$ . However, the two following vehicles have heterogeneous deceleration capabilities, in particular, the weakest vehicle can decelerate at only  $0.6g$ . Hence, to ensure safe emergency braking, the whole platoon has to decelerate at only  $0.6g$ .

As shown in Fig. 7.1, we log the positions of the platoon lead on the road just before it begins braking and continue until it comes to a complete standstill. This is done for both the cases of traveling in isolation and in platoon. The platoon and vehicle cruise velocity is around  $100km/h$  when emergency braking is initiated.

Since the lead vehicle can brake at a maximum deceleration of  $0.7g$  in isolation, its stopping distance is shorter than braking in the platoon. Further, when operating in the platoon due to the reduced aerodynamic force as well, the lead vehicle takes longer to arrive at standstill. This difference is approximately around  $9m$  for this configuration of three vehicles.

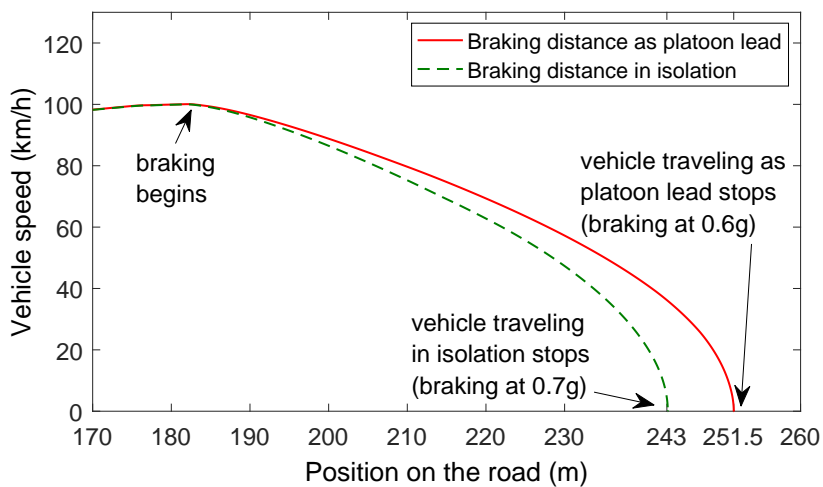


Figure 7.1.: Impact of platoon braking on stopping distance

In conclusion, to account for the heterogeneous deceleration capabilities of vehicles, and also due to the reduced aerodynamic force, a vehicle's stopping distance will always be longer in a platoon than that achieved in isolation.

## 7.2. Braking under idealized conditions

In this section, we assume idealized conditions of braking, i.e., instantaneous deceleration tracking and braking on a flat road, and demonstrate the effectiveness of our Space-Buffer approach. We compare its performance against the intuitive approaches and the Subplatoon approach on the basis of achieved aerodynamic benefits, platoon length, and stopping distance. For this comparison, we consider longer platoons of 20 vehicles and perform our simulations in Matlab/Simulink.

### 7.2.1. Test data

The following vehicle data was randomly generated. Vehicles up to  $3500\text{kg}$  are considered to be passenger cars in Europe. As a result, we chose the vehicle masses  $m$  to be in the range of  $1000\text{kg} - 3500\text{kg}$  and, their frontal areas  $A_f$  in the range of  $2\text{m}^2 - 2.5\text{m}^2$ . The aerodynamic coefficients  $C_D$  of production cars are in the range of  $0.311 - 0.475$  [48] and, hence, the same was chosen.

We consider dry asphalt road conditions and, hence, the coefficient of road adhesion  $\mu$  is 0.85. This also implies that under optimal brake-force distribution to the axles, vehicles can achieve a maximum deceleration of  $0.85g$  (in magnitude). Decelerations greater than  $0.40g$  in magnitude are uncomfortable for in-vehicle passengers [61]. As a result, we treat decelerations above  $0.40g$  as emergency braking. Therefore, to simulate heterogeneous maximum deceleration capabilities of platoon vehicles, we randomly choose a value in the  $0.5g - 0.8g$  range for each vehicle. Note that due to the equivalent mass factor  $\gamma_m$ , with a common value of 1.05, the corresponding maximum decelerations would be lesser in magnitude.

Apart from the equivalent mass factor, there are certain other parameters that are common for all the vehicles. These are the coefficient of rolling resistance  $f_r = 0.015$ , the air-mass density  $\rho = 1.225\text{kg/m}^3$ , acceleration due to gravity  $g = 9.8\text{m/s}^2$ , and a vehicle length of  $5\text{m}$ . Further, all vehicles are assumed to be of the same height for ease of computing aerodynamic benefits. Finally, two important parameters with respect to braking are the platoon cruise velocity, and the dead time of brake-by-wire systems. All vehicles are assumed to be traveling at a common cruise velocity of  $30\text{m/s}$  ( $108\text{km/h}$ ) before emergency braking is initiated. Then, all individual brake-by-wire systems are assumed to have a common dead time of  $0.1\text{s}$ . Therefore, all vehicles travel a distance of  $3\text{m}$  ( $30 \cdot 0.1$ ) before actually starting to decelerate.

### 7.2.2. Method of performing the simulations

Based on the values of vehicle parameters mentioned above, we randomly generate 20 vehicles. This constitutes one dataset. An example dataset is shown in Table 7.1.<sup>1</sup> Then, vehicles represented by  $ID$  join in the same order (i.e., the order of increasing stopping distances), and operate in a platoon. Hence, the number of vehicles gradually increases from 1 to 20. Recall that for the Subplatoon approach, a suitable lead has to be chosen. Table 7.2 shows the corresponding maximum deceleration capability of the selected lead from this dataset

<sup>1</sup>Note that we use  $m$  for mass as well as for the unit meter. However, these can be easily distinguished depending on the context. In addition, for denoting the maximum deceleration we normalize it as  $g$ . This is the acceleration due to gravity, and not the weight unit gram.

Table 7.1.: An example of one dataset of vehicles

ID	$m$ (in $kg$ )	max. $ d $ (in $g$ )	$C_D$	$A_f$ (in $m^2$ )	ID	$m$ (in $kg$ )	max. $ d $ (in $g$ )	$C_D$	$A_f$ (in $m^2$ )
1	2034	0.79	0.384	2.16	11	1138	0.61	0.419	2.44
2	2456	0.78	0.396	2.46	12	1499	0.62	0.370	2.16
3	2493	0.74	0.371	2.36	13	1845	0.60	0.465	2.25
4	1915	0.73	0.419	2.18	14	2207	0.59	0.369	2.34
5	2823	0.72	0.377	2.35	15	3234	0.58	0.406	2.18
6	1376	0.71	0.435	2.05	16	1965	0.57	0.440	2.09
7	1062	0.69	0.453	2.13	17	3180	0.54	0.452	2.38
8	1942	0.67	0.319	2.02	18	2832	0.52	0.442	2.34
9	1661	0.65	0.333	2.04	19	1176	0.51	0.331	2.42
10	2080	0.64	0.440	2.23	20	2753	0.50	0.385	2.35

as the number of vehicles gradually increase — again, only the case of two subplatoons is considered.<sup>2</sup>

For each platoon configuration from 1 to 20 vehicles, we compute the stopping distances as per (2.3.9), initiate emergency braking causing all the vehicles to brake simultaneously 20ms later. The stopping distances for all the four approaches are logged along with the achieved aerodynamic benefits, and the overall platoon length. This whole process is repeated for 100 such datasets. Once this is complete, we finally take the average of all the logged aerodynamic benefits, platoon length, and stopping distance values and present our results.

As previously mentioned in Section 4.5, we employ separations of just  $1m$  ( $SG$ ) in the Least Platoon Length approach. The same separation is also used within a subplatoon. Further, based on the chosen lead, the appropriate inter-subplatoon separation is maintained. The separations in the Least Stopping Distance approach are dependent on the difference in stopping distances of two consecutive vehicles plus  $SG$ . Finally, for the Space-Buffer approach, we vary the space buffer  $B$  as a design parameter and choose values of  $1m$ ,  $2m$ , and  $3m$  thereby, resulting in inter-vehicle separations of  $2m$ ,  $3m$ , and  $4m$  respectively. Recall that for separations of  $5m$  and beyond, there are no fuel/energy savings for the platoon lead [56] [57]. As a result, we do not increase the value of  $B$  beyond  $3m$ .

<sup>2</sup>Every time a new vehicle joins, the lead was selected by an exhaustive search, i.e., trying out each and every vehicle as the lead and choosing the one with more benefits. This results in a linear complexity on the number of vehicles joining the platoon.

Table 7.2.: Selected lead for the Subplatoon approach

Vehicle joining	max. $ d $ (in $g$ )	Vehicle joining	max. $ d $ (in $g$ )
1	0.79	11	0.72
2	0.79	12	0.79
3	0.78	13	0.79
4	0.74	14	0.71
5	0.73	15	0.71
6	0.74	16	0.71
7	0.73	17	0.71
8	0.73	18	0.71
9	0.72	19	0.71
10	0.72	20	0.71

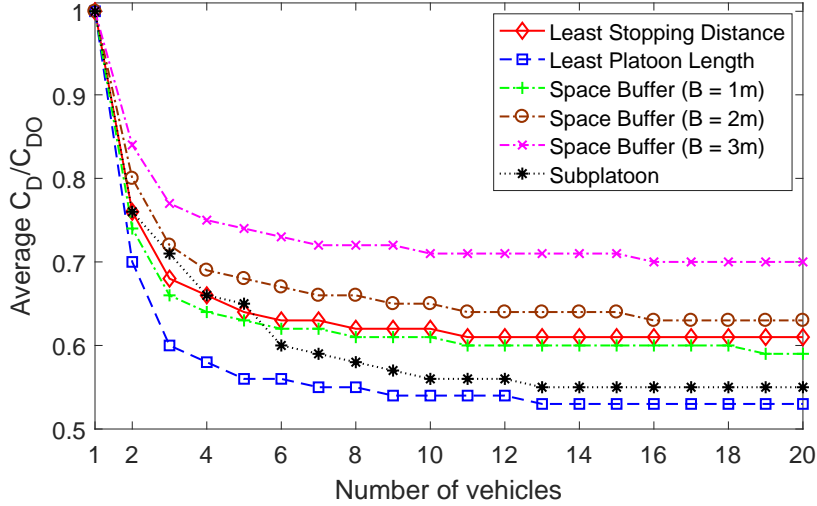


Figure 7.2.: Average drag coefficient ratio vs. number of vehicles

### 7.2.3. Aerodynamic savings, platoon length, and stopping distance

Fig. 7.2 shows the average drag coefficient ratio for the approaches as the number of vehicles increase (i.e., as vehicle 1 to 20 join the platoon). Clearly, at large separations of  $4m$  ( $B=3m$ ), the overall aerodynamic savings for the Space-Buffer approach are less. However, in comparison to the existing separations employed in platooning, i.e.,  $5$  to  $10m$  and beyond, these benefits are much better as even the lead vehicle has benefits.

In contrast to the Space-Buffer approach ( $B=3m$ ), Least Platoon Length achieves optimum values by around 17% from 3 vehicles onwards. This is because it maintains inter-vehicle separations of just  $1m$ . Similarly, the Subplatoon approach has a deviation of only 2% from the optimum for 13 vehicles and more. This slight difference is due to the large inter-subplatoon separation.

At inter-vehicle separations of  $2m$  ( $B=1m$ ) for 20 vehicles, the Space-Buffer approach has a maximum deviation of just 6% when compared to the optimum and only 4% when compared to the Subplatoon approach. For  $3m$  ( $B=2m$ ) separations, this deviation with respect to the optimum increases to 10%. The Least Stopping Distance approach also achieves approximately the same benefits but performs slightly better. This is because in case of vehicles with similar braking capabilities the separations will be very close to  $SG$ , where as in the Space-Buffer approach the separations are always constant.

Interestingly, all approaches' aerodynamic benefits stagnate for more than 12 vehicles. As previously mentioned in Section 2.2.2, these savings become smaller and asymptotically approach a value of around 0.50 as the number of vehicles increase.

**An example:** Consider a vehicle cruising with a constant velocity  $V$  on a flat road. Its mass  $m$  is  $2000kg$ , coefficient of aerodynamic resistance  $C_D$  is 0.4, frontal area  $A_f$  is  $2m^2$ , coefficient of rolling resistance  $f_r$  is 0.015, and the air-mass density  $\rho$  is  $1.225kg/m^3$ . The ratio of liters of fuel consumed per kilometer to overcome aerodynamic resistance to the total liters of fuel consumed per kilometer by a vehicle is given by [57]:

$$\frac{[liters/km]_{Aerodyn}}{[liters/km]_{Total}} = \frac{\frac{\rho}{2}C_D A_f V^2}{\frac{\rho}{2}C_D A_f V^2 + f_r W}. \quad (7.2.1)$$

Assume a distance of  $200km$  is covered in isolation consuming 10 liters of fuel. If another vehicle follows at a separation of  $1m$  for the whole distance, there is a reduction of 36% in the aerodynamic resistance on the lead vehicle — see again Fig. 2.3. Substituting these values

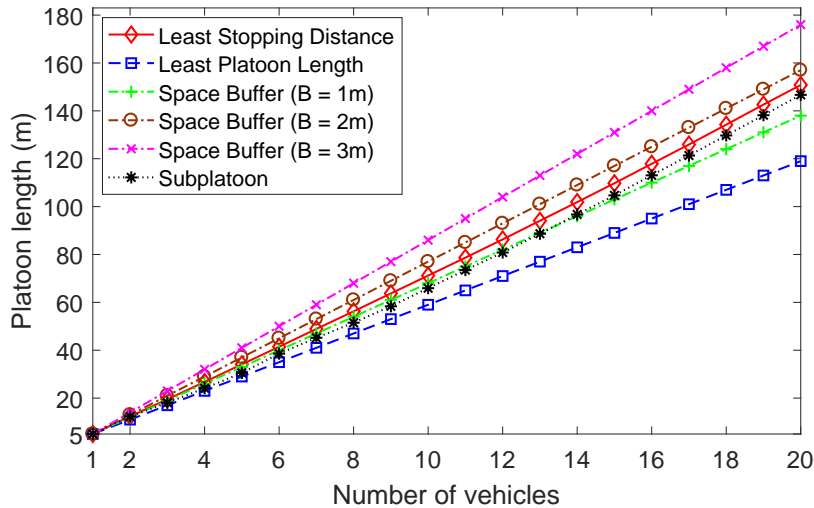


Figure 7.3.: Platoon length vs. number of vehicles

in (7.2.1), the lead vehicle now requires less than 7 liters of fuel to cover the same distance. From Fig. 7.2, for 20 vehicles, there is an average 47% reduction in aerodynamic force (for the optimum Least Platoon Length) leading to more fuel savings at each of the vehicles.

Fig. 7.3 shows the resulting platoon length for the different approaches. With constant inter-vehicle separations of  $1m$ , Least Platoon Length achieves the shortest length of  $119m$  for 20 vehicles making it ideal for coexistence with other road users. The next best platoon length of  $138m$  is achieved by the Space-Buffer approach at inter-vehicle separations of  $2m$  ( $B = 1m$ ). This is around  $9m$  shorter than the Subplatoon approach. This difference is due to the large inter-subplatoon separation.

At large separations of  $4m$  ( $B = 3m$ ), the Space-Buffer approach results in the longest platoon of  $176m$  for 20 vehicles. The Least Stopping Distance approach is approximately 5 vehicle lengths (i.e.,  $25m$ ) shorter than this longest platoon. However, at separations of  $3m$  ( $B = 2m$ ), this difference reduces to just around 1.2 vehicle lengths (i.e.,  $6m$ ), with the Least Stopping Distance approach being the shorter one. This longer platoon length of the Space-Buffer approach can be reasoned again by the fact that inter-vehicle separations are always constant (either  $3m$  or  $4m$ ), irrespective of whether the difference in deceleration capabilities of consecutive vehicles is very little or significant. On the contrary, in the Least Stopping Distance approach, if the deceleration capabilities are identical, their separations are reduced to just  $1m$   $SG$  leading to shorter platoon length.

Fig. 7.4 shows the stopping distances that can be achieved with these approaches. The platoon cruise speed was  $30m/s$  ( $108km/h$ ) when emergency braking was initiated. The lead vehicle broadcasts the brake command, and  $20ms$  later simultaneously brakes together with all the following vehicles in all of the approaches. This  $20ms$  delay results in all the vehicles traveling a negligible  $0.6m$  ( $30 \cdot 0.02$ ). Further, after the vehicles begin braking, due to the time taken for activation of brakes they cover a distance of  $3m$  ( $30 \cdot 0.1$ ) before beginning to decelerate. Only this  $3m$  traveled is included in the values shown in Fig. 7.4.

Note that the stopping distance values presented here are greater than the stopping distance of the vehicles in isolation. As previously explained in Section 7.1, this is due to the consideration of heterogeneous deceleration capabilities and also partly due to the reduction of aerodynamic force on the vehicles during platoon operation.

The Least Platoon Length approach achieves the worst stopping distance of around  $95m$  for 20 vehicles and, is thereby, unsuitable for emergency braking. Even at  $B = 1m$ , the Space-

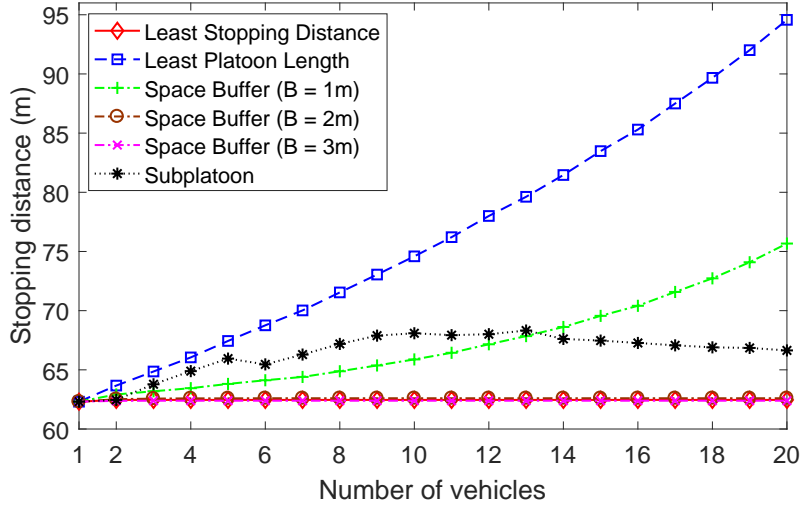


Figure 7.4.: Stopping distance vs. number of vehicles

Buffer approach outperforms Least Platoon Length and achieves a stopping distance that is  $20m$  shorter. In comparison to the Subplatoon approach, the achieved stopping distances are shorter for platoons of up to 13 vehicles. For longer platoons, the Subplatoon approach performs better than our Space-Buffer approach with  $2m$  separations ( $B = 1m$ ) due to the choice of a better braking vehicle as the platoon lead. However, the platoon becomes longer as previously shown in Fig. 7.3. For 20 vehicles, the difference in stopping distance between these approaches is around  $9m$ .

The optimum stopping distance of around  $63m$  for 20 vehicles is achieved by Least Stopping Distance as well as our Space-Buffer approach for separations of  $3m$  ( $B = 2m$ ) and  $4m$  ( $B = 3m$ ). More precisely, at  $3m$  separations ( $B = 2m$ ), our Space-Buffer approach has a difference of only  $0.1m$  to Least Stopping Distance with the latter performing better. However, at separations of  $4m$  ( $B = 3m$ ), our Space-Buffer approach outperforms the Least Stopping Distance approach marginally by  $0.07m$ . This can be explained by the fact that closer the inter-vehicle separations are to  $5m$ , lesser is the magnitude of tail wind experienced by the lead vehicle causing it to reach standstill in a shorter distance. Hence, this result is inline with the results presented in [56] [57].

Finally, one observation with respect to the Space-Buffer approach for all values of  $B$  is that it exhibits stagnation in the achieved stopping distance from 6 vehicles onwards. This can be reasoned by the same choice of vehicle  $x$  leading to the same  $S_{SB}$ .

#### 7.2.4. The impact of braking capacities

In this section, different ranges of maximum deceleration capabilities of vehicles are considered and their impact on the achieved aerodynamic benefits, platoon length, and stopping distance are analyzed. The method used for generating the test data and performing the simulations is the same as mentioned before. Additionally, we vary the range of vehicle braking capacities from  $0.8g - 0.8g$  till  $0.5g - 0.8g$  in steps of  $0.03$  keeping the number of vehicles constant at 20 for each range.

Fig. 7.5 shows the impact of vehicle braking capacities on the achieved aerodynamic benefits. Only the Least Stopping Distance and the Subplatoon approaches show a dependency on the range of braking capacities with higher benefits at identical braking capacities.

However, the achieved aerodynamic benefits by both these approaches at homogeneous braking capacities of  $0.8g$  have a very slight difference to the optimum value of around  $0.53$  achieved by Least Platoon Length. With respect to the Subplatoon approach, the difference is

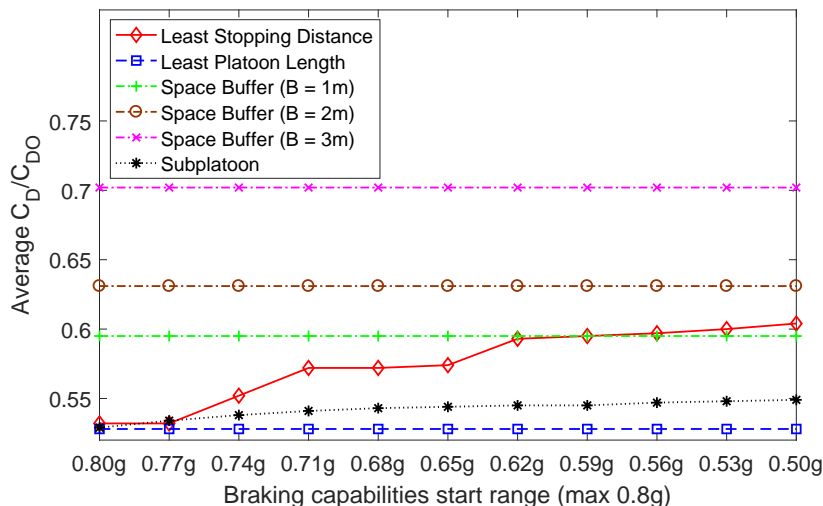


Figure 7.5.: Average drag coefficient ratio vs. range of braking capacities

almost negligible. This negligible deviation from the optimum is due to the inter-subplatoon separation that is a little longer than  $SG$ , whereas in the Least Platoon Length it is always the constant  $1m$ . Similarly, with respect to Least Stopping Distance, the vehicle weights impact their stopping distances and, as a result, separations are a little longer than  $1m$ .

As the range of braking capability increases, the aerodynamic benefits in the Least Stopping Distance and the Subplatoon approaches decrease. For the widest range of  $0.5g-0.8g$ , the ratio is around  $0.60$  for Least Stopping Distance, whereas for Subplatoon it is around  $0.55$  having only a difference of  $2\%$  to the optimum.

The Space-Buffer approach with  $2m$  separations ( $B=1m$ ) exhibits a constant ratio of around  $0.60$ . It has a difference of around  $7\%$  to the optimum. In the widest range of braking capacities, it performs slightly better than Least Stopping Distance. With respect to the Subplatoon approach, it has a deviation of around  $5\%$ .

Similarly, at  $3m$  separations ( $B=2m$ ), the ratio is also a constant  $0.63$  that is greater than the Least Stopping Distance approach across all ranges of braking capacities. With respect to the optimum, the difference is around  $10\%$ .

Finally, the worst aerodynamic benefits is achieved by the Space-Buffer approach at  $4m$  separations ( $B=3m$ ). This is due to the constant  $B$  which is not adapted to the range of braking capacities. Hence, irrespective of the range considered, the ratio is around  $0.70$ . The difference to the optimum is around  $17\%$ . Note that even though this value of  $B$  performs the worst among all the approaches, it is much better in comparison to the existing inter-vehicle separations employed in platooning, i.e.,  $5$  to  $10m$  and beyond.

Fig. 7.6 shows the relation between the range of braking capacities and the overall platoon length. Similar to the previously presented aerodynamic benefits, only the Least Stopping Distance and the Subplatoon approaches exhibit a dependency. With homogeneous braking capacities, the platoon lengths in all the approaches are approximately the same. Shorter, but varying inter-vehicle separations (due to vehicle weights impacting stopping distances) in Least Stopping Distance and slightly longer than  $1m$  inter-subplatoon separation in Subplatoon can be reasoned for these slight differences. The optimum value of  $119m$  is achieved by Least Platoon Length for all the ranges of braking capacities.

As the range gets wider, the platoon length increases linearly for Least Stopping Distance and Subplatoon. In the widest range, their platoon lengths are respectively around  $150m$  and  $145m$ . The shorter length achieved by the Subplatoon approach can be explained by the fact that inter-subplatoon separation is chosen as the difference in deceleration capacities

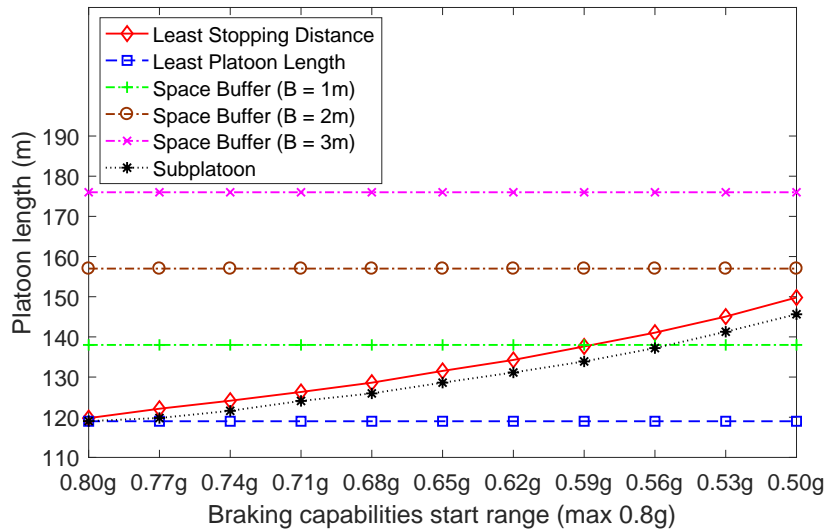


Figure 7.6.: Platoon length vs. range of braking capacities

of the selected platoon lead and the worst braking vehicle. The selected platoon lead is not necessarily the best braking vehicle, thereby, resulting in a smaller difference. However, the achieved stopping distances will be impacted as shown next.

The Space Buffer approach with 2m separations ( $B = 1m$ ), results in a constant length of 138m which is shorter than that achieved by Least Stopping Distance and Subplatoon. At inter-vehicle separations of 4m ( $B = 3m$ ), the longest platoon of around 176m results. This length reduces to 157m for  $B = 2m$ . This 157m length is around 1.2 vehicle lengths longer than the Least Stopping Distance approach. Note again that the nonadaptation of  $B$  as per the range of braking capacities causes this difference.

A comparison of the achieved stopping distances for the different ranges of braking capacities is presented in Fig. 7.7. The Least Stopping Distance and Space Buffer approaches with  $B = 3m$  and  $B = 2m$  achieve optimum values for all ranges of braking capacities. In the widest range, this is around 62m, whereas at identical braking capacities of 0.8g this is

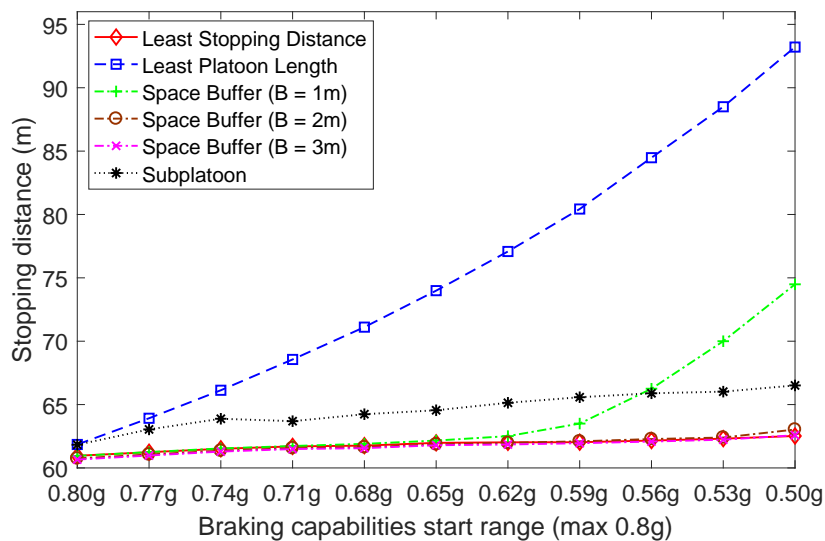


Figure 7.7.: Stopping distance vs. range of braking capacities



around  $61m$ . More precisely, Space Buffer with  $B = 3m$  outperforms the Least Stopping Distance approach by an average negligible margin of around  $0.20m$ . With respect to  $B = 2m$ , it is the contrary where Least Stopping Distance performs better. In the widest range, Least Stopping Distance achieves a stopping distance that is around  $0.5m$  shorter than  $B = 2m$ .

Contrarily, the Least Platoon Length approach achieves the worst stopping distances across all the ranges. For homogeneous capacities, the achieved stopping distance is around  $62m$ , i.e.,  $1m$  longer than the optimum. This is because the vehicle weights impact their stopping distances and, as a result, all vehicles have to adapt to the worst braking vehicle which has a slightly longer distance. However, as the range of capacities gets wider, the difference between the best and the worst stopping distances also increases linearly. For the widest range, there exists a difference of approximately  $31m$ , i.e., more than 6 vehicle lengths, thus, making the Least Platoon Length approach undesirable for emergency situations.

On the other hand, even at  $2m$  separations ( $B = 1m$ ), the Space-Buffer approach achieves a stopping distance that is around  $20m$  shorter than Least Platoon Length in the widest range. In comparison to the best performing approaches,  $B = 1m$  achieves almost similar results starting from homogeneous braking capacities till the  $0.8g - 0.62g$  range. Further, until this range it also outperforms the Subplatoon approach. However, from the  $0.56g - 0.8g$  range till the widest, the Subplatoon approach achieves shorter stopping distances due to a better braking vehicle chosen as the platoon lead. The difference is around  $8m$  in the widest range. However, as mentioned previously, the platoon length get longer (in Subplatoon).

In conclusion, when all platoon vehicles have identical braking capabilities, the stopping distances achieved are almost similar. However, in reality, their deceleration capabilities are not identical, but vary. In such a scenario, especially during emergency braking, it becomes crucial to minimize the stopping distance of the whole platoon in spite of this heterogeneity. This is where our Space-Buffer approach demonstrates its effectiveness even with the lowest value of  $B = 1m$ . The aerodynamic benefits and platoon lengths achieved by the other values of  $B$  might not be optimum, but the corresponding optimum performing approaches have their stopping distance affected in case of Least Platoon Length, and both platoon length and aerodynamic benefits affected in case of Least Stopping Distance.

The Subplatoon approach finds a balance in the performance of these two intuitive approaches, but at the cost of large inter-subplatoon separations, thereby, achieving suboptimal performance. Additionally, the large separation might result in other road traffic merging into it which naturally leads to vehicle collisions during emergency braking, thus, jeopardizing safety. This is never the case with the Space-Buffer approach. Therefore, in the direction of deploying platoons in real world, our Space-Buffer approach performs the best when all the three parameters — achieved aerodynamic benefits, platoon length, and stopping distance — are considered together, and ensures safe emergency braking.

### 7.3. Braking under realistic conditions

Now that the effectiveness of our Space-Buffer approach is demonstrated, in all further sections, we consider realistic conditions of braking, i.e., accounting for controller-related effects in deceleration tracking and braking on varying road profiles. From here on, we employ a shorter platoon of 10 vehicles, whose corresponding data are shown in Table 7.3. This data was also randomly generated in the same manner as mentioned before. The heterogeneity of the vehicles, especially in terms of braking capabilities can be observed.

Each vehicle in the table was modeled in Matlab/Simulink as per Fig. 2.4, i.e., considering even the nonlinear rolling and aerodynamic resistances which were excluded from our LTI model. In addition, the brake-by-wire controllers present at each of these vehicles were designed using the PID technique. For each controller, we chose a sampling time of  $20ms$  and obtained the controllers' integral gains which are also shown in the table. In all the

Table 7.3.: Dataset of vehicles used in the simulation ( $d$  and  $S$  respectively stand for deceleration and stopping distance, where we omit indexes for simplicity. Further, the  $d$ 's shown here also account for the equivalent mass factor  $\gamma_m$ .)

ID	$m$ (in $kg$ )	max. $ d $ (in $g$ )	$C_D$	$A_f$ (in $m^2$ )	Controller's integral gain ( $K_i$ )	Original $S$ (in $m$ )	Desired $S$ at $B = 1m$ (in $m$ )	Desired $ d $ (in $g$ )	Simulated $S$ (for $B = 1m$ ) (in $m$ )
1	3284	0.7430	0.289	2.02	34482	67.78	91.32	0.5377	91.29
2	1317	0.7188	0.273	2.14	13828.5	69.88	92.32	0.5314	92.27
3	1243	0.6927	0.195	2.41	13051.5	72.24	93.32	0.5253	93.28
4	1696	0.6885	0.221	2.35	17808	72.63	94.32	0.5192	94.31
5	2581	0.6701	0.257	2.05	27100.5	74.46	95.32	0.5130	95.39
6	3394	0.6635	0.257	2.48	35637	75.20	96.32	0.5067	96.51
7	3037	0.6635	0.196	2.35	31888.5	75.20	97.32	0.5005	97.63
8	2367	0.5883	0.269	2.16	24853.5	83.96	98.32	0.4947	98.69
9	3413	0.5251	0.273	2.02	35836.5	93.35	99.32	0.4903	99.53
10	3265	0.4864	0.315	2.02	34282.5	100.32	100.32	0.4864	100.28

controllers, the proportional and derivative gains were zero. The steps followed for control design, as well as our vehicle and platoon model can be found in the appendix.

### 7.3.1. The impact of ignoring controller-related effects

We first demonstrate the impact of ignoring controller-related effects in tracking the reference decelerations computed using our Space-Buffer approach. The stopping distances as per (2.3.9) were relied upon for the computations rather than using (5.3.5). To demonstrate the resulting effect, as examples, we consider  $2m$  ( $B = 1m$ ) and  $3m$  ( $B = 2m$ ) separations. Fig. 7.8 shows the trajectories of individual vehicles during an emergency braking on a flat road at inter-vehicle separations of  $2m$ . Trajectories are represented by ribbon-like plots that account for the vehicle length (in our case  $5m$ ). Note that all vehicles travel  $3m$  (due to

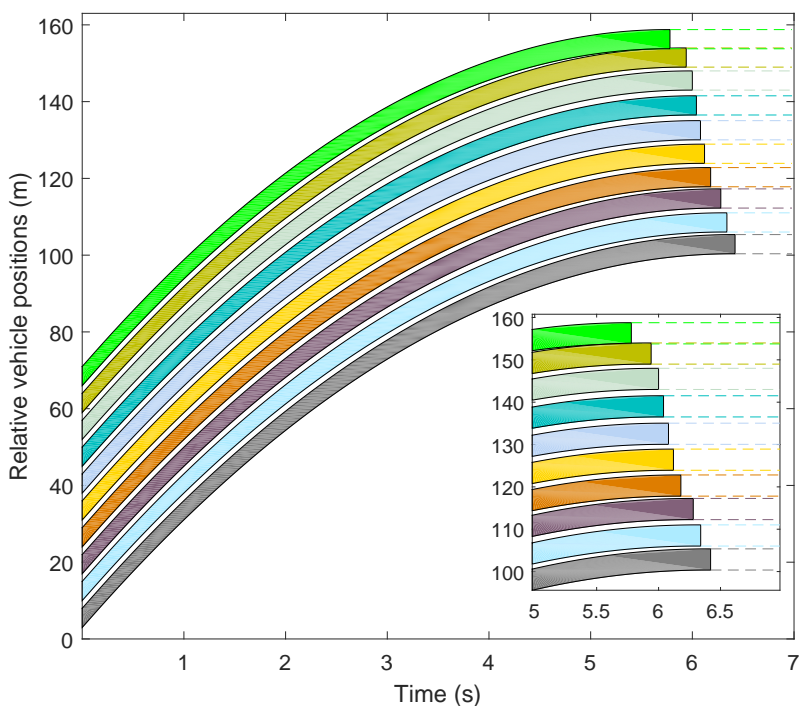


Figure 7.8.: Braking on a flat road by ignoring controller-related effects ( $B = 1m$ )

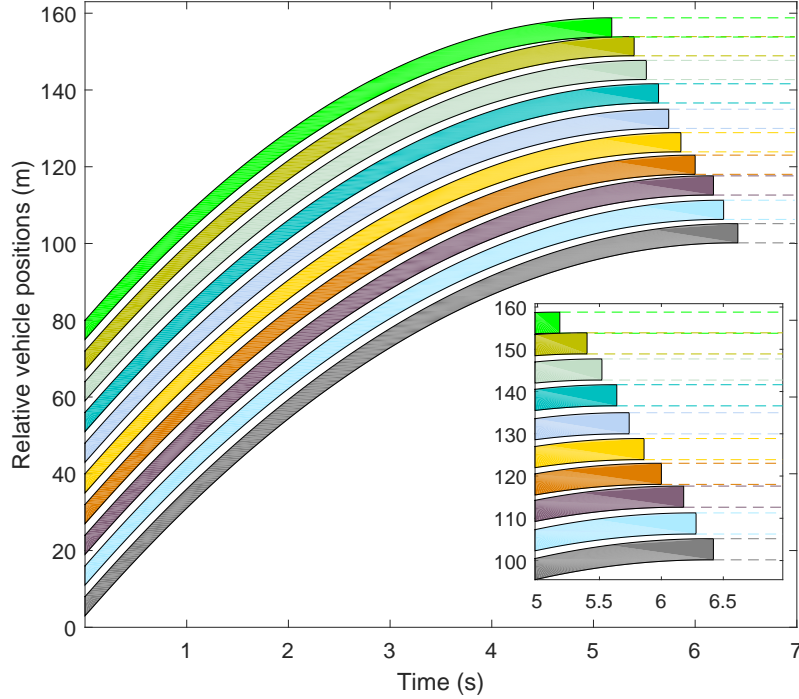


Figure 7.9.: Braking on a flat road by ignoring controller-related effects ( $B = 2m$ )

the actuation’s dead time as discussed above) before beginning to decelerate. After the dead time has elapsed, their positions are plotted in Fig. 7.8. This is why the 10<sup>th</sup> vehicle’s ribbon does not start exactly at (but rather at  $3m$  from) the origin.

Even though emergency braking happens on a flat road, the 2<sup>nd</sup> vehicle crashes into the platoon lead, i.e., the ribbons slightly overlap. Some of the vehicles have consumed even the  $SG$  reserved exclusively for packet losses, for example, the 8<sup>th</sup> vehicle in the platoon. If emergency braking is triggered after few packet losses occur, the number of collisions increase, thereby, impacting safety.

Similar behavior occurs even for inter-vehicle separations of  $3m$  ( $B = 2m$ ) — see Fig. 7.9. Thus, it can be concluded that controller-related effects in tracking an assigned deceleration should not be ignored as it impacts the platoon safety even when braking on a flat road.

### 7.3.2. Braking on a flat road

Considering the controller-related effects, we now rely on stopping distances computed as per (5.3.5), and perform our space buffer computations. We resimulate the same platoon to brake on a flat road. As seen in Fig. 7.10, all vehicles in the platoon brake to complete standstill without collisions, i.e., ribbons do not overlap, while minimizing the overall stopping distance from  $100.28m$  (i.e., that of the worst braking vehicle) to  $91.29m$ . Vehicles’ individual stopping distances after complete standstill are also presented in the last column of Table 7.1 (for  $B = 1m$ ). These differ by few centimeters when compared to the required stopping distance (also shown in the table). This is mainly due to rounding errors and can be easily fixed by rounding up the stopping distances (7<sup>th</sup> column from the left) before computing space buffers or by slightly increasing the value of  $SG$ .

Similar collision-free braking behavior can also be observed for inter-vehicle separations of  $3m$  ( $B = 2m$ ) with an overall stopping distance of around  $82m$  — see Fig. 7.11. It is interesting to note that the overall stopping distance in this case is around  $10m$  shorter than for  $B = 1m$ . This is due to the greater value of  $B$ , but also partly due to increased

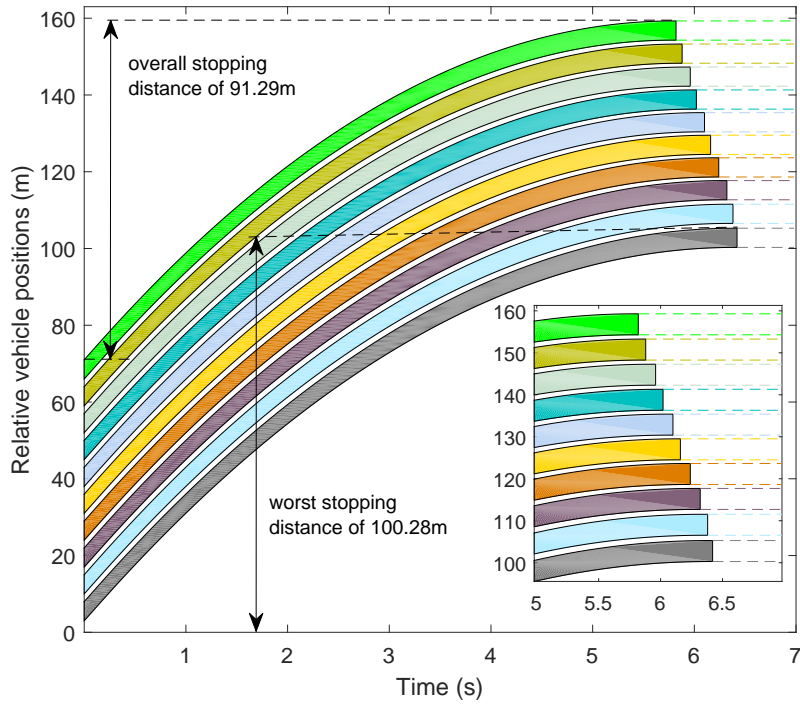


Figure 7.10.: Braking on a flat road ( $B = 1m$ )

aerodynamic force acting on the lead vehicle as a consequence of the larger inter-vehicle separations (which is again in line with the results in [56] [57]).

For  $4m$  separations ( $B = 3m$ ), the overall stopping distance is around  $73m$  — see Fig. 7.12. This stopping distance is around 4 vehicle lengths shorter than that achieved by  $B = 1m$ , and around 2 vehicle lengths shorter than  $B = 2m$ .

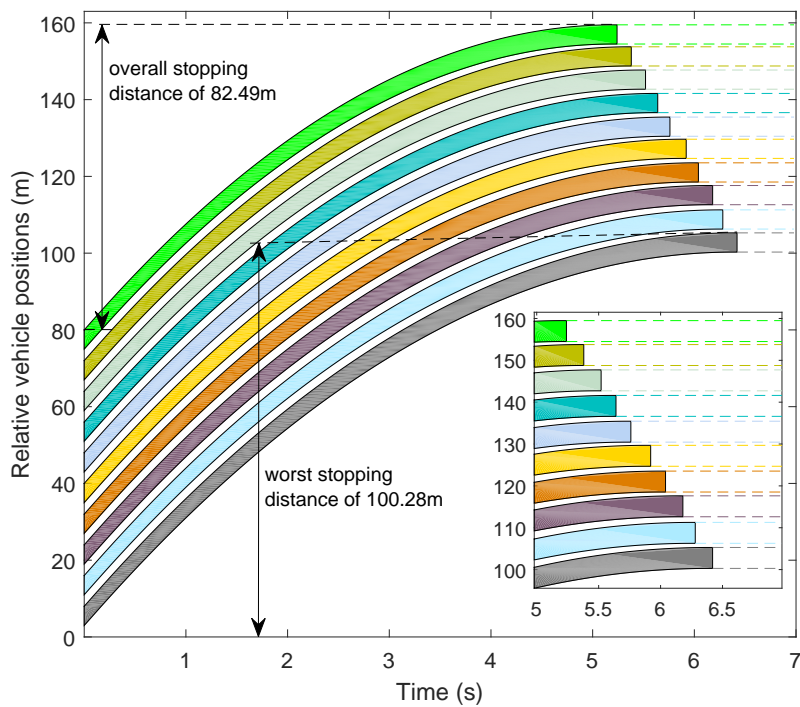


Figure 7.11.: Braking on a flat road ( $B = 2m$ )

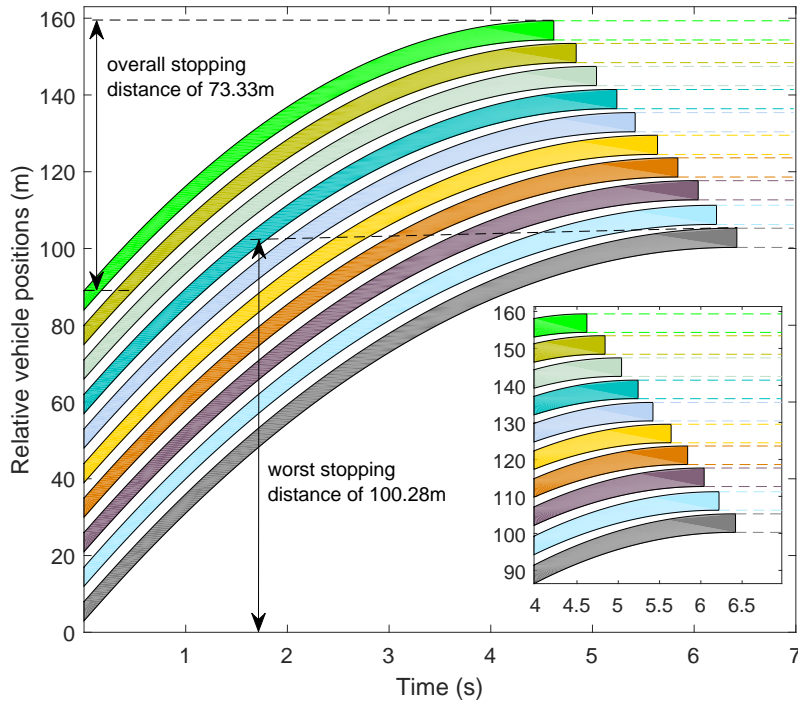


Figure 7.12.: Braking on a flat road ( $B = 3m$ )

### 7.3.3. Braking in a downhill

We now demonstrate how certain vehicles fail to track their reference decelerations (computed for a flat road) in a downhill and, as a result, vehicular collisions happen. Even though road profiles have a maximum slope of  $8^\circ$ , Fig. 7.13 ( $B = 1m$ ) shows that even a  $4^\circ$  slope downhill

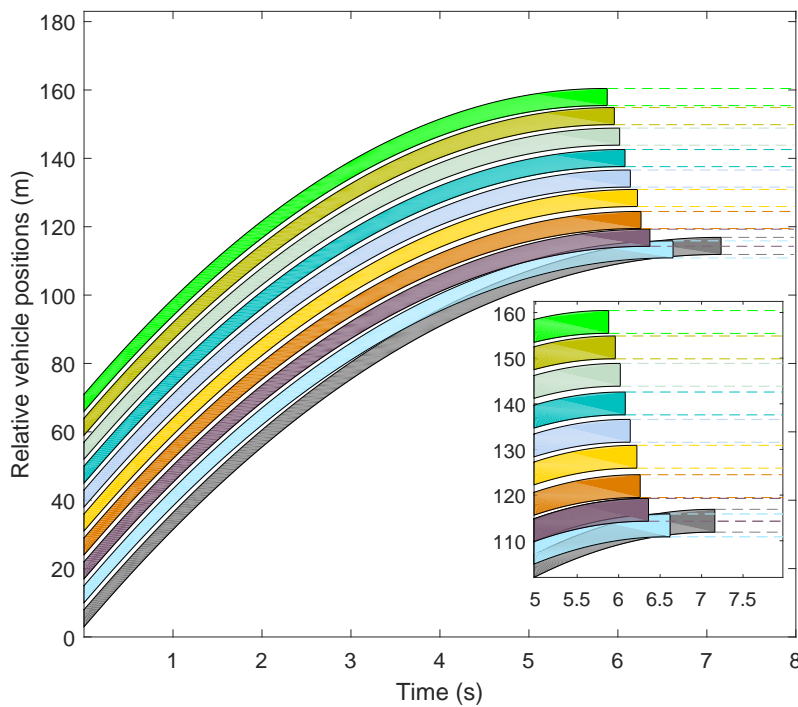


Figure 7.13.: Braking on  $4^\circ$  slope downhill ( $B = 1m$ )

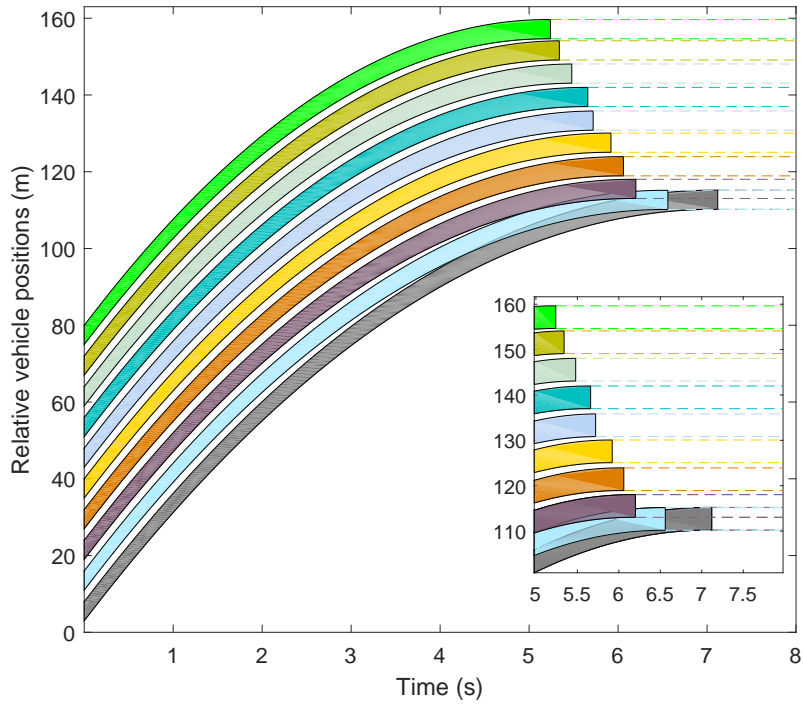


Figure 7.14.: Braking on  $4^\circ$  slope downhill ( $B = 2m$ )

results in vehicle collisions, i.e., ribbons overlap. In this test, all vehicles remain on the same  $4^\circ$  slope for the whole brake maneuver.

From Table 7.3, we see that 9<sup>th</sup> and 10<sup>th</sup> vehicles are already required to brake close to/at their maximum deceleration magnitudes even on a flat road. In downhill, they simply cannot

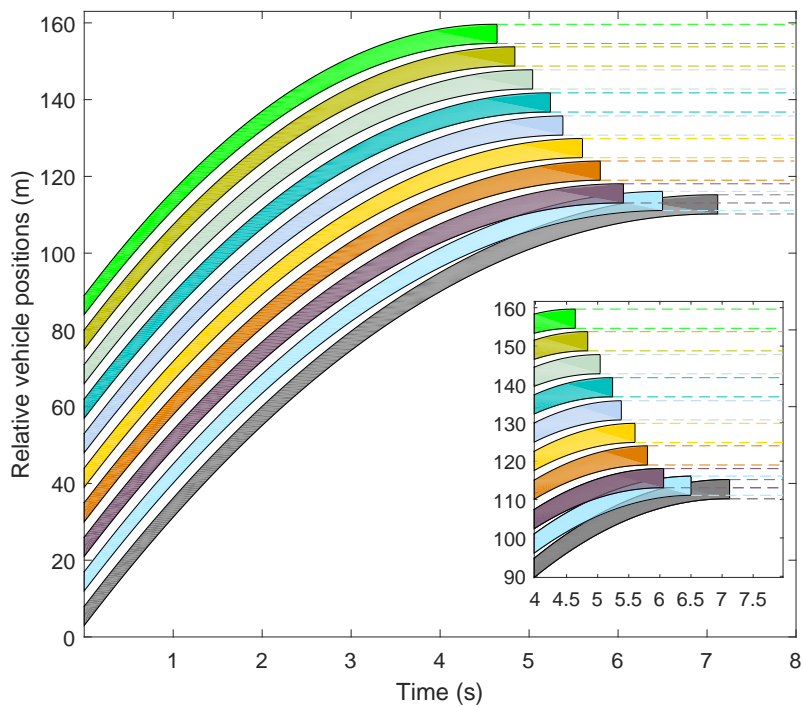


Figure 7.15.: Braking on  $4^\circ$  slope downhill ( $B = 3m$ )

counter the disturbing grade force. As a result, they consume the space buffers to their respective immediately leading vehicles, finally, colliding into each other and into the 8<sup>th</sup> vehicle. These simulated collisions can be more catastrophic in reality as they may lead to collisions with the 7<sup>th</sup> vehicle and beyond. The same behavior can also be observed with  $B = 2m$  and  $B = 3m$  — see Fig. 7.14 and Fig. 7.15 respectively.

#### 7.3.4. Avoiding collisions by distress messages

The inter-vehicle collisions presented previously can be avoided by a distress message broadcast. Upon an emergency, once the settling time of  $400ms$  has elapsed, vehicles 9 and 10 know that they fail to track their references and, hence, broadcast distress messages. As a result, the distress message of the 10<sup>th</sup> vehicle is considered by all the other vehicles as it is more distressed, i.e, it has the most deviation from tracking its assigned deceleration.

All vehicles (including the 9<sup>th</sup> vehicle) perform their computations within  $20ms$  as described in Section 6.2. From  $420ms$  onwards, they simultaneously adapt their decelerations and begin tracking the same. This coordination among the vehicles ensures that the inter-vehicle collisions are avoided, thereby, resulting in a safe brake maneuver, i.e., the ribbons now do not overlap. However, the stopping distance gets affected and it is clearly longer than that achieved on a flat road. For  $B = 1m$ , this is  $101.37m$  — see Fig. 7.16.

However, when the value of  $B$  is larger than  $1m$ , i.e.,  $2m$  and  $3m$ , the overall stopping distances will be much shorter than that achieved by  $B = 1m$ . The same can be observed in Fig. 7.17 and Fig. 7.18 (corresponding to inter-vehicle separations of  $3m$  and  $4m$  respectively). These stopping distances are around  $92m$  and  $83m$  respectively.

Note that there are slight differences in the achieved stopping distances. For example, the lead vehicle in Fig. 7.16 stops in a distance of  $101.37m$  rather than the required  $101.21m$ . This is again due to the rounding errors which can be fixed by rounding up the required stopping distance.

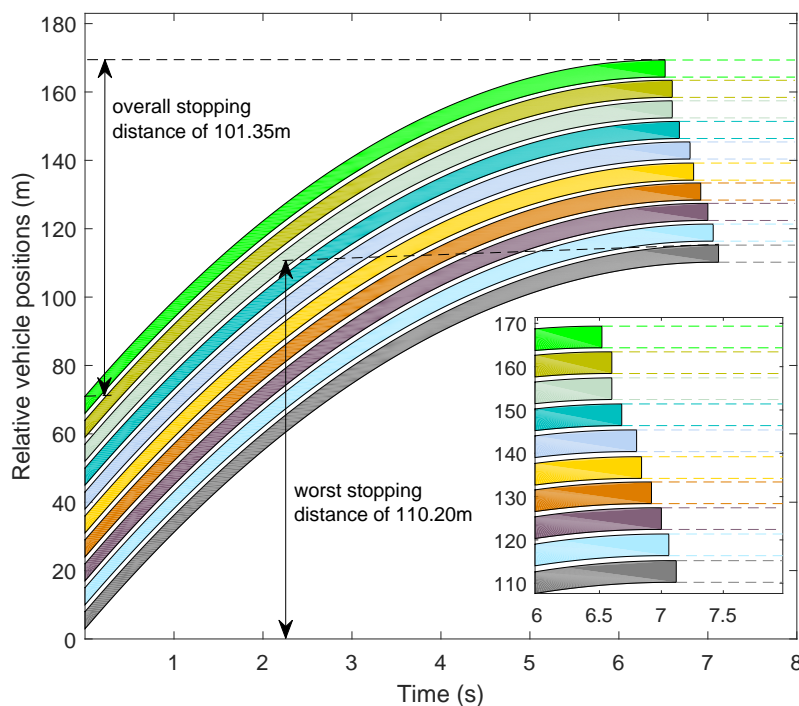


Figure 7.16.: Braking on  $4^\circ$  slope downhill with distress message ( $B = 1m$ )

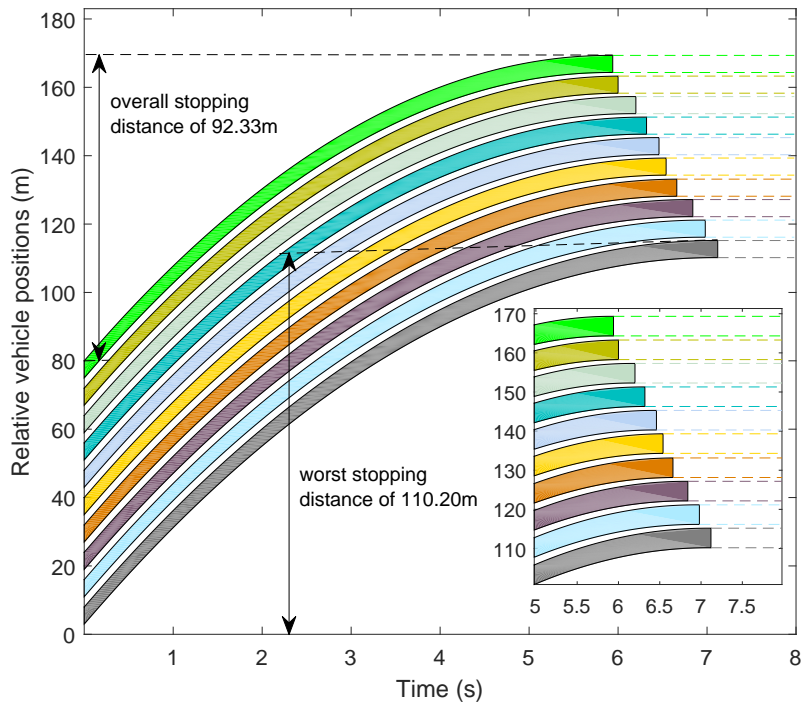


Figure 7.17.: Braking on 4° slope downhill with distress message ( $B = 2m$ )

### 7.3.5. Braking in a steep downhill

In this section, we demonstrate the worst case of braking in a steep downhill. For the entire brake maneuver, all the vehicles will be on the same downhill slope of 8°, i.e., the maximum allowed on European highways as explained before. Due to the steeper downhill, even the 8<sup>th</sup>

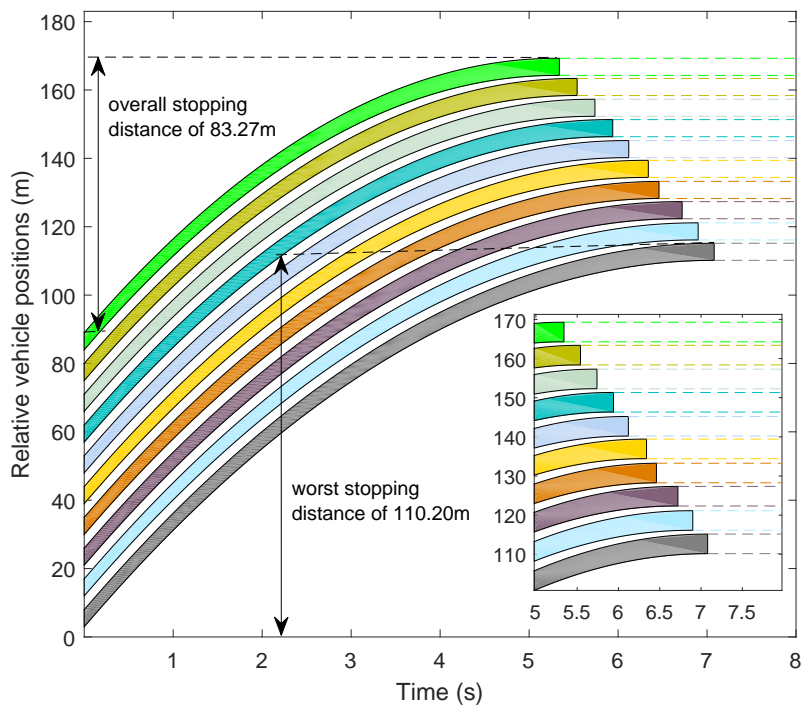


Figure 7.18.: Braking on 4° slope downhill with distress message ( $B = 3m$ )



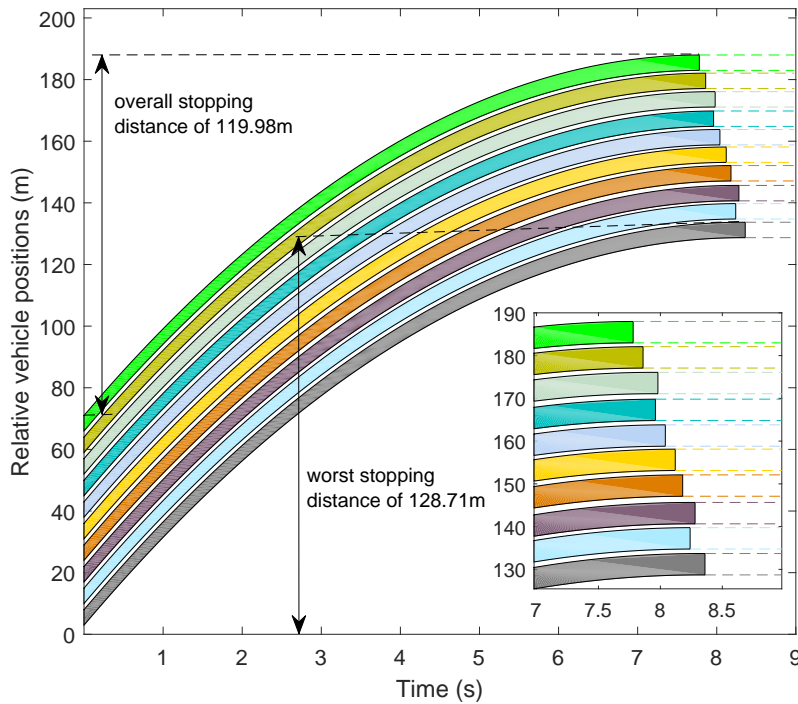


Figure 7.19.: Braking on  $8^\circ$  slope downhill with distress message ( $B = 1m$ )

vehicle is now distressed along with the previously distressed vehicles 9 and 10. These vehicles now need a longer stopping distance than that achieved on a  $4^\circ$  slope. As a result, this leads to a worst stopping distance of around  $128m$ , as opposed to the  $110m$  on the  $4^\circ$  slope. The overall stopping distance is now reduced to around  $120m$  for  $B = 1m$  — see Fig. 7.19.

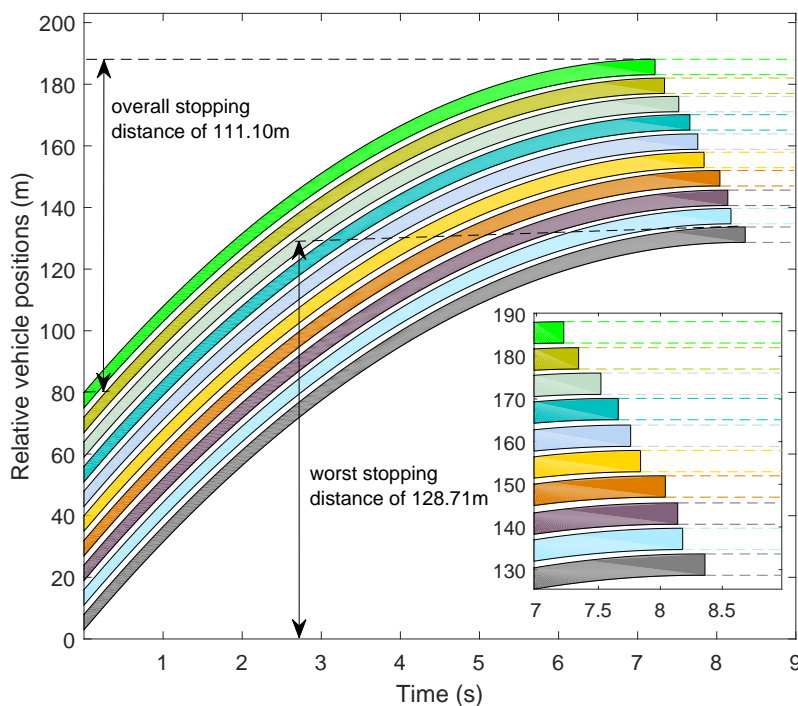


Figure 7.20.: Braking on  $8^\circ$  slope downhill with distress message ( $B = 2m$ )

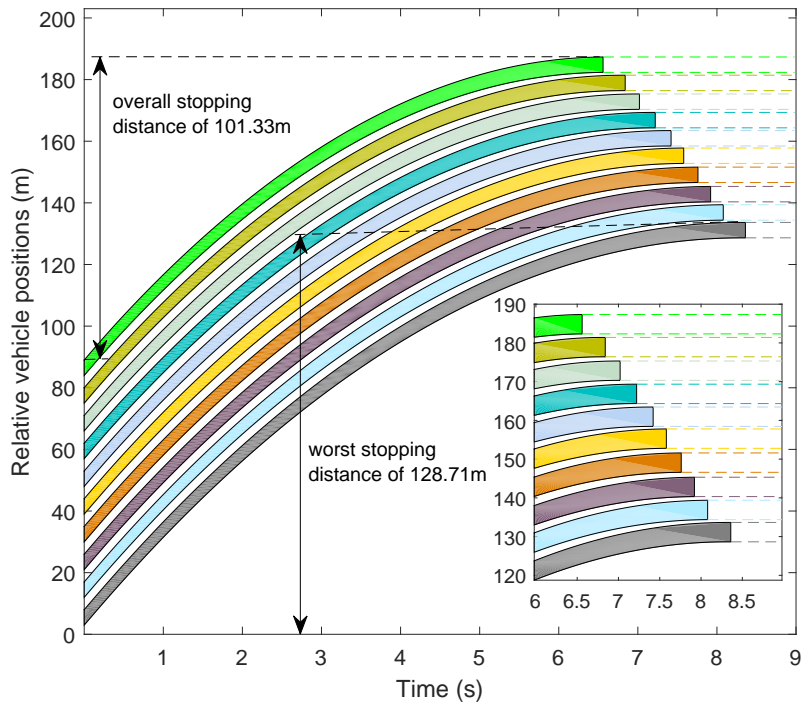


Figure 7.21.: Braking on  $8^\circ$  slope downhill with distress message ( $B = 3m$ )

For  $B = 2m$  and  $B = 3m$ , the overall stopping distance reduces to around  $111m$  and  $101m$  respectively — see Fig. 7.20 and Fig. 7.21.

### 7.4. Packet losses during platoon operation

The inter-vehicle separations employed in this work are below  $5m$ . As a result, packet losses in the inter-vehicle communication impacts the safety of a platoon. Hence, in this section, we analyze the number of packets that can be safely lost in all the presented approaches.

As shown in Fig. 7.22, the packet losses can be analyzed from the perspectives of brake command and live signals separately. These individual losses can be viewed as overlapping subsets with the overlapping region representing the worst-case situation, where both the live signals and brake command are lost. Hence, we consider this worst case for our analysis.

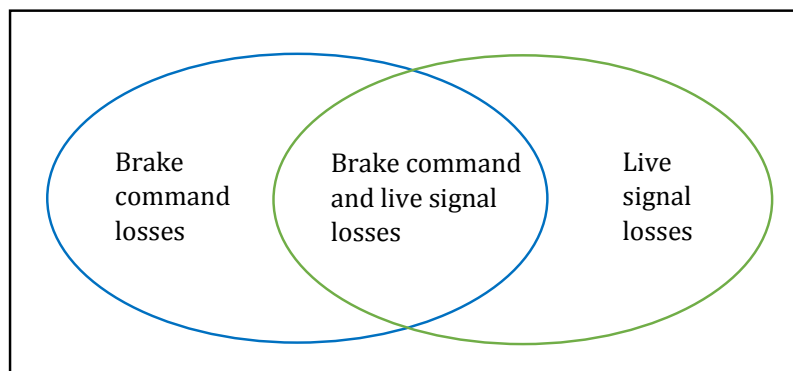


Figure 7.22.: Packet loss analysis

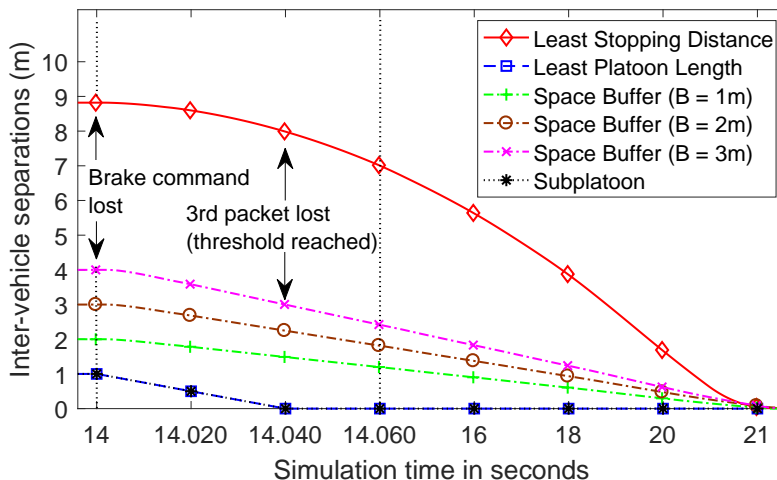


Figure 7.23.: Effect of packet losses on inter-vehicle separation

As mentioned before, whenever a vehicle experiences communication problems, it assumes the worst-case scenario, i.e., its immediately leading vehicles are already braking, and initiates a (decentralized) emergency brake maneuver and communicates the same to all of its following vehicles. The platoon then disintegrates ensuring safety. This behavior is initiated immediately after the number of consecutive packets lost crosses a threshold.

This threshold is a function of both the platoon cruise velocity and the inter-vehicle separation. In our work, to address packet losses, a  $SG$  value of  $1m$  in the inter-vehicle separations is chosen for all the approaches. With respect to the platoon cruise velocity, a higher number of packets can be lost at low cruise speeds compared to high speeds. All the approaches — Least Platoon Length, Least Stopping Distance, Subplatoon, and Space Buffer — exhibit this behavior. In our analysis, we consider high and low speeds of  $90km/h$  and  $50km/h$  respectively.

For simplicity, we consider a 2-vehicle platoon and assume an instantaneous deceleration tracking by both the vehicles. Fig. 7.23 shows the effect of packet losses on the inter-vehicle separation at high platoon speeds. Note that in Fig. 7.23, we use a  $20ms$  scale from  $14s$  up to  $14.060s$  (region enclosed by vertical dotted lines). From then onwards we change to a  $2s$  scale (to be able to show the points in time at which the inter-vehicle separation of all the approaches reduces to zero). In all the approaches, an emergency situation caused the lead vehicle to broadcast the brake command, initiating a simultaneous braking  $20ms$  later. The trail vehicle under test neither received this brake command nor the appropriate live signals.

In the Least Stopping Distance approach, the necessary separation including the  $SG$  between the two vehicles under test was  $8.8m$ . When the second consecutive live signal after the brake command is lost, the following vehicle initiates emergency braking. The inter-vehicle separation gradually reduces to zero at standstill.

At high speeds, including the brake command loss, a packet loss threshold of 3 packets can be observed. This generally applies to all pairs of consecutive vehicles irrespective of the number of vehicles in the platoon. This is because the separations account for the difference in their respective stopping distances and packet loss has to be dealt only with  $SG$ .

The above mentioned threshold is the same for the Least Platoon Length and the Subplatoon approaches as well. However, as soon as the third packet is lost, the separation reduces to zero and remains the same until standstill. This implies that the following vehicle's front bumper is in contact with its immediately leading vehicle's rear bumper. Such an undesirable scenario, in particular, because there is no margin for errors, can be eliminated by choosing the value of  $SG$  slightly greater than  $1m$ .

For the Space-Buffer approach, the difference in stopping distances between any two consecutive vehicles differs by  $B$  and their separation is the sum of the  $SG$  and  $B$ . As a result, again, only the safeguard can account for packet loss and, hence, the above mentioned threshold of 3 packets does not change. Unlike Least Platoon Length and Subplatoon, and similar to Least Stopping Distance, the inter-vehicle separation gradually reduces to zero at standstill.

In conclusion, at speeds of  $90\text{km/h}$ , assuming the lead vehicle is braking, the inter-vehicle distance reduces by  $0.5\text{m}$  per packet lost. Increasing the value of  $SG$  allows for more packet loss threshold. However, this also negatively impacts platoon length and the achieved aerodynamic benefits in particular.

On the other hand, keeping the  $SG$  constant, provided the platoon cruises at low speeds, the allowable number of packet losses is slightly more. More precisely at  $50\text{km/h}$ , the threshold increases to 4 consecutive packets including the loss of brake command, as the reduction in separation is only  $0.28\text{m}$  per packet lost. Additionally, note that in this case, non-zero inter-vehicle separations result at standstill for all the approaches.

## 7.5. Summary

In this chapter, we performed the experimental evaluation of our Space-Buffer approach. We began by considering idealized conditions of braking, and demonstrated the effectiveness of our approach against the intuitive — Least Platoon Length and Least Stopping Distance — and Subplatoon approaches on the basis of achieved aerodynamic benefits, platoon length, and stopping distance.

Least Platoon Length achieved optimum aerodynamic benefits and platoon length. However, when heterogeneous deceleration capabilities of vehicles were considered, it performed the worst in terms of the achieved stopping distance. Thus, this approach is more suitable for cruise scenarios rather than emergency braking. On the other hand, the Least Stopping Distance approach achieves optimum stopping distance. However, the varying inter-vehicle separations lead to lesser fuel/energy savings and longer platoons. In comparison, the Subplatoon approach performs better in terms of the achieved fuel benefits and the platoon length. However, the achieved stopping distance is less than the optimum and longer platoon results due to the large inter-subplatoon separation.

The design parameter  $B$  in our Space-Buffer approach was varied from 1 to  $3\text{m}$ . For  $B = 1\text{m}$ , the achieved stopping distance was around  $20\text{m}$  shorter than that of the worst performing Least Platoon Length. The achieved aerodynamic benefits had a difference of only 6% to the optimum and the platoon lengths were much shorter than the Subplatoon and Least Stopping Distance approaches. Hence, the Space-Buffer approach with  $B = 1\text{m}$  performs the best when all the three parameters are considered simultaneously.

At  $B = 2\text{m}$  and  $B = 3\text{m}$ , the optimum stopping distance similar to the Least Stopping Distance approach was achieved. The platoon length and aerodynamic benefits for  $B = 2\text{m}$  was almost similar to that of the Least Stopping Distance approach.

Even though  $B = 3\text{m}$  achieved optimum stopping distance, the achieved aerodynamic benefits and platoon length are the worst among all the presented approaches. However, these are significantly better in comparison to the values achieved with the current inter-vehicle separations of 5 to  $10\text{m}$  and beyond.

The Space-Buffer approach was also tested under the action of brake-by-wire controllers on different road profiles. Especially, for distress situations, our proposed coordination scheme demonstrated safe and collision-free braking, while simultaneously minimizing the overall stopping distance. Finally, packet losses in the inter-vehicle communication was considered and the number of packets that can be lost in all the approaches was analyzed without compromising on safety.

## Chapter 8.

### Concluding remarks

In this chapter, we present the concluding remarks with respect to this work and identify possible future extensions and developments.

This thesis is motivated by the fact that the existing inter-vehicle separations in platoons can be further reduced to less than  $5m$  to increase the throughput on highways and maximize the fuel/energy benefits. At such short separations, to address the challenges of emergency braking we proposed our cyber-physical approach named Space-Buffer, which efficiently utilizes the space buffers present in all the inter-vehicle separations and minimizes the overall stopping distance of the platoon.

The design parameter  $B$ , i.e., the space buffer between any two vehicles, was varied from 1 to  $3m$  in this work. The resulting aerodynamic benefits, platoon length, and stopping distance were compared against the intuitive approaches — Least Platoon Length and Least Stopping Distance — and the Subplatoon approach. The intuitive approaches achieve optimum fuel/energy savings and platoon length (in Least Platoon Length), and optimum stopping distance (in Least Stopping Distance) respectively.

The shortcomings of these intuitive approaches were partly overcome in the Subplatoon approach. The achieved stopping distance was much shorter than with Least Platoon Length and the aerodynamic benefits was better than with Least Stopping Distance. However, the platoon length was longer, almost similar to that of the Least Stopping Distance approach. This is due to the large inter-subplatoon separation. Further, with this approach, there is always the risk of non-platooning traffic merging into this large separation making emergency brake maneuvers extremely dangerous.

This risk is completely eliminated by our Space-Buffer approach. Particularly, at  $2m$  ( $B = 1m$ ) separations apart from the shorter platoon length, the difference in the achieved aerodynamic benefits is only 4% (for 20 vehicles). Further, the difference to the optimum (i.e., Least Platoon Length) is only 6%. With respect to the stopping distance, our Space-Buffer approach achieves shorter distances than the Subplatoon approach for platoons of up to 13 vehicles. For longer platoons, the Subplatoon approach performs better due to the choice of a better braking vehicle as the platoon lead, but at the cost of a longer platoon length as mentioned before.

Even with  $2m$  ( $B = 1m$ ) separations, our Space-Buffer approach achieves a  $20m$  shorter stopping distance than that of the worst performing Least Platoon Length. At  $3m$  ( $B = 2m$ ) separations, the achieved stopping distance has a negligible difference to the optimum. However, the achieved platoon length and aerodynamic benefits are almost similar to that of Least Stopping Distance. Similarly, at  $4m$  ( $B = 3m$ ) separations, the achieved stopping distance is optimum. In fact, it is slightly better than the optimum, but the difference is negligible. This slightly better performance is due to higher aerodynamic force on the platoon lead. Further increasing the value of  $B$  beyond  $3m$  leads to a negligible decrease in stopping distance mainly due to the greater aerodynamic force on the lead.

Thus, it can be stated that, for inter-vehicle separations below  $5m$ , our Space-Buffer approach with  $2m$  ( $B = 1m$ ) separations results in the most overall benefits, obtaining the best trade-off between stopping distance, platoon length, and aerodynamic benefits. The other values of  $B$  are, even though they incur into longer platoons and lesser aerodynamic benefits,

considerably better in comparison to current platoons employing separations of 5 to 10m and even larger values with the constant time headway policy.

For further maximizing the benefits at  $B = 2m$  and  $B = 3m$ , the separations between similarly braking vehicles can be kept to  $SG$ , i.e., safeguard, or very close to it. Another possible solution is to develop hybrid approaches based on the concept of space buffer, where similarly braking vehicles in the platoon use a different braking approach, for example, Least Stopping Distance.

In conclusion, when platooning becomes a part of real traffic, the challenges in the design of emergency brake maneuvers can be overcome through our Space-Buffer approach. Especially, the coordination mechanism in situations of distress ensures safe braking, irrespective of the road profile, while simultaneously minimizing the stopping distance in this situation. Though more work is still needed, particularly from the standardization perspective of inter-vehicle communication, the presented simulation results demonstrate benefits and, especially, the feasibility of the proposed approach.

## 8.1. Outlook

To conclude, we now identify possible future extensions. In this direction, one possible extension is to consider emergency brake maneuvers on road surfaces other than dry asphalt, i.e., snow/ice/glaze/oil exists on the road. In such scenarios, the vehicle tires cannot grip the surface and, clearly, vehicles cannot track their assigned reference decelerations. Even though this is similar to the distress situation, it is more challenging. This is because the error in tracking the reference is large as a vehicle can only achieve a maximum deceleration magnitude of  $0.2g$ , for example on snowy surfaces (due to the low coefficient of road adhesion).

Further, the best braking vehicles at the beginning of the platoon might travel on such road surfaces, whereas vehicles towards the end may still be on dry asphalt. Additionally, the stretch of the road with such low adhesion might be short or long. Then, depending on the current velocities of vehicles, each one or very few of them may travel through this stretch. Hence, the emergency brake maneuver and the coordination mechanism have to address all such possible combinations making them more complex.

Another possible extension of this work is to consider failures in the operation of the brake-by-wire control systems. Even though a complete failure of such a system is an exception, certain electrical components in the system might malfunction resulting in a low deceleration magnitude. Then, the affected vehicle will be on the course to a collision with its immediately leading vehicle. Even though a distress message broadcast will ensure safe braking, the resulting long stopping distance might be unacceptable due to other road traffic ahead.

Hence, one possible solution is to perform a controlled collision. As per this, the immediately leading vehicle adapts its velocity such that the difference to the affected vehicle's velocity is almost zero at the time of impact. Even though there will be (negligible) damage to the vehicles, the lives of in-vehicle passengers are protected. Then, once the impact has happened, the immediately leading vehicle can decelerate together with the affected vehicle by applying its maximum brake force. Depending on the momentum of this controlled collision, more than one immediately leading vehicles might be required to brake this affected vehicle to standstill in a short distance. The complexity of such maneuvers further increases when there are multiple vehicles experiencing such failures in their brake-by-wire systems.

# Bibliography

- [1] <http://www.sartre-project.eu/en/Sidor/default.aspx>, Retrieved July 2016.
- [2] [https://standards.ieee.org/content/ieee-standards/en/standard/1609\\_0-2019.html](https://standards.ieee.org/content/ieee-standards/en/standard/1609_0-2019.html), Retrieved December 2019.
- [3] <https://www.etsi.org/>, Retrieved December 2019.
- [4] <https://www.ika.rwth-aachen.de/en/research/publications/articles-and-presentations/automated-driving-department/1083-the-konvoi-project-development-and-investigation-of-truck-platoons-on-highways.html>, Retrieved December 2019.
- [5] [https://ec.europa.eu/clima/policies/transport\\_en](https://ec.europa.eu/clima/policies/transport_en), Retrieved March 2020.
- [6] <https://www.aeromobil.com>, Retrieved March 2020.
- [7] <https://www.iso.org/standard/46549.html>, Retrieved August 2020.
- [8] A. Alam and A. Gattami and K. H. Johansson and C. J. Tomlin. Guaranteeing safety for heavy duty vehicle platooning: Safe set computations and experimental evaluations. *Control Engineering Practice*, 2014.
- [9] A. Alam and J. Mårtensson and K. H. Johansson. Experimental evaluation of decentralized cooperative cruise control for heavy-duty vehicle platooning. *Control Engineering Practice*, 2015.
- [10] A. Böhm and K. Kunert. Data age based retransmission scheme for reliable control data exchange in platooning applications. In *IEEE International Conference on Communication Workshop*, 2015.
- [11] A. Böhm and K. Lidström and M. Jonsson and T. Larsson. Evaluating CALM M5-based vehicle-to-vehicle communication in various road settings through field trials. In *IEEE Local Computer Network Conference*, 2010.
- [12] A. Böhm and M. Jonsson. Real-Time Communication Support for Cooperative, Infrastructure-Based Traffic Safety Applications. *International Journal of Vehicular Technology*, 2011.
- [13] A. Böhm and M. Jonsson and E. Uhlemann. Co-existing Periodic Beaconing and Hazard Warnings in IEEE 802.11p-based Platooning Applications. In *Proceeding of the Tenth ACM International Workshop on Vehicular Inter-networking, Systems, and Applications*, 2013.
- [14] A. Böhm and M. Jonsson and E. Uhlemann. Performance comparison of a platooning application using the IEEE 802.11p MAC on the control channel and a centralized MAC on a service channel. In *IEEE International Conference on Wireless and Mobile Computing, Networking and Communications*, 2013.
- [15] A. Borri and D.V. Dimarogonas and K.H. Johansson and M.D. Di Benedetto and G. Pola. Decentralized symbolic control of interconnected systems with application to vehicle platooning. *International Federation of Automatic Control Proceedings Volumes*, 2013.

## BIBLIOGRAPHY

- [16] A. Day. *Braking of Road Vehicles*. Butterworth-Heinemann, 2014.
- [17] A. Dávila and M. Nombela. SARTRE: SAfe Road TRains for the Environment. Technical report, European Commission FP7, 2010.
- [18] A. Gattami and A. A. Alam and K. H. Johansson and C. J. Tomlin. Establishing Safety for Heavy Duty Vehicle Platooning: A Game Theoretical Approach. *International Federation of Automatic Control Proceedings Volumes*, 2011.
- [19] A. Vinel and N. Lyamin and P. Isachenkov. Modeling of V2V Communications for C-ITS Safety Applications: A CPS Perspective. *IEEE Communications Letters*, 2018.
- [20] B. Harker. PROMOTE-CHAUFFEUR II & 5.8 GHz vehicle to vehicle communications system. In *International Conference on Advanced Driver Assistance Systems*, 2001.
- [21] B. van Arem and C. J. G. van Driel and R. Visser. The Impact of Cooperative Adaptive Cruise Control on Traffic-Flow Characteristics. *IEEE Transactions on Intelligent Transportation Systems*, 2006.
- [22] C. Bergenheim and E. Hedin and D. Skarin. Vehicle-to-Vehicle Communication for a Platooning System. *Procedia - Social and Behavioral Sciences*, 2012.
- [23] C. Bergenheim and H. Pettersson and E. Coelingh and C. Englund and S. Shladover and S. Tsugawa. Overview of platooning systems. In *Proceedings of the ITS World Congress*, 2012.
- [24] C. Bergenheim and Q. Huang and A. Benmimoun and T. Robinson. Challenges of Platooning On Public Motorways. Technical report, European Commission FP7, 2010.
- [25] C. Garcia-Costa, and E. Egea-Lopez, and J. Garcia-Haro. A stochastic approach for vehicle safety modeling in a platoon of vehicles equipped with vehicular communications. In *International Conference on Transparent Optical Networks*, 2013.
- [26] C. K. Song and M. Uchanski and J. K. Hedrick. Vehicle Speed Estimation Using Accelerometer and Wheel Speed Measurements. In *SAE Technical Paper*, 2002.
- [27] C. Miller and C. Valasek. Adventures in Automotive Networks and Control Units. In *DEF CON 21 Hacking Conference*, 2013.
- [28] C. Miller and C. Valasek. A Survey of Remote Automotive Attack Surfaces. In *Black Hat USA*, 2014.
- [29] C. Sommer and F. Dressler. *Vehicular Networking*. Cambridge University Press, 2014.
- [30] D. K. Murthy and A. Masrur. Exploiting space buffers for emergency braking in highly efficient platoons. In *IEEE International Conference on Embedded and Real-Time Computing Systems and Applications*, 2017.
- [31] D. K. Murthy and M. Zhang and A. Masrur. Analyzing the Impact of Secure CAN Networks on Braking Dynamics of Cooperative Driving. In *Euromicro Conference on Digital System Design*, 2019.
- [32] D. Yanakiev and I. Kanellakopoulos. Nonlinear spacing policies for automated heavy-duty vehicles. *IEEE Transactions on Vehicular Technology*, 1998.
- [33] European Telecommunications Standards Institute. Intelligent Transport Systems; Communications Architecture, 2010.



- [34] European Telecommunications Standards Institute. Intelligent Transport Systems; Decentralized Congestion Control Mechanisms for Intelligent Transport Systems operating in the 5 GHz range; Access layer part, 2011.
- [35] European Telecommunications Standards Institute. Intelligent Transport Systems; Access Layer specification for Intelligent Transport Systems using LTE Vehicle to everything communication in the 5,9 GHz frequency band, 2018.
- [36] European Telecommunications Standards Institute. Intelligent Transport Systems; Vehicular Communications; Basic Set of Applications; Part 2: Specification of Cooperative Awareness Basic Service, 2019.
- [37] European Telecommunications Standards Institute. Intelligent Transport Systems; Vehicular Communications; Basic Set of Applications; Part 3: Specification of Decentralized Environmental Notification Basic Service, 2019.
- [38] European Telecommunications Standards Institute. Intelligent Transport Systems; ITS-G5 Access layer specification for Intelligent Transport Systems operating in the 5 GHz frequency band, 2020.
- [39] G. C. KeSSLer and M. Hakenberg and S. Deutschle and D. Abel. Lateral Control of Heavy-Duty Vehicle Platoons Using Model-Based Predictive Control. *International Federation of Automatic Control Proceedings Volumes*, 2010.
- [40] G. Giordano and M. Segata and F. Blanchini and R. L. Cigno. A joint network/control design for cooperative automatic driving. In *IEEE Vehicular Networking Conference*, 2017.
- [41] G. J. L. Naus and R. P. A. Vugts and J. Ploeg and M. J. G. van de Molengraft and M. Steinbuch. String-Stable CACC Design and Experimental Validation: A Frequency-Domain Approach. *IEEE Transactions on Vehicular Technology*, 2010.
- [42] G. Xu and L. Liu and Y. Ou and Z. Song. Dynamic Modeling of Driver Control Strategy of Lane-Change Behavior and Trajectory Planning for Collision Prediction. *IEEE Transactions on Intelligent Transportation Systems*, 2012.
- [43] H. Fritz. Longitudinal and lateral control of heavy duty trucks for automated vehicle following in mixed traffic: experimental results from the CHAUFFEUR project. In *Proceedings of the IEEE International Conference on Control Applications*, 1999.
- [44] H. Hao and P. Barooah. Stability and robustness of large platoons of vehicles with double-integrator models and nearest neighbor interaction. *International Journal of Robust and Nonlinear Control*, 2013.
- [45] H. Stübting. *Multilayered Security and Privacy Protection in Car-to-X Networks*. Springer Vieweg, 2013.
- [46] J. Larson and K. Liang and K. H. Johansson. A Distributed Framework for Coordinated Heavy-Duty Vehicle Platooning. *IEEE Transactions on Intelligent Transportation Systems*, 2015.
- [47] J. Ploeg and B. T. M. Scheepers and E. van Nunen and N. van de Wouw and H. Nijmeijer. Design and experimental evaluation of cooperative adaptive cruise control. In *IEEE International Conference on Intelligent Transportation Systems*, 2011.
- [48] J.Y. Wong. *Theory of Ground Vehicles*. Wiley, 2001.

## BIBLIOGRAPHY

- [49] K. Bilstrup and E. Uhlemann and E. G. Ström and U. Bilstrup. On the Ability of the 802.11p MAC Method and STDMA to Support Real-Time Vehicle-to-Vehicle Communication. *EURASIP Journal on Wireless Communications and Networking*, 2009.
- [50] K. Hong and J. B. Kenney and V. Rai and K. P. Laberteaux. Evaluation of Multi-Channel Schemes for Vehicular Safety Communications. In *IEEE Vehicular Technology Conference*, 2010.
- [51] K. Liang and A. Assad and A. Gattami. The impact of heterogeneity and order in heavy duty vehicle platooning networks. In *IEEE Vehicular Networking Conference*, 2011.
- [52] K. Liang and J. Mårtensson and K. H. Johansson. Fuel-saving potentials of platooning evaluated through sparse heavy-duty vehicle position data. In *IEEE Intelligent Vehicles Symposium Proceedings*, 2014.
- [53] K.B. Kelly and H. J. Holcombe. Aerodynamics for Body Engineers. In *SAE Technical Paper*, 1964.
- [54] L. Junwei and W. Jian. Design of antilock braking system based on variable structure control. In *IEEE International Conference on Intelligent Computing and Intelligent Systems*, 2009.
- [55] L. Xu and L. Y. Wang and G. Yin and H. Zhang. Communication Information Structures and Contents for Enhanced Safety of Highway Vehicle Platoons. *IEEE Transactions on Vehicular Technology*, 2014.
- [56] M. Michaelian and F. Browand. Field Experiments Demonstrate Fuel Savings for Close-Following. Technical report, University of Southern California, 2000.
- [57] M. Zabat and N. Stabile and S. Frascaroli and F. Browand. The Aerodynamic Performance of Platoons. Technical report, University of California, 1995.
- [58] N. Cheng and N. Lu and P. Wang and X. Wang and F. Liu. A QoS-provision multi-channel MAC in RSU-assisted vehicular networks (poster). In *IEEE Vehicular Networking Conference*, 2011.
- [59] N. K. Sharma and A. Hamednia and N. Murgovski and E. R. Gelso and J. Sjöberg. Optimal Eco-Driving of a Heavy-Duty Vehicle Behind a Leading Heavy-Duty Vehicle. *IEEE Transactions on Intelligent Transportation Systems*, 2020.
- [60] N. S. Nise. *Control Systems Engineering*. John Wiley & Sons, Inc., 2011.
- [61] P. Greibe. Braking distance, friction and behavior. Technical report, Trafitec, 2007.
- [62] R. Liu and N. G. Kil and I. Lee and H. S. Seo. Automated Highway Systems and the Effects of Emergency Braking. Technical report, University of California, 2015.
- [63] R. Rajamani. *Vehicle Dynamics and Control*. Springer, 2006.
- [64] R. Rajamani and H. Tan and B. K. Law and W. Zhang. Demonstration of integrated longitudinal and lateral control for the operation of automated vehicles in platoons. *IEEE Transactions on Control Systems Technology*, 2000.
- [65] R. Zheng and K. Nakano and S. Yamabe and M. Aki and H. Nakamura and Y. Suda. Study on Emergency-Avoidance Braking for the Automatic Platooning of Trucks. *IEEE Transactions on Intelligent Transportation Systems*, 2014.

- [66] S. Choi. Antilock Brake System With a Continuous Wheel Slip Control to Maximize the Braking Performance and the Ride Quality. *IEEE Transactions on Control Systems Technology*, 2008.
- [67] S. Darbha. *String Stability of Interconnected Systems: An Application to Platooning in Automated Highway Systems*. PhD thesis, University of California, 1995.
- [68] S. Darbha and J. K. Hedrick. String stability of interconnected systems. *IEEE Transactions on Automatic Control*, 1996.
- [69] S. Darbha and J.K. Hedrick and C. C. Chien and P. Ioannou. A Comparison of Spacing and Headway Control Laws for Automatically Controlled Vehicles. *Vehicle System Dynamics*, 1994.
- [70] S. E. Shladover and D. Su and X. Lu. Impacts of Cooperative Adaptive Cruise Control on Freeway Traffic Flow. *Transportation Research Record*, 2012.
- [71] S. Eichler. Performance Evaluation of the IEEE 802.11p WAVE Communication Standard. In *IEEE Vehicular Technology Conference*, 2007.
- [72] S. Eilers and J. Mårtensson and H. Pettersson and M. Pillado and D. Gallegos and M. Tobar and K. H. Johansson and X. Ma and T. Friedrichs and S. S. Borojeni and M. Adolfson. COMPANION – Towards Co-operative Platoon Management of Heavy-Duty Vehicles. In *IEEE International Conference on Intelligent Transportation Systems*, 2015.
- [73] S. Hasan. *Fail-Operational and Fail-Safe Vehicle Platooning in the Presence of Transient Communication Errors*. PhD thesis, Mälardalen University, 2020.
- [74] S. Hasan and A. Balador and S. Girs and E. Uhlemann. Towards Emergency Braking as a Fail-Safe State in Platooning: A Simulative Approach. In *IEEE Vehicular Technology Conference*, 2019.
- [75] S. Linsenmayer and D. V. Dimarogonas and F. Allgöwer. Nonlinear Event-Triggered Platooning Control with Exponential Convergence. *International Federation of Automatic Control*, 2015.
- [76] S. Mangan and J. Wang and Q. H. Wu. Measurement of the road gradient using an inclinometer mounted on a moving vehicle. In *Proceedings. IEEE International Symposium on Computer Aided Control System Design*, 2002.
- [77] S. Solyom and A. Idelchi and B. B. Salamah. Lateral Control of Vehicle Platoons. In *IEEE International Conference on Systems, Man, and Cybernetics*, 2013.
- [78] S. van de Hoef and K. H. Johansson and D. V. Dimarogonas. Coordinating Truck Platooning by Clustering Pairwise Fuel-Optimal Plans. In *IEEE International Conference on Intelligent Transportation Systems*, 2015.
- [79] S. van de Hoef and K. H. Johansson and D. V. Dimarogonas. Computing Feasible Vehicle Platooning Opportunities for Transport Assignments. *International Federation of Automatic Control*, 2016.
- [80] T. K. Mak, and K. P. Laberteaux and R. Sengupta. A Multi-channel VANET Providing Concurrent Safety and Commercial Services. In *Proceedings of the ACM International Workshop on Vehicular Ad Hoc Networks*, 2005.
- [81] T. Massel and E. L. Ding and M. Arndt. Identification of road gradient and vehicle pitch angle. In *IEEE International Conference on Control Applications*, 2004.

## BIBLIOGRAPHY

- [82] T. Robinson and E. Chan and E. Coelingh. Operating Platoons On Public Motorways: An Introduction To The SARTRE Platooning Programme. Technical report, European Commission FP7, 2010.
- [83] Trans-European North-South Motorway (TEM) Project. TEM Standards and Recommended Practice, 2002.
- [84] V. Milanés and S. E. Shladover and J. Spring and C. Nowakowski and H. Kawazoe and M. Nakamura. Cooperative Adaptive Cruise Control in Real Traffic Situations. *IEEE Transactions on Intelligent Transportation Systems*, 2014.
- [85] V. Turri and B. Besselink and J. Martensson and K. H. Johansson. Fuel-efficient heavy-duty vehicle platooning by look-ahead control. In *IEEE Conference on Decision and Control*, 2014.
- [86] V. Turri and B. Besselink and K. H. Johansson. Cooperative Look-Ahead Control for Fuel-Efficient and Safe Heavy-Duty Vehicle Platooning. *IEEE Transactions on Control Systems Technology*, 2017.
- [87] W. Choi and S. Darbha. Assessing the safety benefits due to coordination amongst vehicles during an emergency braking maneuver. In *Proceedings of the American Control Conference*, 2001.
- [88] X. Liu and A. Goldsmith and S. S. Mahal and J. K. Hedrick. Effects of communication delay on string stability in vehicle platoons. In *IEEE Intelligent Transportation Systems*, 2001.
- [89] Y. Lee and W. Lee. Hardware-in-the-loop Simulation for Electro-mechanical Brake. In *SICE-ICASE International Joint Conference*, 2006.
- [90] Y. Liu and B. Xu. Improved Protocols and Stability Analysis for Multivehicle Cooperative Autonomous Systems. *IEEE Transactions on Intelligent Transportation Systems*, 2015.

# Appendix A.

## Principles and Fundamentals

### A.1. Platoon joining and operation

In this section, we present an example algorithm to induce a new vehicle into an existing platoon. For the sake of simplicity, we assume that the Least Platoon Length braking approach is used. However, the below algorithm can be easily extended to any of the other braking approaches presented in this work.

Whenever a car wants to join an existing platoon it sends a wireless request to the manager of the platoon, usually the platoon lead, with the necessary information like its maximum deceleration rate and maximum speed achievable. The platoon manager uses the below algorithm to induce the new car into the platoon.

---

**Algorithm 1** Algorithm for a new car joining a platoon

---

**Input:** Request for platoon joining

**Output:** New vehicle joins platoon

- 1: read current max speed of platoon
- 2: read current max deceleration rate of platoon
- 3: read car's max speed and max deceleration rate
- 4: compare platoon's values with car's values
- 5: **if** platoon's values are greater **then**
- 6:   make car's values as platoon's values
- 7:   create packet with new values
- 8: **else**
- 9:   create packet with platoon values
- 10:   inform about new car in packet
- 11: **end if**
- 12: broadcast packet to all vehicles and the new car
- 13: wait for acknowledgment from all vehicles
- 14: **if** all\_acknowledgment\_received() **then**
- 15:   create message with needed inter-vehicle distance
- 16:   send message to new car
- 17:   wait\_for\_acknowledgment
- 18:   **if** acknowledgment\_received() **then**
- 19:     broadcast message about new car in platoon
- 20:   **end if**
- 21: **end if**

---



# Appendix B.

## Braking under realistic conditions

### B.1. Control design, vehicle and platoon model

In this section, we outline the steps performed in Matlab/Simulink for controller design, vehicle and platoon models. Initially, we load all the necessary vehicle parameters, i.e., its mass, maximum deceleration, aerodynamic drag coefficient, frontal area, etc., in the Matlab workspace. Then, using the Simulink and the PID controller blocks, we construct a LTI car model, i.e., which considers only the input force generated by the brake system. Further, we assume no disturbances ( $\theta = 0$ ) to account for flat road conditions. The model is as below:

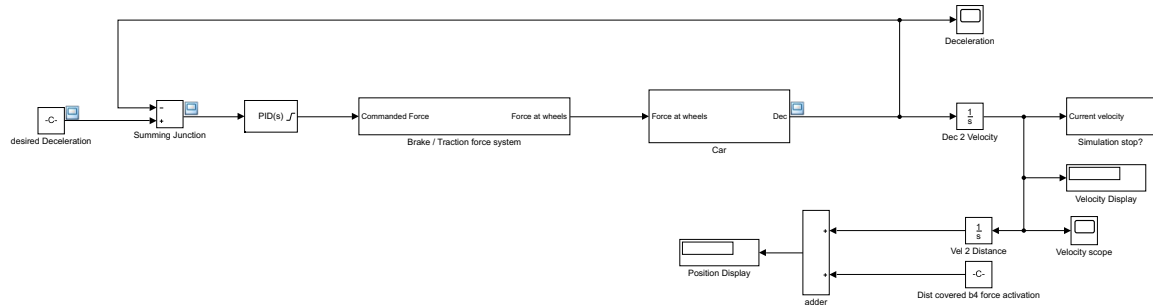


Figure B.1.: LTI vehicle model

Then, we tune our controller to meet the performance specifications shown in Table 5.1. Double clicking on the PID block opens up the controller parameters dialog as below:

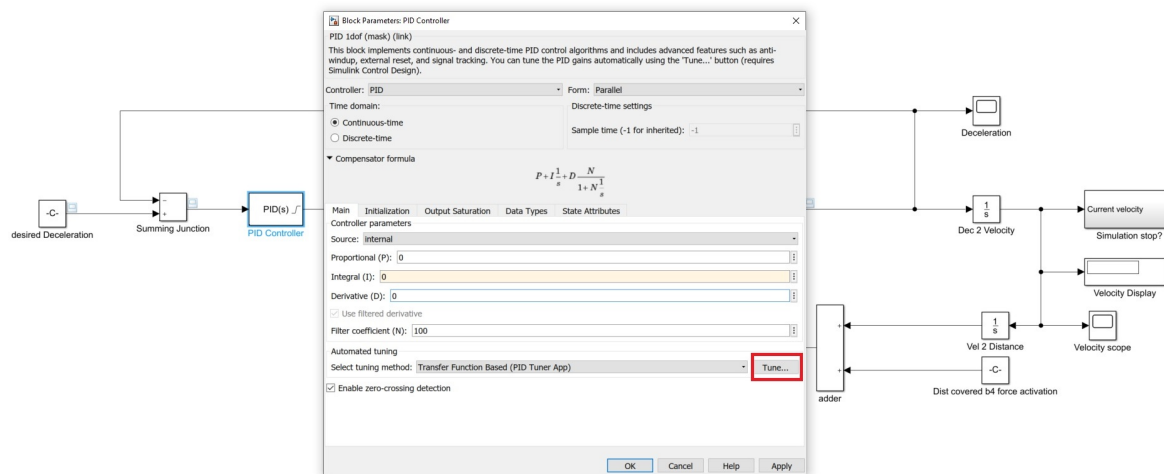


Figure B.2.: Controller parameters dialog before tuning

## Appendix B. Braking under realistic conditions

Clicking the highlighted **Tune** button shown in the previous figure launches the *PID Tuner App*. Once the performance specifications are entered in the app and the tuning is performed, the corresponding proportional, integral and derivative gains are updated in the controller parameters dialog as shown below:

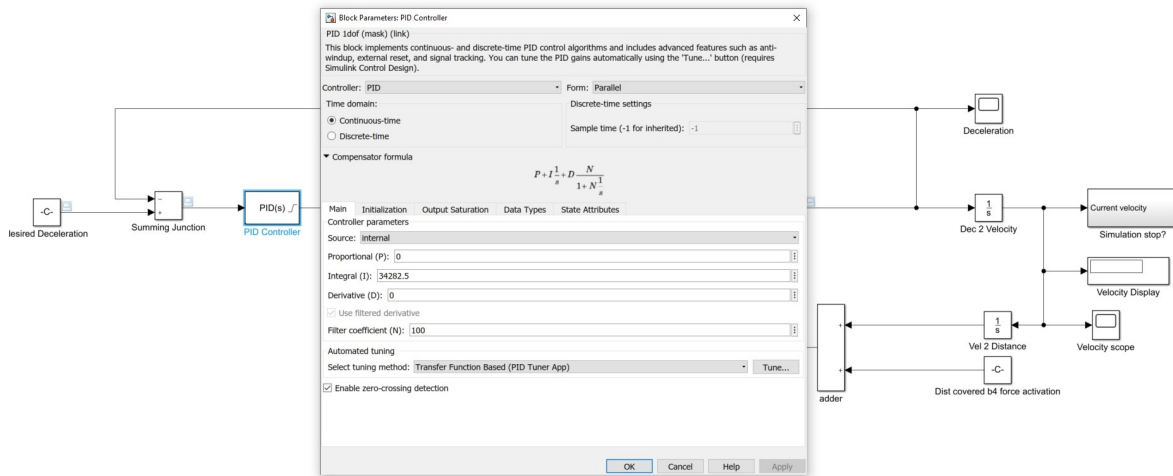


Figure B.3.: Controller parameters dialog after tuning

Note that the proportional (P) and derivative (D) gains are 0 and the integral gain (I) has a value of 34282.5 for this particular vehicle. This process is repeated for all the platoon vehicles and the controllers' integral gains are obtained. Simultaneously, we also analytically compute the stopping distance for every vehicle under controller action as explained in Section 5.3. Then, using our Space-Buffer approach, we calculate the individual vehicle decelerations to be tracked during an emergency.

Now that the controller gains are obtained for each vehicle in the platoon, our next step is to employ these gains in the controllers that are present in the high-fidelity vehicle models, i.e., we include all the nonlinear forces shown in Fig. 2.4 and construct the vehicle models in Simulink. An example vehicle is shown below. Clearly, the complexity increases due to the implementation of cooperative scheme during emergency braking, the necessary inter-vehicle communication, and simulating the grade force as the vehicle undergoes a road profile transition.



## B.1. Control design, vehicle and platoon model

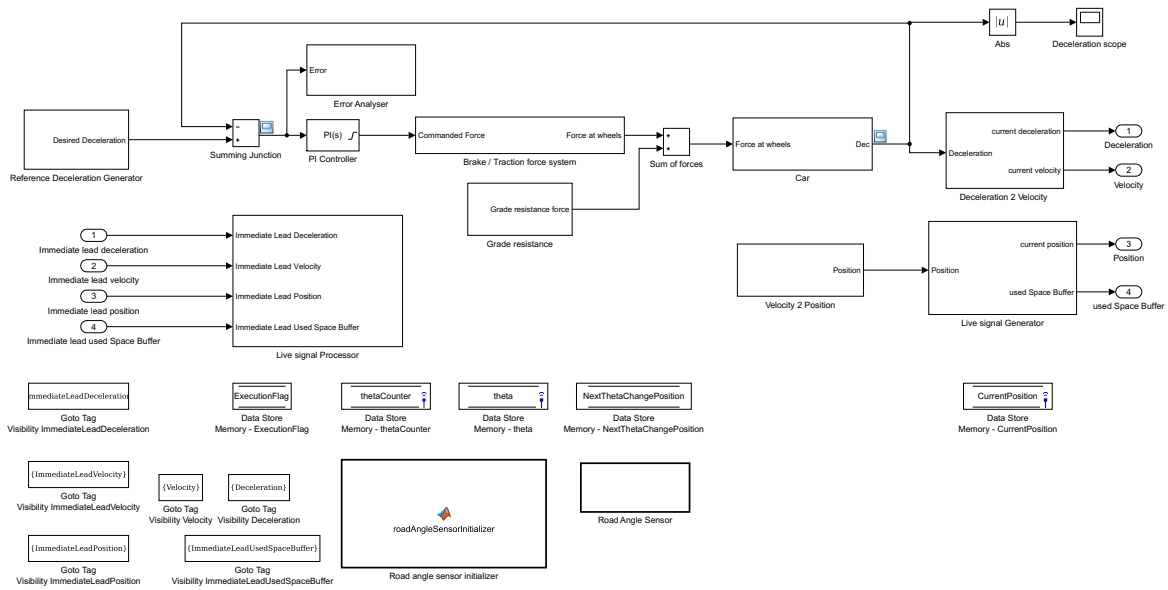


Figure B.4.: Nonlinear vehicle model

The above vehicle model is implemented as a masked model so that it can be replicated to form a platoon. Then, the individual vehicles are parametrized based on their characteristics shown in Table 7.3. For example, parametrization of the platoon lead is as below:

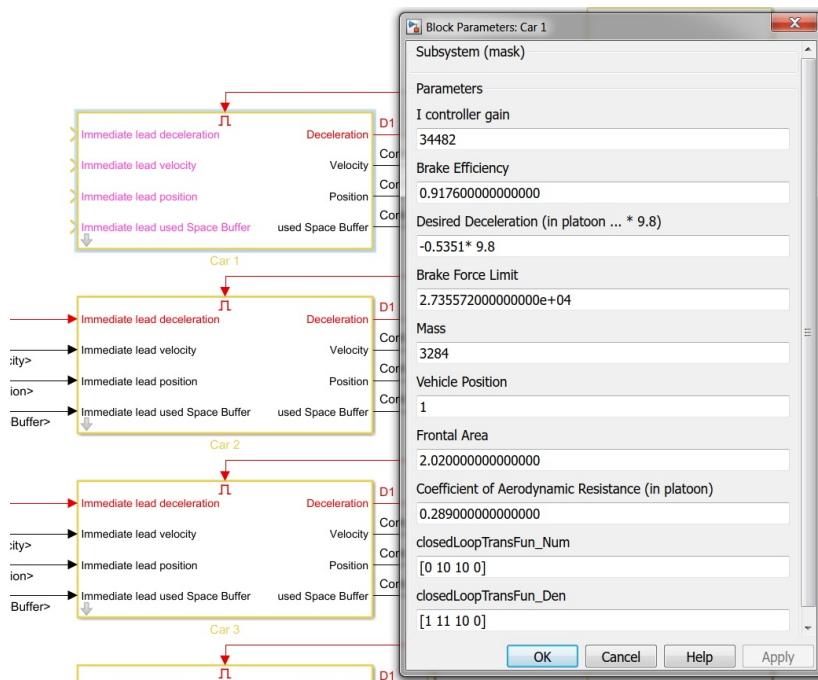


Figure B.5.: An example parametrization of the masked vehicle model

## Appendix B. Braking under realistic conditions

Once all the vehicles are parametrized, the vehicles are interconnected to form a platoon as shown below and the graphs were generated.

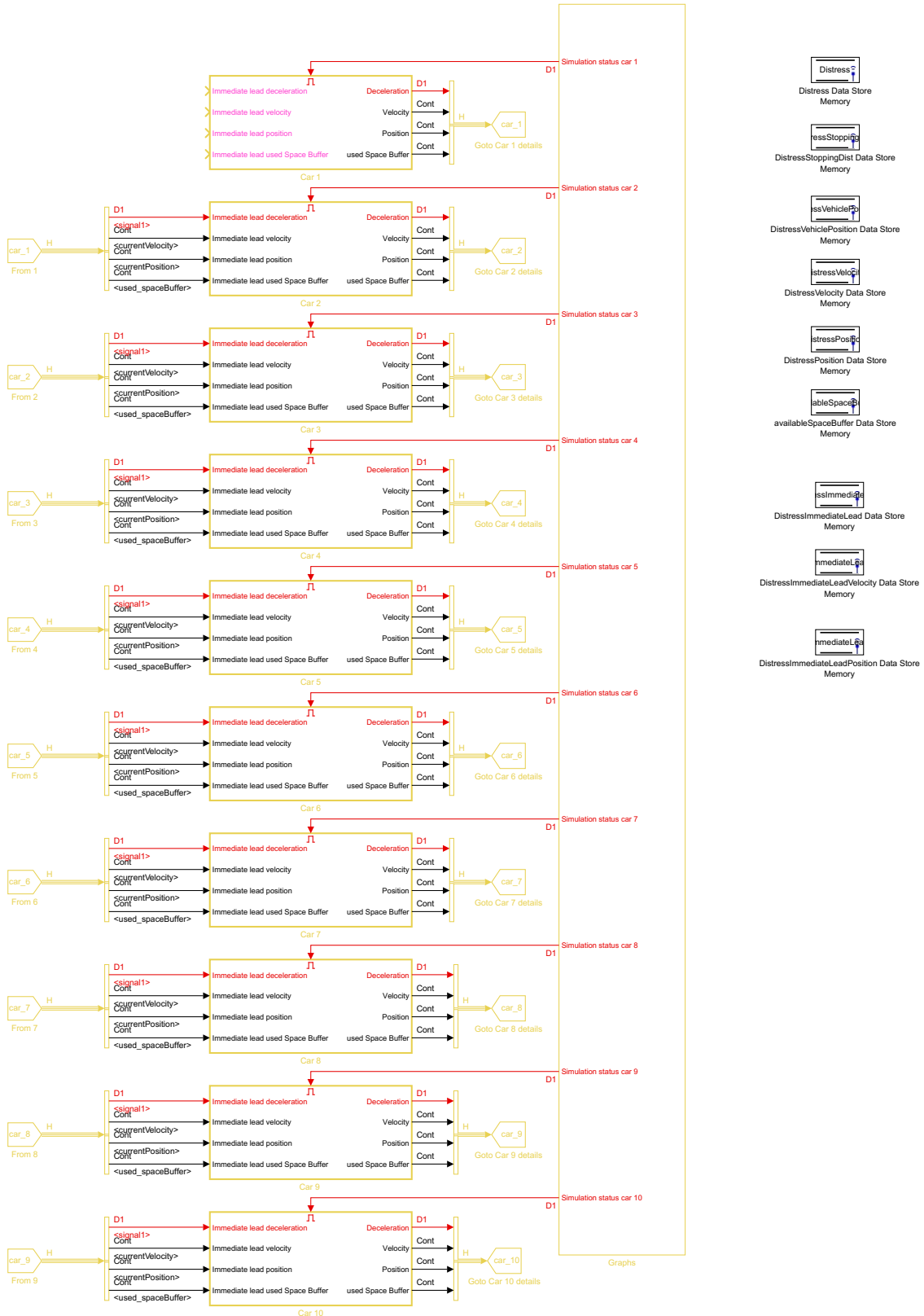


Figure B.6.: The entire platoon model

# Appendix C.

## List of Symbols

$s_c$	inter-vehicle separation in constant spacing policy ( $m$ )
$s_0$	minimum inter-vehicle separation in constant time headway policy ( $m$ )
$\dot{x}$	platoon cruise velocity when using the constant time headway policy ( $m/s$ )
$h$	time headway or time gap in the constant time headway policy ( $s$ )
$s_{des}$	inter-vehicle separation in constant time headway policy ( $m$ )
$R_a$	aerodynamic resistance ( $N$ )
$\rho$	air-mass density ( $kg/m^3$ )
$C_D$	vehicle's aerodynamic drag coefficient when traveling in a platoon
$A_f$	frontal area of a vehicle along its travel direction ( $m^2$ )
$V_r$	vehicle's speed relative to the wind ( $m/s$ )
$C_{DO}$	vehicle's aerodynamic drag coefficient when traveling in isolation
$R_{rf}$	rolling resistance at the front axle tires ( $N$ )
$R_{rr}$	rolling resistance at the rear axle tires ( $N$ )
$h_a$	height from the ground at which aerodynamic resistance acts on a vehicle ( $m$ )
$F_{bf}$	brake force at a vehicle's front-axle tires ( $N$ )
$F_{br}$	brake force at a vehicle's rear-axle tires ( $N$ )
$W_f$	weight on a vehicle's front axle ( $N$ )
$W_r$	weight on a vehicle's rear axle ( $N$ )
$R_d$	draw-bar load of a vehicle ( $N$ )
$h_d$	height from the ground at which a draw-bar load acts on a vehicle ( $m$ )
$d$	deceleration of a vehicle ( $m/s^2$ )
$g$	acceleration due to gravity ( $m/s^2$ )
$h$	height from the ground at which a vehicle's center of gravity is located ( $m$ )
$l_1$	distance from midpoint of a vehicle's front axles to its center of gravity ( $m$ )
$l_2$	distance from midpoint of a vehicle's rear axles to its center of gravity ( $m$ )
$L$	wheel base of a vehicle ( $m$ )

### Appendix C. List of Symbols

$\theta$	road angle/grade/inclination with respect to the horizontal ground (degrees)
$F_{total}$	total decelerating force acting on a vehicle ( $N$ )
$F_b$	brake force at both the front and rear axles of a vehicle combined into one ( $N$ )
$f_r$	coefficient of rolling resistance
$W$	total weight of a vehicle ( $N$ )
$\mu$	coefficient of road adhesion
$F_{bfmax}$	maximum brake force at a vehicle's front axle tires without them locking ( $N$ )
$F_{brmax}$	maximum brake force at a vehicle's rear axle tires without them locking ( $N$ )
$T_b$	brake torque at a wheel ( $N.m$ )
$T_t$	moment at a tire's center due to brake force ( $N.m$ )
$\dot{\omega}$	a tire's angular deceleration ( $rad/s^2$ )
$I_\omega$	mass moment of inertia of a tire about its center ( $kg.m^2$ )
$r$	radius of a tire ( $m$ )
$d_c$	longitudinal deceleration of a tire's center ( $m/s^2$ )
$w$	angular velocity of a tire ( $rad/s$ )
$K_{bf}$	proportion of a vehicle's total brake force acting at its front axle
$K_{br}$	proportion of a vehicle's total brake force acting at its rear axle
$S$	stopping distance of a vehicle assuming instantaneous deceleration tracking ( $m$ )
$\gamma_m$	equivalent mass factor
$C_A$	aerodynamic constant for a vehicle computed as the product of $\frac{\rho}{2}C_D A_f$
$V_{init}$	vehicle's initial velocity before it begins braking ( $m/s$ )
$\eta_b$	vehicle's braking efficiency
$m$	mass of a vehicle ( $kg$ )
$i, j$	indices to represent a vehicle's position in a platoon
$n$	index of a platoon's trail vehicle and also the total number of platoon vehicles
$d_i$	vehicle $i$ 's deceleration ( $m/s^2$ )
$V_i$	vehicle $i$ 's velocity ( $m/s$ )
$P_i$	vehicle $i$ 's position relative to the platoon lead ( $m$ )
$t_i$	time at which vehicle $i$ 's deceleration, velocity, and position were measured to compose the live signal ( $s$ )
$B_i$	space buffer remaining between vehicle $i$ and its immediately leading vehicle at the time of composing the live signal ( $m$ )

$SG$	safeguard ( $m$ )
$B$	space buffer ( $m$ )
$S_j$	stopping distance of vehicle $j$ ( $m$ )
$x$	index of a vehicle that has the longest stopping distance in spite of using all the space buffers from its position ( $1 \leq x \leq n$ ) till the platoon lead
$S_{SB}$	required stopping distance of a platoon lead as per Space-Buffer approach ( $m$ )
$K_1$	used for simplification to denote $\frac{\gamma_m W}{2gC_A}$
$K_2$	used for simplification to denote $C_A V_{init}^2$
$K_3$	used for simplification to denote $f_r W \cos(\theta) \pm W \sin(\theta)$ with $\theta = 0$
$t$	time ( $s$ )
$\Delta d_{i,i+1}$	difference in deceleration magnitudes between two consecutive vehicles $i$ and $i + 1$ ( $m/s^2$ )
$s$	frequency domain $s$
$Gp(s)$	transfer function of a vehicle's LTI model
$Gc(s)$	transfer function of a brake-by-wire controller
$H(s)$	transfer function of an accelerometer
$R_i(s)$	transfer function of the vehicle $i$ 's reference deceleration
$D_i(s)$	transfer function of the vehicle $i$ 's achieved deceleration
$E_i(s)$	transfer function of the error calculated as $R_i(s) - D_i(s)$
$U_i(s)$	transfer function of the vehicle $i$ 's input brake force
$Y_i(s)$	transfer function of the vehicle $i$ 's velocity
$Z_i(s)$	transfer function of (disturbance) grade force acting on the vehicle $i$
$G_i(s)$	closed-loop transfer function involving $Gp_i(s)$ , $Gc_i(s)$ , and $H(s)$
$R_1 - R_4$	residues of the closed-loop transfer function $G_i(s)$ for an input $D_i(s)$
$p_1 - p_4$	poles of the closed-loop transfer function $G_i(s)$
$d_i(t)$	vehicle $i$ 's deceleration expression in time domain under its controller action
$v_i(t)$	vehicle $i$ 's velocity expression in time domain under its controller action
$C_1, C_2$	constants of integration
$s_i(t)$	vehicle $i$ 's position expression in time domain under its controller action
$S_{init}$	vehicle's initial position before braking ( $m$ )
$K_i$	brake-by-wire controller's integral gain
$dis$	index of the distressed vehicle ( $1 \leq dis \leq n$ )

$B_{min}$	the least remaining space buffer that is considered by vehicles when adapting their decelerations during distress situations ( $m$ )
$S_{dis}$	stopping distance or final position at standstill of the most distressed vehicle computed at the time of distress message broadcast ( $m$ )
$S_{max}$	$S_{dis}$ minus the distance covered by the most distressed vehicle in $20ms$ after distress message broadcast ( $m$ )
$B_{dis}$	remaining space buffer between the distressed and its immediately leading vehicle ( $m$ )
$V_{dis}$	velocity of a distressed vehicle at the time of distress message broadcast ( $m/s$ )
$V_{dis-1}$	velocity of a distressed vehicle's immediate lead received through its live signal ( $m/s$ )
$d_{dis-1}$	deceleration of a distressed vehicle's immediate lead received through its live signal ( $m/s^2$ )
$t_{dis-1}$	time at which a distressed vehicle's immediate lead measured its deceleration, velocity, and position to compose its live signal ( $s$ )
$t_{dis}$	time of distress message broadcast ( $s$ )
$d_{dis}$	deceleration of the distressed vehicle at the time of distress message broadcast ( $m/s^2$ )
$S_i^{new}$	required distance to be covered by vehicle $i$ after it begins tracking its new deceleration during distress situations ( $m$ )
$d_i^{new}$	deceleration that brings the vehicle $i$ to standstill in a distance $S_i^{new}$ assuming instantaneous deceleration switching ( $m/s^2$ )
$S_i$	position of vehicle $i$ relative to the moment of braking at $20ms$ after distress message broadcast ( $m$ )
$C_3, C_4$	constants of integration
$\Delta D_i(s)$	difference in magnitudes of $d_i$ and $d_i^{new}$ in the frequency domain $s$
$\tilde{R}_1 - \tilde{R}_4$	residues of the closed-loop transfer function $G_i(s)$ for an input $\Delta D_i(s)$
$\Delta d_i(t)$	time domain output expression of the closed loop transfer function $G_i(s)$ for an input that is the difference in magnitudes of $d_i$ and $d_i^{new}$ in the frequency domain $s$ for vehicle $i$
$\Delta v_i(t)$	time domain velocity expression obtained after integrating $\Delta d_i(t)$
$\Delta s_i(t)$	time domain position expression obtained after integrating $\Delta v_i(t)$
$d_{i,k}^{new}$	deceleration of vehicle $i$ computed numerically and iteratively during distress situations with $k$ denoting the iteration ( $m/s^2$ )
$S_{i,k}^{new}$	distance covered by vehicle $i$ when transitioning to the corresponding deceleration $d_{i,k}^{new}$ ( $m$ )



# Summary of findings

1. The existing inter-vehicle separations in platoons can be further reduced to below  $5m$  (to maximize the benefits) without compromising on safety, especially, when braking in an emergency.
2. At such short separations, the space buffers in the inter-vehicle separations can be efficiently utilized to minimize the overall stopping distance of the platoon as shown by our Space-Buffer approach. In this direction, once emergency braking is initiated, vehicles have to track their respective reference decelerations.
3. The computations of our approach rely on stopping distances of vehicles from a common cruise velocity. The controller-related effects (i.e., rise time, settling time, etc.) in tracking a reference deceleration impact a vehicle's stopping distance. Since these effects are neglected by the standard expression of stopping distance, the same cannot be used. Hence, an expression that computes a vehicle's stopping distance under controller action was derived, and the resulting stopping distance values were used in our approach.
4. The road profile transitions the vehicles undergo during emergency braking impacts safety. Some controllers cannot counter the (disturbing) grade force in a downhill (as they are already braking at their limit on a flat road to minimize the overall stopping distance). As a result, they incur actuator saturation and fail to continue tracking their assigned decelerations. In such situations, through a distress message broadcast, and our proposed coordination scheme we ensure vehicular collisions are avoided and a safe maneuver results, while simultaneously minimizing the stopping distance.
5. At  $2m$  ( $B = 1m$ ) separations, our Space-Buffer approach results in the most benefits, obtaining the best trade-off between stopping distance, platoon length, and aerodynamic benefits in comparison to the intuitive (Least Platoon Length and Least Stopping Distance) and the Subplatoon approaches.
6. At  $3m$  ( $B = 2m$ ) and  $4m$  ( $B = 3m$ ) separations, our approach achieves the optimum stopping distance. Even though at these separations, the platoon becomes longer and the aerodynamic benefits decrease when compared to  $B = 1m$  and the other approaches, the performance is significantly much better in comparison to platoons that employ separations of  $5$  to  $10m$  and above.



# List of own publications

---

The following publications were published in the context of this work.

## Journal publications

- D. K. Murthy and A. Masrur, *A Cyber-Physical Approach for Emergency Braking in Close-Distance Driving Arrangements*, In ACM Transactions on Cyber-Physical Systems (TCPS), **under review**

## Peer-reviewed conferences (acceptance ratio < 30 %)

- D. K. Murthy, Mingqing Zhang and A. Masrur, *Analyzing the Impact of Secure CAN Networks on Braking Dynamics of Cooperative Driving*, In Proceedings of the 22nd Euromicro Conference on Digital Systems Design (DSD), 2019
- D. K. Murthy, and A. Masrur, *A Subplatooning Strategy for Safe Braking Maneuvers*, In Proceedings of the 20th Euromicro Conference on Digital Systems Design (DSD), 2017
- D. K. Murthy, and A. Masrur, *Exploiting space buffers for emergency braking in highly efficient platoons*, In Proceedings of the 23rd IEEE International Conference on Embedded and Real-Time Computing Systems and Applications (RTCSA), 2017
- D. K. Murthy, and A. Masrur, *Braking in Close Following Platoons: The Law of the Weakest*, In Proceedings of the 19th Euromicro Conference on Digital Systems Design (DSD), 2016

Dharshan Krishna Murthy

## Curriculum Vitae

### Personal Details

**Name:** Dharshan Krishna Murthy

**Marital Status:** Single

**Nationality:** Indian

**Email:** dharshankrishna@gmail.com

---

### Work Experience

10/2015 – present

#### **Technische Universität Chemnitz, Germany**

Doctoral Candidate and Research Fellow

Dissertation Title: Emergency Braking in Compact Vehicle Platoons: A Cyber-Physical Design

- Study of impact of Vehicle Dynamics on Braking capabilities
- Design of Emergency Braking approaches for Cooperative Autonomous Driving at vehicle separations below 5 meters
- Modelling, Design and Simulation of a Brake-by-wire Controller for participating in such autonomous vehicle arrangements
- Published Research Articles:  
<https://ieeexplore.ieee.org/document/8875018>  
<https://ieeexplore.ieee.org/document/8046308>  
<https://ieeexplore.ieee.org/document/8049813>  
<https://ieeexplore.ieee.org/document/7723607>

04/2015 – 09/2015

#### **Technische Universität Chemnitz, Germany**

Tutor and Master Thesis in Car-to-Car communication

- Modelling, Design and Simulating a self-driven Trailer with Distance Controller for cruise operation
- Car-to-X communication with its lead/parent car
- 3D Visualization of their movement & wireless communication
- Tutor for *Timing Aware Programming for Embedded Systems*

10/2014 – 02/2015

#### **Technische Universität Chemnitz, Germany**

Tutor and Internship in Car-to-X communication

- Overview of Wireless communication protocols
- Interfacing RFID reader & *Nanett* board for wakeup & data exchange
- Programming Pololu 3pi Robots and Tutor for *Software Platforms for Automotive Systems*

Dharshan Krishna Murthy

03/2012 – 09/2013

**SAP Labs, Bangalore, INDIA**

Programmer in Enterprise Resource Planning System

- Programming and Application enhancements with C#, ABAP(Advanced Business Application Programming)
- Consultant for Application Design
- Tutor for ABAP Programming Language

07/2009 – 02/2012

**Infosys, Bangalore, INDIA**

Programmer in Banking and Capital Markets area

- Programming and Application Enhancements of trading solution - *Sophis Risque* with C#, C and C++
- Design and programming of Batch Jobs with C#, C and C++

---

**Educational Background**

10/2013 – 09/2015

**Technische Universität Chemnitz, Germany**

Master Automotive Software Engineering

*Focus on:* Design of Software for Embedded systems, Real Time Systems, Hardware Development, Multicore Programming, Hardware/Software Co-Design, Software Platforms for Automotive Systems, Timing Aware Programming for Embedded Systems, Machine Learning and AUTOSAR

09/2005 – 06/2009

**Dr. Ambedkar Institute of Technology, Bangalore, India**

Bachelor in Computer Science and Engineering

*Focus on:* C, Data Structures, Operating Systems, Database, Programming Languages, Design of Algorithms, Simulation, UNIX, Networks and Microprocessor Architectures

---

**Skills**

**Programming Languages:**

(Level: Intermediate)

**Automotive Buses:**

**Simulation Tools:**

(Level: Advanced)

C#, C, C++, Python

CAN, Flexray, Automotive Ethernet

Matlab & Simulink, Control Design Toolbox,

OMNeT++, dSPACE -- MotionDesk (3D Visualization) and Automotive Simulation Models

**Languages:**

**Awards:**

Deutsch (B1), English (very good)

Best Developer award at SAP Labs, India (March 2013)

**Hobbies/Interests:**

Cooking and Reading

Chemnitz, November 2020

Dharshan Krishna Murthy

## Erklärungen

Ich versichere, dass die vorgelegte Arbeit weder im Inland noch im Ausland in gleicher oder in ähnlicher Form einer anderen Prüfungsbehörde zum Zwecke einer Promotion oder eines anderen Prüfungsverfahrens vorgelegt wurde und auch noch nicht veröffentlicht wurde.

Es fand ein früheres Promotionsverfahren statt.  Ja  Nein  
(wenn ja)

Thema:

Bescheid:

Zeit:

Hochschule:

Ich versichere, dass die vorliegende Arbeit ohne unzulässige Hilfe und ohne Benutzung anderer als der angegebenen Hilfsmittel angefertigt wurde und die aus fremden Quellen direkt oder indirekt übernommenen Gedanken in der Arbeit als solche kenntlich gemacht sind.

Ich versichere, dass weitere Personen bei der geistigen Herstellung der vorliegenden Arbeit nicht beteiligt waren, insbesondere auch nicht die Hilfe eines Promotionsberaters in Anspruch genommen wurde, und dass Dritte vom Bewerber weder unmittelbar noch mittelbar geldwerte Leistungen für Arbeiten erhalten haben, die im Zusammenhang mit dem Inhalt der vorgelegten Dissertation stehen.

Ich bin mit der elektronischen Überprüfung meiner Dissertation auf etwaige Plagiate hin einverstanden.

---

Datum

---

Unterschrift